

E-proceedings of

# The 7<sup>th</sup> Biotechnology International Congress (BIC 2023)



6-7<sup>th</sup> September 2023  
BITEC, Bangkok, Thailand  
Advances in Biotechnology for Attaining BCG Goals

Copyright © 2023 Thai Society for Biotechnology (TSB)

All rights reserved. This book or any portion thereof may not be reproduced or used in any manner whatsoever without the express written permission of the publisher except for the use of brief quotations in a book review.

Published by Thai Society for Biotechnology (TSB), in Thailand

First printing, 2023.

ISBN (e-book) 978-616-92027-0-7

Thai Society for Biotechnology (TSB)

National Science and Technology Development Agency Building

73/1 Rama VI Road, Thung Phaya Thai, Ratchathewi, Bangkok 10400

Email: [tsb@biotec.or.th](mailto:tsb@biotec.or.th)      [www.bictsb.com](http://www.bictsb.com)

# TABLE OF CONTENTS

<b>WELCOME MESSAGE</b>	<b>1</b>
<b>COMMITTEE</b>	<b>2</b>
<b>CONGRESS PROGRAMME</b>	<b>4</b>
<b>KEYNOTE SPEAKERS</b>	
<b>Pursuing BCG's goals of producing biolubricant from vegetable oil</b>	<b>8</b>
<i>Prof. Penjit Srinophakun</i>	
<b>Potentiality of using salt-tolerant plant-growth-promoting rhizobacteria as biofertilizer for climate-smart agriculture in the coastal areas</b>	<b>9</b>
<i>Prof. Muhammad Manjurul Karim</i>	
<b>Future of food resiliency and security - crucial roles of biotechnology</b>	<b>10</b>
<i>Prof. Pavinee Chinachoti</i>	
<b>Realizing the goal of Bio-Circular Green (BCG) economy through bioconversion of lignocellulosic biomass to bioethanol</b>	<b>11</b>
<i>Prof. Virendra Swarup Bisaria</i>	
<b>From insect farming to insect biorefining with biotechnology and bioprocessing</b>	<b>12</b>
<i>Prof. Yu-Shen Cheng</i>	
<b>Conversion of lignocelluloses to commodity and specialty biochemicals by microbial cell factory and enzymatic process</b>	<b>13</b>
<i>Dr. Verawat Champreda</i>	
<b>INVITED SPEAKERS</b>	
<b>Sustainable BCG model in butanol production using CRISPR cas tools</b>	<b>14</b>
<i>Dr. Ranjita Biswas</i>	
<b>Yeast biotechnology for green energy and clean environment</b>	<b>15</b>
<i>Assoc. Prof. Choowong Auesukaree</i>	
<b>Anti-invasion activities of heat-killed lactic acid bacteria isolates against <i>Salmonella enterica</i> serovar Typhimurium</b>	<b>16</b>
<i>Assoc. Prof. Dr. Sharifah Aminah Syed Mohamad</i>	
<b>Developing synbiotics for the prevention of pathogens through a simulated human gut model</b>	<b>17</b>
<i>Assoc. Prof. Massalin Nakphaichit</i>	
<b>Gut health benefits and potential prebiotic effects of marine seaweeds</b>	<b>18</b>
<i>Asst. Prof. Suvimol Charoensiddhi</i>	

# TABLE OF CONTENTS

## INVITED SPEAKERS

**Biomass polymer-based bioink for 3D bioprinting in vitro multicellular brain-like tissue** 19

*Assoc. Prof. Yi-Chen Ethan Li*

***Streptococcus suis*, a new pathogen of snakeskin gourami (*Trichopodus pectoralis*) and evidence of cross-species transmission** 20

*Dr. Saengchan Senapin*

## ORAL PRESENTATION

### AGRICULTURAL AND FOOD BIOTECHNOLOGY

**Peptides from soy flake koji and their molecular docking to umami receptors** 21

*Aniwat Kaewkrod*

**Chemical composition and nitric oxide inhibition of Sugarcane molasses on LPS-induced inflammatory response in Raw 264.7 macrophage cell** 22

*Fatikah Luebaeteh*

**Development of a low-cost cultivation medium for an industrial-scale spore production of *Priestia megaterium* RS91** 30

*Chaipat Chaemsuwankul*

**Inhibition of *C. gloeosporioides* growth using lemongrass crude extracts combined with pullulan film** 31

*Wanaree Suwannatrai*

### BIOCATALYSIS AND BIOTRANSFORMATION

**Building a sustainable biomanufacturing business: solving human crises with bio-based solutions** 37

*Natthaporn Takpho*

**Characterization of flavin-containing Monooxygenase (FMO) from *Microbacterium esteraromaticum* SBS1-7** 38

*Sathita Meeasa*

# TABLE OF CONTENTS

## ORAL PRESENTATION

### BIOENERGY, BIOREFINERY AND ENVIRONMENTAL BIOTECHNOLOGY

- Influence of culture media on biomass production and pigments of the  
freshwater alga *Chaetophora* sp. (Chlorophyta) 39

*Narin Chansawang*

### BIOPHARMACEUTICAL AND MEDICAL BIOTECHNOLOGY

- Effects of an organic nitrogen supplement on production of  
recombinant HPV52 L1 capsid protein in *Hansenula polymorpha* 47

*Wichitra Phimsen*

- Formulating *Thunbergia laurifolia* Lindl. cream with nanostructured  
lipid carriers for bacterial skin infection treatment 52

*Esther Thongaram*

- Marine actinomycetes isolation from mangrove sediment and partial  
purification of their anticancer activity 59

*Tepakorn Kongsaya*

### MOLECULAR BIOTECHNOLOGY AND NANOBIOENGINEERING

- Phosphatidylserine production via a two-stage carbon dioxide  
utilization technology 68

*Liang-Jung Chien*

- Minocycline encapsulation in PEG-PLGA nanoparticles 69

*Monthira Rattanatayarom*

- Encapsulation of anti-DENV E mAbs in polymeric nanoparticle for  
intracellular delivery 76

*Nutthanicha Intrarakasem*

- Combination of multiplex PCR and CRISPR detection enables  
simultaneous diagnosis of major pathogens in penaeid shrimp 83

*Suthasinee Kanitchinda*

### OTHER RELATED AREAS

- Preliminary study on free radical scavenging activity in the different  
fractions of lactic acid bacteria-derived postbiotics 96

*Sareeya Reungpatthanaphong*

# WELCOME MESSAGE



**Dear friends and colleagues,**

On behalf of the Thai Society for Biotechnology (TSB), the Asian Federation of Biotechnology-Thailand Regional Branch Office of (AFOB – Thailand RBO) and the Organizing Committee of 7<sup>th</sup> Biotechnology International Congress (BIC 2023), I am delighted to welcome you to the Congress and Thailand LAB INTERNATIONAL in Bangkok from September 6-8, 2023.

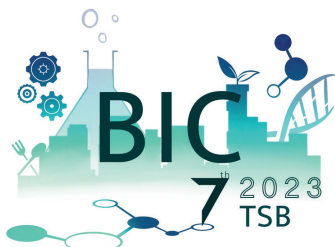
Thai Society for Biotechnology (TSB) and Thailand LAB INTERNATIONAL started the TSB International Forum in 2013 and became Biotechnology International Congress (BIC) in 2015 and used to be annually organized. However, the Congress was canceled for 3 years due to COVID-19 pandemic. This year BIC 2023 is served as community hubs, encouraging collaboration, exchange of ideas and technology focusing on various aspects of biotechnology. The Congress collaborated with Thai Probiotics and Lactic Acid Bacteria Group to update the research on the impact of probiotics on the gut immune system, and the Asian Federation of Biotechnology Association (AFOB) to strengthen the linkage.

The theme of this Congress is “Advances in Biotechnology for Attaining BCG Goals”. The BCG model has been promoted as a new economic model by the Thai Government for inclusive and sustainable growth. Therefore, our society has an essential role to promote industries in the areas of agriculture and food; medical and wellness; bioenergy, biomaterial and biochemical based on transforming biodiversity to a value-based and innovation-driven economy. We believe that the events would be a vital platform providing opportunities for cooperation and support among participants from various sectors during these 3 days of Thailand LAB INTERNATIONAL, 2023.

Finally, I wish you all success, fruitful meetings, and well-spent visits at this 7<sup>th</sup> Biotechnology International Congress and Thailand LAB INTERNATIONAL 2023.

Sincerely yours,

**Associate Prof. Chuenchit Boonchird, Ph.D.**  
**President TSB**  
**Vice President AFOB - Thailand**  
**Chairman Organizing Committee BIC 2023**



**The 7<sup>th</sup> Biotechnology International Congress (BIC 2023)**  
**Advances in Biotechnology for Attaining BCG Goals**  
**6-7 September 2023**

# COMMITTEE

## **Chairperson:**

Associate Professor Dr. Chuenchit Boonchird (President TSB)

Mahidol University

## **Secretary:**

Associate Professor Dr. Prakrit Sukyai (Vice President TSB)

Kasetsart University

## **Advisory Board:**

Professor Takeshi Omasa (President AFOB, Osaka University – Japan)

Professor Dr. Penjit Srinophakun (Former President TSB, KasetsartUniversity – Thailand))

Professor Wen-Chien Lee (Former President AFOB, National Chung Cheng University – Taiwan)

Professor Dr. Suraini Abd Aziz (President AFOB-Malaysia Chapter, Universiti Putra Malaysia – Malaysia)

## **Organizing Committee:**

Regional Branch Office-AFOB Thailand Committee

TSB Committee

## **Scientific Committee:**

Chair: Professor Dr. Vilai Rungsardthong

King Mongkut's University of Technology North Bangkok

Co-chair: Professor Dr. Penjit Srinophakun

Kasetsart University

## **Scientific Committee Members:**

Professor Janardan Lamichhan

Kathmandu University

Professor Dr. Muhammad Manjurul

University of Dhaka

Professor Dr. Mark Stadler

Helmholtz Center for Infection Research

Professor Dr. Pavinee Chinachoti

Former President and Advisor FoSTAT

Professor Dr. Yu-Shen Cheng

National Yulin University of Science and Technology

Professor Dr. Virendra Swarup Bisaria

Regional Centre for Biotechnology

Associate Professor Dr. Sharifah Aminah Syed Mohamad

Universiti Teknologi MARA

Dr. Ranjita Biswas

MAKA University of Technology

# COMMITTEE

## Local Committee:

Associate Professor Dr. Aphichart Karnchanatat	Chulalongkorn University
Associate Professor Dr. Choowong Auesukaree	Mahidol University
Associate Professor Dr. Chuenchit Boonchird	Mahidol University
Associate Professor Dr. Massalin Nakphaichit	Kasetsart University
Associate Professor Dr. Prakrit Sukyai	Kasetsart University
Associate Professor Dr. Ratchaneewan Aunpad	Thammasat University
Associate Professor Dr. Rujikan Nasanit	Silpakorn University
Associate Professor Dr. Sehanat Prasongsuk	Chulalongkorn University
Associate Professor Dr. Tatsaporn Todhanakasem	King Mongkut's Institute of Technology Ladkrabang
Associate Professor Dr. Theppanya Charoenrat	Thammasat University
Assistant Professor Dr. Adisak Romsang	Mahidol University
Assistant Professor Dr. Suvimol Charoensiddhi	Kasetsart University
Dr. Saengchan Senapin	National Center for Genetic Engineering and Biotechnology
Dr. Verawat Champreda	National Center for Genetic Engineering and Biotechnology
Dr. Selorm Torgbo	Kasetsart University

## Proceedings:

Associate Professor Dr. Ratchaneewan Aunpad	Thammasat University
Assistant Prof. Adisak Romsang	Mahidol University



# CONGRESS PROGRAMME

DAY 1 | 06.09.2023 | ROOM MR211

08:00 - 09:00		Registration
09:00 - 09:30		Welcome speech & Opening
09:30 - 10:00	<b>Keynote speaker</b> Prof. Dr. Penjit Srinophakun	Pursuing BCG's goals of producing biolubricant from vegetable oil
10:00 - 10:30	<b>Keynote speaker</b> Prof. Dr. Muhammad Manjurul Karim	Potentiality of using salt-tolerant plant-growth-promoting rhizobacteria as biofertilizer for climate-smart agriculture in the coastal areas
10:30 - 10:50	<b>Coffee Break</b>	
10:50 - 11:05	Aniwat Kaewkrod	Peptides from soy flake koji and their molecular docking to umami receptors
11:05 - 11:20	Fatikah Luebaeteh	Chemical composition and nitric oxide inhibition of Sugarcane molasses on LPS-induced inflammatory response in Raw 264.7 macrophage cell
11:20 - 11:35	Chaipat Chaemsuwankul	Development of a low-cost cultivation medium for an industrial-scale spore production of <i>Priestia megaterium</i> RS91
11:35 - 11:50	Wanaree Suwannatrai	Inhibition of <i>C. gloeosporioides</i> growth using lemongrass crude extracts combined with pullulan film
11:50 - 13:00	<b>Lunch</b>	

# CONGRESS PROGRAMME

DAY 1 | 06.09.2023 | ROOM MR211

13:00 - 13:30	<b>Keynote speaker</b> Prof. Dr. Pavinee Chinachoti	Future of food resiliency and security - crucial roles of biotechnology
13:30 - 14:00	<b>Keynote speaker</b> Prof. Dr. Virendra Swarup Bisaria	Realizing the goal of Bio-Circular Green (BCG) economy through bioconversion of lignocellulosic biomass to bioethanol
14:00 - 14:20	<b>Invited speaker</b> Assoc. Prof. Ranjita Biswas	Sustainable BCG model in butanol production using CRISPR cas tools
14:20 - 14:50	<b>Coffee Break</b>	
14:50 - 15:20	<b>Keynote speaker</b> Prof. Dr. Yu-Shen Cheng	From insect farming to insect biorefining with biotechnology and bioprocessing
15:20 - 15:40	<b>Invited Speaker</b> Assoc. Prof. Choowong Auesukaree	Yeast biotechnology for green energy and clean environment
15:40 - 15:55	Narin Chansawang	Influence of culture media on biomass production and pigments of the freshwater alga <i>Chaetophora</i> sp. (Chlorophyta)
15:55 - 16:10	Dr. Sareeya Reungpatthanaphong	Preliminary study on free radical scavenging activity in the different fractions of lactic acid bacteria-derived postbiotics

# CONGRESS PROGRAMME

DAY 2 | 07.09.2023 | ROOM MR211

08:00 - 09:00		Registration
09:00 - 09:30	<b>Keynote speaker</b> Dr. Verawat Champreda	Conversion of lignocelluloses to commodity and specialty biochemicals by microbial cell factory and enzymatic process
09:30 - 09:50	<b>Invited speaker</b> Assoc.Prof. Sharifah Aminah Syed Mohamad	Anti-Invasion activities of heat-killed lactic acid bacteria isolates against <i>Salmonella enterica</i> Serovar Typhimurium
09:50 - 10:05	Dr. Natthaporn Takpho	Building a sustainable biomanufacturing business: Solving human crises with bio-based solutions
10:05 - 10:20	Sathita Meeasa	Characterization of Flavin-containing Monooxygenase (FMO) from <i>Microbacterium esteraromaticum</i> SBS1-7
10:20 - 10:40	<b>Coffee Break</b>	
10:40 - 11:00	<b>Invited speaker</b> Assoc.Prof. Massalin Nakphaichit	Developing synbiotics for the prevention of pathogens through a simulated human gut model
11:00 - 11:20	<b>Invited speaker</b> Asst.Prof. Suvimol Charoensiddhi	Gut health benefits and potential prebiotic effects of marine seaweeds
11:20 - 11:35	Wichitra Phimsen	Effects of an organic nitrogen supplement on production of recombinant HPV52 L1 capsid protein in <i>Hansenula polymorpha</i>

# CONGRESS PROGRAMME

DAY 2 | 07.09.2023 | ROOM MR211

11:35 - 11:50	Esther Thongaram	Formulating <i>Thunbergia laurifolia</i> Lindl. cream with nanostructured lipid carriers for bacterial skin infection treatment
11:50 - 12:05	Tepakorn Kongsaya	Marine Actinomycetes Isolation from mangrove sediment and partial purification of their anticancer activity
12:05 - 13:15	Lunch	
13:15 - 13:35	<b>Invited speaker</b> Assoc.Prof. Yi-Chen Ethan Li	Biomass polymer-based bioink for 3D bioprinting in vitro multicellular brain-like tissue
13:35 - 13:55	<b>Invited speaker</b> Dr. Saengchan Senapin	Streptococcus suis, a new pathogen of snakeskin gourami ( <i>Trichopodus pectoralis</i> ) and evidence of cross-species transmission
13:55 - 14:15	Leo Lin	The applications of bioreactors in different field of laboratory and industries
14:15 - 14:30	Dr. Liang-Jung Chien	Phosphatidylserine production via a two-stage carbon dioxide utilization technology
14:30 - 14:45	Monthira Rattanatayaron	Minocycline encapsulation in PEG-PLGA nanoparticles
14:45 - 15:00	Nutthanicha Intrarakasem	Encapsulation of anti-DENV E mAbs in polymeric nanoparticle for intracellular delivery
15:00 - 15:15	Suthasinee Kanitchinda	Combination of multiplex PCR and CRISPR detection enables simultaneous diagnosis of major pathogens in penaeid shrimp

**Closing Ceremony**

**Coffee Break**

## Pursuing BCG's goals of producing biolubricant from vegetable oil

**Penjit Srinophakun, Kritpornpawee Pindit, Anusith Thanapimmetha, Maythee Saisriyoot  
and Nutchapon Chiarasamran**

*Chemical Engineering, Kasetsart University, Thailand*

**ABSTRACT:** BCG goals are promising achievements in Thailand and Southeast Asia for biochemicals and biomaterials development from vegetable oils, particularly biolubricant. The market for biolubricant is increasing gradually due to green industrial growth and the good properties of bi-polar biolubricant, which attaches to metal surfaces better than petroleum lubricant. After extracting fatty acid from the vegetable oil, biolubricant molecules can be built. In this presentation, vegetable oils were hydrolyzed to fatty acid and formed biolubricant molecules through 5-step reactions. First, hydrolysis of vegetable oils was applied. Then urea crystallization was made to separate unsaturated fatty acids. Later, epoxidation and esterification reactions were sequentially performed to obtain high-quality biolubricant. H-NMR and C-NMR were used to identify the intermediates and products. Finally, the biodegradable biolubricant (Synthetic ester types) ISO 15380 was produced. ISO V32 specification was categorized as viscosity at 40 °C of 28.8-35.2 cSt, viscosity at 100 °C of higher than 5.0 cSt, viscosity index higher than 104, pour point of -18 °C, and flash point of higher than 175 °C.

## Potentiality of using salt-tolerant plant-growth-promoting rhizobacteria as biofertilizer for climate-smart agriculture in the coastal areas

Muhammad Manjurul Karim

*Department of Microbiology, University of Dhaka, Dhaka 1000, Bangladesh*

**ABSTRACT:** The coastal lands contribute hugely for agriculture and agro-based livelihood. Saltwater intrusion, however, emerged as a growing concern for affecting agriculture. Application of salt-tolerant, plant-growth-promoting rhizobacteria (PGPR) as biofertilizer emerged as microbiotechnology to improve salt tolerance in plants. Here, we isolated 53 PGPR from saline and non-saline areas in Bangladesh. Bacteria isolated from saline areas were able to grow in up to 2.60 mol/L salt concentration, contrary to the isolates collected from non-saline areas. Among the salt-tolerant isolates, *Bacillus aryabhatai* MS3, identified by comparing respective sequences of 16S rRNA using the NCBI GenBank, exhibited a higher amount of atmospheric nitrogen fixation, phosphate solubilization, and indoleacetic acid production at 200 mmol/L salt stress. While in soil, rice growth under non-saline condition was comparable in between *B. aryabhatai* MS3-fertilized and control pots, the scenario was statistically significant when challenged with 200 mmol/L salts, 42.60% and 8% survival were recorded respectively. Biochemical analyses revealed that *B. aryabhatai* MS3 supported the plants under salinity by increasing the availability of nutrients (Fe, P), accelerating the levels of IAA and chlorophyll content, enhancing proline accumulation and decreasing malondialdehyde formation. Further, rice growth was found to be favored by enhanced expression of a set of at least four salt-responsive plant genes: *BZ8*, *SOS1*, *GIG*, and *NHX1*. Fertilization of rice with osmoprotectant-producing PGPR therefore, could be a climate-change-adaptation framework with a view to building a climate-smart agriculture for coastal ecosystems.

\*Presenting and corresponding author: +8801715 490535 and [manjur@du.ac.bd](mailto:manjur@du.ac.bd)

## Future of food resiliency and security – crucial roles of biotechnology

Pavinee Chinachoti<sup>1\*</sup>

<sup>1</sup>*FIRN (Food Innovation and Regulation Network), FoSTAT (Food Science and Technology Association of Thailand), Bangkok, 10400, Thailand*

*\*Correspondence to: FoSTAT (Food Science and Technology Association of Thailand), , 7<sup>th</sup> Floor Amorn Bhumirat Bldg., Kasetsart University, Ngamwongwan Rd. Khwang Latyao, Khet Chatuchak, Bangkok 10900 Bangkok, 10400, Thailand. E-mail Chair@FIRN.or.th*

**ABSTRACT:** Food system currently is under threats from man-made and natural phenomena that disturb and disrupts the fragile bioresources. In order to make sure of food availability to fast growing world population, more resilient and sustainable food systems will need to be implement in the next decade. But existing agricultural practices do not match the world demands for BCG (bio-, circular, and green) technology. Biotechnological approach to improve agricultural practices for the future is one of the needed areas for implementation in future food systems to improve or replace out-of-date, poor agriculture practices. This is a race against the rapidly growing climate change and human conflicts or “food war” that may become inevitable if or when adversity will strike again and most likely all beings will be at risk. Biotechnology can be a part of future food where a more controllable production can be secured and food abundance protected from threats and human can still benefit from healthy sources of food products. As the world population is aging rapidly, occurrence of non-communicable diseases (NCD) an imbalanced metabolic disease and poor food availability (hunger) will add to a major campaign on healthier and affordable food products. Development of food system from up-stream to down-stream (from raw materials to end products), therefore, is one of the key development areas for future survivability and well-being of man-kind. Micro-, macro- nutrients as well as bioactive compounds (functional compounds such as anti-oxidants, peptides and probiotics) should be made more readily available for safe and functional foods and related products. Innovative development with combined use of biotechnology and food technology will be highlighted.

**Keyword:** food security, future food, BCG, agriculture, health function

## Realizing the goal of Bio-Circular Green (BCG) economy through bioconversion of lignocellulosic biomass to bioethanol

Virendra Swarup Bisaria

*Dept. of Biochemical Engineering and Biotechnology  
Indian Institute of Technology-Delhi (Former Organization)  
New Delhi, India  
Email: vsbisaria@hotmail.com*

**ABSTRACT:** Bioconversion of abundant lignocellulosic resources to renewable commodity products such as energy, food, feed, and chemicals through application of green technologies which employ biological processes is being intensively explored to safeguard the environment and to give a push to bioeconomy. The conversion of lignocellulosic biomass to bioethanol is a promising approach to reduce GHG emissions as the carbon dioxide generated during ethanol production is balanced by the carbon dioxide absorbed by the plants used as feedstocks. This renewable biomass, which contains the carbohydrate polymers, cellulose and hemicellulose, can be enzymatically hydrolyzed to hexose (mainly glucose) and pentose (mainly xylose) sugars that serve as building blocks for their bioconversion into ethanol. Out of the three main processes, that is, separate hydrolysis and fermentation (SHF), simultaneous saccharification and fermentation (SSF) and consolidated bioprocessing (CBP) for conversion of cellulose to ethanol, SSF and CBP are being intensively studied to realize this goal. Development of SSF which employs compatible cellulases and thermo-tolerant yeasts makes this process very attractive for large scale trials. CBP in which the saccharolytic enzyme production, hydrolysis of cellulose and hemicellulose, and fermentation of the resultant sugars by an organism to ethanol takes place within a single bioreactor is being looked upon as a preferred option as it improves cellulose conversion efficiency and decreases lignocellulosic biomass processing costs. The presentation will describe the recent research efforts that have been made to develop SSF and CBP processes for efficient production of ethanol from lignocellulosic biomass.



## From insect farming to insect biorefining with biotechnology and bioprocessing

Yu-Shen Chen<sup>1\*</sup>, Nina Hartin<sup>1</sup>, Zong-Xuan Zheng<sup>1</sup>, Erika Wijaya<sup>1</sup>, Ya-Jun Zeng<sup>1</sup>, Wei-Ting Tseng<sup>1</sup>, Guan-Ming Huang<sup>1</sup>, Po-Kai Hsu<sup>1</sup>, and Hui Suan Grrace Ng<sup>2</sup>

<sup>1</sup>*Department of Chemical and Materials Engineering, National Yunlin University of Science and Technology, Douliou, Yunlin 64002, Taiwan*

<sup>2</sup>*Centre for Research and Graduate Studies, University of Cyberjaya, Cyberjaya 63000, Selangor, Malaysia*

**ABSTRACT:** In the pursuit of achieving the global goals of Bio-Circular Green development, the integration of innovative biotechnological methods in insect farming and biorefining stands as a vital pathway. The present talk explores this rapidly advancing frontier, shedding light on the interdisciplinary nexus between insect farming, biochemical engineering, and circular economy. Insect farming, as a sustainable protein source, has emerged as an essential component of the modern agricultural landscape. The application of biotechnology in insect breeding, feed optimization, and waste utilization demonstrates a promising stride towards resource efficiency and ecological responsibility. The transition from insect farming to insect biorefining leverages bioprocessing technologies that are key to valorizing insect biomass. Insect biorefining, transforming insects into high-value products like proteins, lipids, chitin, and more, symbolizes an evolution of traditional bioprocessing paradigms. By detailing the optimization of enzymatic processes, fermentation techniques, and extraction methods, this talk will highlight the commercial aspect and environmental benefits of insect biorefining. Lastly, the synthesis of insect farming and biorefining within the overarching framework of a circular economy will be explored. An in-depth analysis of life cycle assessment, techno-economic evaluation, and the alignment with principles of green bioproducts will be provided. Special attention will be dedicated to the role of policy, innovation, and global collaboration in advancing this bio-based economy. The insights from this talk aim to inspire collaboration across academia, industry, and policy to further explore and harness this burgeoning field. This endeavor not only aligns with the principles of sustainable development but also serves as a beacon for the future of biotechnological innovation in the pursuit of a Bio-Circular Green world.

**Keyword:** Insect biorefinery, circular economy, sustainable development, biomass, agroindustrial wastes

## Conversion of lignocelluloses to commodity and specialty biochemicals by microbial cell factory and enzymatic process

Verawat Champreda<sup>1\*</sup>, Weerawat Runguphan<sup>1</sup>, Benjarat Bunternngsook<sup>1</sup>, Marisa Raita<sup>1</sup>, Pattanop Kanokratana<sup>1</sup>, Warasirin Sornlek<sup>1</sup>, Wuttchai Mhuantong, Pornkamol Unrean<sup>1</sup>, Xinqing Zhao<sup>2</sup>, Chenguang Liu<sup>2</sup>, Dongqing Wei<sup>2</sup>

<sup>1</sup>*Biorefinery and Bioproduct Technology Research Group, National Center for Genetic Engineering and Biotechnology, Patumthani 12120, Thailand*

<sup>2</sup>*State Key Laboratory of Microbial Metabolism, School of Life Science and Biotechnology, Shanghai Jiao Tong University, Shanghai, China*

**\*Correspondence to:** *Biorefinery and Bioproduct Technology Research Group, National Center for Genetic Engineering and Biotechnology, 113 Thailand Science Park, Pahonyothin Road, Khlong Luang, Patumthani 12120, Thailand. E-mail: verawat@biotec.or.th*

**ABSTRACT:** Lignocellulosic biomass represents a promising renewable carbon resource for production of fuels, chemicals, and materials in biorefineries. At BIOTEC, we developed an integrated workflow on biomass conversion, starting from pretreatment and fractionation of the raw materials by green hydrothermal and organosolv process. The cellulose fraction was saccharified to fermentation sugar and converted to various commodity biochemicals, including ethanol, isobutanol, and lactic acid by engineered *Saccharomyces cerevisiae*, designed by synthetic biology in combination with cross-breeding, resulting in robust cell factories with high productivity and tolerances to inhibitors in the biomass hydrolysate. Machine learning was applied for optimization of promoter strengths of key metabolic genes, resulting in improved ethanol production at high temperature. The hemicellulose fraction was converted to xylooligosaccharides, a potent pre-biotic, using an engineered hyperthermophilic endo-xylanase with high specificities towards the X3-X6 products. The isolated lignin was converted to polyhydroxyalkanoate bioplastic by consolidated bioprocessing using a *Pseudomonas* strain. The work demonstrates utilization of all the major biopolymers in lignocellulosic materials to bioproducts of industrial interest.

**Keyword:** Biorefinery; Biochemicals; Bioplastics; Synthetic biology; Enzyme engineering

## Sustainable BCG model in butanol production using CRISPR cas tools

**Ranjita Biswas**

*Department of Biotechnology, Maulana Abul Kalam Azad University of Technology, West Bengal, NH-12, Simhat, Haringhata, West Bengal- 741249.*

**ABSTRACT:** Production of butanol using lignocellulose is desirable for a sustainable BCG model. There are some solventogenic thermophiles in nature that produces biofuels using lignocellulosic biomass. The metabolic engineering of its pathway by redirecting carbon and electron flux can improve the yield significantly. The widely used CRISPR-cas9 editing is not suitable for thermophiles as the enzymatic machinery is unstable above 37°C. The suitability of thermophilic microbes for industrial-scale production of fuels and chemicals from lignocellulosic biomass emphasizes the need for advance genome editing tools. Harnessing endogenous CRISPR-cas system for genome editing can allow precise chromosomal modifications. The CRISPR-cas system in thermophiles will be discussed with reference to *Clostridium thermocellum* and *Thermoanaerobacterium virendrii* strains. In this study, endogenous Type I CRISPR is being repurposed for genetic modification of its butanol synthesizing pathway.

**Keywords:** CRISPR-cas, Type-I CRISPR, Thermopiles, Butanol production

## Yeast biotechnology for green energy and clean environment

Choowong Auesukaree<sup>1,2</sup> \*

<sup>1</sup>Department of Biotechnology, Faculty of Science, Mahidol University, Bangkok 10400, Thailand

<sup>2</sup>Mahidol University-Osaka University Collaborative Research Center for Bioscience and Biotechnology, Bangkok 10400, Thailand

\*E-mail :choowong.aue@mahidol.ac.th

**ABSTRACT:** The budding yeast *Saccharomyces cerevisiae* has long been used in industrial ethanol production. Meanwhile, *S. cerevisiae* is one of the most widely used eukaryotic model organisms for basic life science research. Our main research focuses include yeast responses to fermentation-associated stresses and environmental pollutants, and their biotechnological applications to the production of renewable biofuel and environmental remediation. For the studies on cellular responses to fermentation-associated stresses, we investigate the molecular mechanisms required for tolerance to various stresses present during fermentation. A better understanding of mechanisms underlying adaptive stress responses will provide a direct clue for improving the productivity of beneficial biological products including biofuels. On the other hand, we use *S. cerevisiae* as the eukaryotic model to elucidate the cellular toxicities of key environmental pollutants such as pesticides and heavy metals. Meanwhile, we have developed the yeast system for examining the potential roles of herbal extracts in pollutant detoxification. Moreover, we also evaluate the potential of modified yeast cells for use as efficient biosorbents for toxic pollutants. These research outcomes are expected to provide novel biotechnological approaches for environmental remediation, alternative therapeutic options for environmental poisoning, and also precision detection methods for environmental pollutants.

**Keywords :** Biofuel; Environment; Fermentation; Pollutant; Stress Response; Yeast

## Anti-invasion activities of heat-killed lactic acid bacteria isolates against *Salmonella enterica* serovar Typhimurium

Anis Syahirah Saifor Adzuan<sup>1</sup>, Sharifah Aminah Syed Mohamad<sup>1,2,\*</sup>, Nur Intan Hasbullah<sup>1,3</sup>, Nurliana Abd Mutalib<sup>2</sup>, Maimunah Mustakim<sup>4</sup>, Rozila Alias<sup>5</sup>

<sup>1</sup>Faculty of Applied Sciences, Universiti Teknologi MARA, 40450 Shah Alam, Selangor, Malaysia.

<sup>2</sup>Atta-ur-Rahman Institute for Natural Product Discovery, Universiti Teknologi MARA Cawangan Selangor, 42300 Puncak Alam, Selangor, Malaysia.

<sup>3</sup>Faculty of Applied Sciences, Universiti Teknologi MARA, Cawangan Negeri Sembilan, Kampus Kuala Pilah, 72000 Kuala Pilah, Negeri Sembilan, Malaysia

<sup>4</sup>Faculty of Health Sciences, Universiti Teknologi MARA Cawangan Selangor, 42300 Puncak Alam, Selangor, Malaysia

<sup>5</sup>Institute of Bio-IT Selangor, Universiti Selangor, Jalan Zirkon A7/A, Seksyen 7, 40000 Shah Alam Campus, Selangor, Malaysia

**Correspondence to:** Atta-ur-Rahman Institute for Natural Product Discovery, Universiti Teknologi MARA Cawangan Selangor, 42300 Puncak Alam, Selangor, Malaysia.  
sharifah459@uitm.edu.my

**ABSTRACT:** The most common cause of severe foodborne salmonellosis is *S. Typhimurium*. Despite its emergence as a major foodborne pathogen, little is known on how *S. Typhimurium* interacts with intestinal epithelial cells. Lactic acid bacteria (LAB) have been recognized as prominent probiotic gastrointestinal microbiota of the human and animal that confer health-promoting effects and protection against pathogens. The aim of this study is to determine the capability of heat killed LAB (HK-LAB) isolates to inhibit the invasion of *S. Typhimurium* towards human intestinal cells. We observed the adhesion and invasion pattern of *S. Typhimurium* on intestinal epithelial cells (Caco-2) and also assessed the effect of LAB on the *S. Typhimurium*-host cell interaction with the hypothesis that LAB would reduce *S. Typhimurium* infectivity. In this study, 12 HK-LAB isolates from 3 sources of origin (stingless bee, plant, and food) were tested for adhesion on Caco-2 cells and anti-invasion activities against *S. Typhimurium*. The HK-LAB identified as *Lactobacillus paracasei* from plant origin demonstrated adhesion of  $17 \pm 0.70$  per 10 Caco-2 cells, which is similar as the control strain (*Lactobacillus casei*). Meanwhile, isolate from food origin (tairu) has the highest adhesion rate with  $19 \pm 1.32$  per 10 Caco-2 cells. In anti-invasion assay, pre-exposure of Caco-2 cells to the two HK-LAB isolates that had the strongest adherence to Caco-2 cells led to increased suppression of *S. Typhimurium*. When compared to the positive control ( $63.81 \pm 1.15\%$ ), R-isolate inhibited at  $64.76 \pm 9.02\%$  and Tairu-isolate inhibited at  $78.1 \pm 3.06\%$ . R and Tairu were then tested for their antibacterial ability against *S. Typhimurium* based on their excellent anti-invasion properties. Both isolates displayed very strong inhibition zones ( $27 \pm 0.06$  mm for R and  $23 \pm 0.06$  mm for Tairu) against *S. Typhimurium*. These findings suggest that the anti-invasion activities of HK-LAB R and Tairu may correlate to their bactericidal effects that serve to protect the host from infection.

**Keyword:** *Salmonella* Typhimurium, Heat-killed lactic acid bacteria, intestinal Caco-2 cells, adhesion, anti-invasion

## Developing synbiotics for the prevention of pathogens through a simulated human gut model

**Massalin Nakphaichit<sup>1,2\*</sup>, Kevin Mok<sup>1,2</sup>, Patkakorn Udomsri<sup>1,2</sup>, Witida Sathitkowitchai<sup>1,2</sup>, and Sunee nitisinprasert<sup>1,2</sup>**

<sup>1</sup>*Department of Biotechnology, Faculty of Agro-Industry, Kasetsart University, Bangkok, Thailand*

<sup>2</sup>*Specialized Research Unit: Probiotics and Prebiotics for Health, Faculty of Agro-Industry, Kasetsart University, Bangkok, Thailand*

**\*Correspondence to:** <sup>1</sup>*Department of Biotechnology, Faculty of Agro-Industry, Kasetsart University, Bangkok, Thailand, fagimln@ku.ac.th*

**ABSTRACT:** Synbiotics are mixtures that contain live microorganisms and substrates selectively utilized by host microorganisms, which confer a health benefit on the host. According to the environmental conditions of the gut microbiota in each individual, synbiotics are designed to enhance the efficacy of probiotics or prebiotics for health promotion. *Lactococcus lactis* KA-FF 1-4 can produce antimicrobial substances that inhibit Vancomycin-resistant enterococcus (VRE). Through commercial prebiotic selection, Fibersol was found to enhance the inhibition activity of probiotic KA-FF 1-4. In addition, combining *Lactococcus lactis* KA-FF 1-4 with Fibersol could reduce VRE levels by 0.5 log copy number when tested in a simulated human gut model. The synbiotic also promoted the production of short-chain fatty acids. To design a synbiotic that reduces the amount of *Salmonella* in humans, it was found that a water-based plant consisting of *Ulva regida* and *Wolffia globosa* promoted the growth of *Limosilactobacillus reuteri* KUB-AC5, especially *Ulva regida*, which promoted the production of butyric acid by KUB-AC5. In a simulated gut fermentation system with *Salmonella* challenge, only KUB-AC5 with *Ulva regida* supplement reduced *Salmonella* by approximately 1 log copy number compared to the control group. Additionally, the synbiotic produced the highest levels of short-chain fatty acids, including acetic, propionic, and butyric acids, and promoted beneficial bacteria such as *Faecalibacterium*, *Blutia*, and *Lactobacillus*. Therefore, synbiotics are suitable as functional foods that can enhance the efficacy of probiotics or prebiotics and contribute to the future development of the health food industry.

**Keyword:** Probiotic, Prebiotic, Synbiotics, a stimulated human gut model

## Gut health benefits and potential prebiotic effects of marine seaweeds

Suvimol Charoensiddhi<sup>1\*</sup>

<sup>1</sup>*Department of Food Science and Technology, Faculty of Agro-Industry, Kasetsart University, 50 Ngamwongwan Road, Ladyao, Chatuchak, Bangkok 10900 Thailand*

*\*Correspondence to: Department of Food Science and Technology, Faculty of Agro-Industry, Kasetsart University, 50 Ngamwongwan Road, Ladyao, Chatuchak, Bangkok 10900 Thailand.  
E-mail: suvimol.ch@ku.th*

**ABSTRACT:** Marine macroalgae or seaweeds are important sources of bioactive compounds with diverse structures and functionalities. The aim of this study was to investigate the potential of using seaweeds as dietary supplements with gut health benefits demonstrated in both *in vitro* and *in vivo*. Dietary fiber or polysaccharide, a common main component of seaweeds accounting for up to 70% of the dry weight, shows promise as prebiotics as it was resistant to digestion by enzymes presented in the gastrointestinal tract and was readily fermentable in the gut by resident microbiota. Seaweed polysaccharides can benefit health through impacts on gut microbiota modulation and production of microbial metabolites, including the formation of short-chain fatty acids (SCFAs) when added to an *in vitro* anaerobic batch fermentation system containing human fecal inocula that mimic the environment of the human large bowel. More importantly, these positive *in vitro* results correspond to the investigations *in vivo* animal model. In addition, seaweed polyphenols, the new candidates to prebiotics, can also modulate gut microbial balance by stimulating the growth of gut microbiota recognized as prebiotic targets and increase the production of SCFAs, particularly butyric acid. The key findings achieved from this work contribute to develop and expand new platform of seaweed utilization for higher-value products, particularly to functional food and nutraceutical industries in order to serve the social demand for health awareness and support economic development.

**Keyword:** Gut microbiota; Polyphenol; Polysaccharide; Prebiotic activity; Seaweed; Short-chain fatty acid

## Biomass polymer-based bioink for 3D bioprinting an in vitro multicellular brain-like tissue

Yi Chen Ethan Li\*

<sup>1</sup> *Department of Chemical Engineering, Feng Chia University, Taiwan*  
E-mail: yicli@fcu.edu.tw

**ABSTRACT:** To provide a reliable in vitro drug testing platform for brain diseases, it is crucial to create three-dimensional (3D) multi-cell-based environments that mimic cell-cell configurations and interactions. However, existing 2D cultures fail to fully recapitulate the complex features of 3D environments, resulting in brain disease models that lack accurate specific 3D configurations and 3D neuron-astrocyte interactions. In this study, we aim to develop a bioink based on biomass polymers for 3D bioprinting of a brain-like construct. Using this bioprinting technique, a neuron-laden bioink will be printed within an astrocyte-laden soft hydrogel with a brain-like stiffness, effectively resembling brain tissue. This construct will recapture synapse functions and possess the ability to synthesize glutamate, thus recapitulating neuron-astrocyte interactions for controlling glutamate levels in the printed brain. By employing this 3D biomimetic brain model, we expect to achieve higher confidence in drug testing results, enabling accurate predictions of human responses to treatments and reducing the need for animal testing in the pre-clinical phase.

**Keywords:** Biomass polymers, 3D bioprinting, stem cells, co-culture.



***Streptococcus suis*, a new pathogen of snakeskin gourami  
(*Trichopodus pectoralis*) and evidence of cross-species transmission**

Saengchan Senapin<sup>1,2\*</sup>, Nguyen Dinh-Hung<sup>3</sup>, Ha Thanh Dong<sup>4</sup>,

Satid Chatchaiphon<sup>5</sup> and Pakorn Aiewsakun<sup>6,7</sup>

<sup>1</sup>*Fish Health Platform, Center of Excellence for Shrimp Molecular Biology and Biotechnology (Centex Shrimp), Faculty of Science, Mahidol University, Bangkok, 10400, Thailand*

<sup>2</sup>*National Center for Genetic Engineering and Biotechnology (BIOTEC), National Science and Technology Development Agency (NSTDA), Pathum Thani, 12120, Thailand*

<sup>3</sup>*Center of Excellence in Fish Infectious Diseases (CE FID), Department of Veterinary Microbiology, Faculty of Veterinary Science, Chulalongkorn University, Bangkok, 10330, Thailand*

<sup>4</sup>*Department of Food, Agriculture and Bioresources, Aquaculture and Aquatic Resources Management Program, Asian Institute of Technology (AIT), School of Environment, Resources and Development, Klong Luang, Pathum Thani, 12120, Thailand*

<sup>5</sup>*Department of Aquaculture, Faculty of Fisheries, Kasetsart University, Bangkok, 10900, Thailand*

<sup>6</sup>*Department of Microbiology, Faculty of Science, Mahidol University, Bangkok, 10400, Thailand*

<sup>7</sup>*Pornchai Matangkasombut Center for Microbial Genomics, Department of Microbiology, Faculty of Science, Mahidol University, Bangkok, 10400, Thailand*

**\*Correspondence to:** S. Senapin. E-mail [saengchan@biotec.or.th](mailto:saengchan@biotec.or.th)

**ABSTRACT:** *Streptococcus suis*, primarily recognized as a pathogen in pigs, has recently emerged as the causative agent of farmed snakeskin gourami (*Trichogaster pectoralis*).

A comprehensive examination of the bacterial strain originating from a natural disease outbreak, using both microbiological and molecular methods, identified the Gram-positive bacteria infecting snakeskin gourami as *S. suis*. Experimental infections in both juvenile and adult fish demonstrated dose- and size-dependent morbidity and mortality, with mortality rates reaching up to 92.5%. The infected fish exhibited clinical manifestations similar to those observed in naturally infected fish. The results not only fulfilled Koch's postulates but also established *S. suis* as a novel piscine pathogen. Genomic analysis of *S. suis* strain 3112, the first known fish-infecting isolate, identified it as serotype 6 with a unique sequence type likely originating from swine. Furthermore, genome sequencing revealed the presence of specific genes closely correlated with antimicrobial resistance phenotypes in the bacterium. These findings enhance our understanding of *S. suis* pathogenicity and genome characteristics, as well as highlight the importance of heightened awareness, active surveillance, and mitigation measures to prevent the wider spread of this pathogen. The discovery of *S. suis* cross-species transmission underscores the interconnectedness of human, animal, and environmental health, in alignment with the One Health paradigm.

**Keywords:** Fish, Pig, Streptococcosis, Genome, One Health

## Peptides from soy flake koji and their molecular docking to umami receptors Aniwat Kaewkrod<sup>1</sup>, Nuttawee Niamsiri<sup>1</sup>, Angkana Wpatanawin<sup>1</sup>, Napassorn Punyasuk and Sittiwat Lertsiri<sup>1\*</sup>

<sup>1</sup>Department of Biotechnology, Faculty of Science, Mahidol University, Bangkok, 10400

\*Correspondence to: Department of Biotechnology, Faculty of Science, Mahidol University,  
Bangkok, 10400, E-mail: [sittiwat.ler@mahidol.edu](mailto:sittiwat.ler@mahidol.edu)

Umami peptides are short peptides that contain glutamic acid residue and have a molecular weight less than 3,000 Da. These peptides are generally found in natural foods and fermented food products. In this work, umami peptides were isolated from soy flake koji fermented by three strains of *Aspergillus oryzae* i.e., mutk, 9252, and mu4. Protease activity, soluble protein content, and primary amine content were investigated during fermentation. *A. oryzae* mu4 had the highest level of protease activity ( $0.60 \pm 0.01$  U/ml), soluble protein ( $263.33 \pm 18.49$  M/ml), and primary amine ( $92.11 \pm 0.90$  M/ml). Crude peptide extracted from *A. oryzae* mu4 was separated using membrane filtration and reverse-phase high-performance liquid chromatography. Umami taste of the peptide fraction was predicted by In-silico analysis. Molecular docking was used to study the interaction between the peptides and the umami receptors. Five peptides that showed umami tastes were glutamic acid-rich with glutamic acid residuals near the N-terminal. These peptides were evaluated through GOLD molecular docking against the T1R1-T1R3 binding pocket. The GOLD fitness scores of glutamic acid-rich peptides show the best fitness score of 15.98 with a binding energy (-22.44) Kcal/mol. Moreover, hydrogen bonding was the important interaction for amino acid residues to bind with the receptor pocket.

**Keyword:** Umami peptide, Umami receptor, *Aspergillus oryzae*, Soy flake.

## Chemical composition and nitric oxide inhibition of Sugarcane molasses on LPS-induced inflammatory response in Raw 264.7 macrophage cell

Fatikah Luebaeteh<sup>1</sup>, Rajnibhas Sukeaw Samakdhamrongthai<sup>2</sup>, Bandhita Wanikorn<sup>3</sup> and Chutha Takahashi Yupunqui<sup>4\*</sup>

<sup>1</sup>Functional Foods and Nutrition programs, Faculty of Agro – Industry, Prince of Songkla University, Songkhla, 90110 Thailand

<sup>2</sup>Division of Product Development Technology, Faculty of Agro-Industry, Chiang Mai University, 50100 Thailand

<sup>3</sup>Biotechnology department, Faculty of Agro – Industry, Kasetsart University, Bangkok, 10900 Thailand

<sup>4</sup>Center of Excellence in Functional Foods and Gastronomy, Faculty of Agro – Industry, Prince of Songkla University, Songkhla, 90110 Thailand

\*Correspondence to: Center of Excellence in Functional Foods and Gastronomy, Faculty of Agro – Industry, Prince of Songkla University, Songkhla, 90110 Thailand Email: chuthatakahashi@gmail.com

### ABSTRACT:

Sugar crystallization produces a by-product called sugarcane molasses (SM). It is the most common biological compound and can be utilized to offer health benefits. The aims of study to proximate analysis, chemical composition, its effect on cell viability, and production of nitric oxide decreasing in raw 264.7 macrophage cells. The results of the proximate analysis indicate that the main compositions of SM are carbohydrate, moisture, and ash in the 11 SM samples. The total phenolic content (TPC) and total flavonoid content (TFC) of NE8 exhibited a significant difference ( $p < 0.05$ ) when compared to all other samples, with values of  $88.33 \pm 13.82$  mg GAE/g sample and  $1.36 \pm 0.08$  mg CE/g sample, respectively. NE8 was identified as a component containing polyphenols, including ferulic acid, quercetin, gallic acid, and rutin. Cell viability, as determined by the MTT assay, was greater than 90% for SM concentrations ranging from 0.1 to 6.4 mg/ml. Notably, at concentrations between 0.1 and 1.6 mg/ml, SM exhibited a concentration-dependent increase in cell viability. Additionally, cell viability at concentrations of 3.2 and 6.4 mg/mL demonstrated similar trends. Meanwhile, SM demonstrated the ability to reduce NO production induced by LPS-induced inflammation in raw 264.7 macrophage cells. The cells treated with SM at concentrations ranging from 0.1 to 6.4 mg/ml were assessed using Griess's reagent. NE8 exhibited the highest inhibition of NO production, significantly differing ( $p < 0.05$ ) compared to all other samples, with a value of  $59.74 \pm 0.03\%$  ( $IC_{50} = 3.57 \pm 0.07$  mg/ml). Therefore, SM at concentrations less than 3.2 mg/ml was found to be non-toxic to raw 264.7 macrophage cells. The polyphenolic compounds present in SM, such as the phenolic compounds found in sugarcane molasses, may contribute to the enhancement of their functional capabilities

**Keyword:** Sugarcane molasses, phenolic, flavonoid, anti-inflammation, raw 264.7 cell

### 1. INTRODUCTION

Sugarcane molasses (SM) has dark brown liquid viscosity characteristics, an aroma like a caramel. SM has a part of by-product throughout crystallized process of sugar production [1]. SM can be as use feedstock in profile of microbial fermentation of biomass [2]. In addition, SM has been employed for animal fed, baking, fuel, and ethanol, among organics other [3]. SM in animal feed with nonnutritive and dieted benefits but addition sweetness diet [4] was identified in SM is the mainly compound carbohydrate.

The quality and type of chemical composition of SM were as SM with 76 – 85% dry matter, 1 – 2% reducing sugar, 1% of raffinose, 0.2 – 1% invert sugar, 2 – 4% of pigments and 6% of ash [5], and minerals. The dark brown color as a rich nutrients and minerals, main compound is carbohydrate with mainly sucrose [6]. General chemical composition of SM consists of crude protein content with value of  $6.7 \pm 1.8\%$  dry matter, and organic acid [7]. Few years, researchers more consider of SM on health benefits of on sugar production and by – product of sugar productions [8].

Phenolics and flavonoids which are functional component there were reported that previous study of SM flavonoids and other compound of SM with antioxidant activity [9], by quantitative of phenolics contents and flavonoids contents using colorimetric methods of SM ethanol extract revealed 17.4 mg GAE/g and 5.2 mg CE/g, respectively [10] water extract of SM showed  $184 \pm 12.9$  mg GAE/g DW and  $79.5 \pm 2.93$  mg RE/g DW [11] respectively. The compounds of SM were identified by an UHPLC-MSMS system methods which found that phenyl valeric acid, quinic acid, tannic acid, apigenin and gallic acid [12]. Several reported that phenolics compounds can be use as antioxidant scavenger namely flavonoids as higher antioxidants activity [13] to health promoting properties such as antimicrobial and anticancer activities [14]

The objectives of our research are to determine the proximate and chemical composition of SM and to identify its phenolic compounds. Subsequently, the sample with the highest phenolic compound content can be selected for the study of pharmacological properties and potential human benefits.

## 2. MATERIALS AND METHODS

### 2.1. Materials

Sugarcane molasses was collected from sugar production factories and stored in a polypropylene (PPE) bottle at 4°C until it was used. Gallic acid, ferulic acid, quercetin, rutin, and catechin standards were employed for the chemical composition analysis of SM. Raw 264.7 macrophage cells were utilized to assess cytotoxicity and the inhibition of NO production

### 2.2 Proximate and physician analysis

The proximate composition of 100 g of sugarcane molasses was analyzed by Central Laboratory (Thailand) Co., Ltd in Hat Yai, Songkhla, Thailand, following the AOAC 2019 standards. All parameters were analyzed in triplicate

### 2.3 Identification of phenolic and flavonoid composition

The total phenolic content (TPC) and total flavonoid content (TFC) were determined using colorimetric assays. The samples were diluted with distilled water to a 10-fold dilution from the stock samples. TPC was determined using the Folin-Ciocalteu colorimetric assay, with gallic acid used to create a standard curve for TPC calculations. TFC was determined through a colorimetric assay, using catechin for the standard curve calculation. Polyphenol analysis was performed to assess the phenolic and flavonoid profile using HPLC analysis. The sample powder extract was diluted to a concentration of 10 mg/ml and filtered before being added to vials for HPLC analysis.

### 2.4 Cell viability assay and inhibition NO production assay

The cytotoxicity of sugarcane molasses on an animal cell culture was evaluated using a methyl thiazolyl tetrazolium (MTT) assay. Raw 264.7 macrophage cells were cultured in RPMI-1640 medium containing 10% fetal bovine serum and maintained in a humidified atmosphere of 5% CO<sub>2</sub> and 95% air at 37°C. The cells were seeded at a density of  $7 \times 10^4$  cells per well onto a 96-well plate in complete medium and incubated for 24 hours. The cells were then treated with sugarcane molasses at concentrations ranging from 0.1 to 6.4 mg/ml. Subsequently, the cells were exposed to the MTT reagent (5 mg/ml in PBS) for 2 hours at 37°C in a 5% CO<sub>2</sub> environment. After aspirating the culture supernatants, 200 µl of DMSO was added to each well, and the absorbance was measured at 570 nm using a microplate reader. For the inhibition of NO production assay, 100 µl of 1 µg/ml

LPS was added to the cells, and they were incubated for 24 hours. Equal volumes of the cell culture supernatants and Griess' reagent were mixed thoroughly. Nitrite concentrations, indicative of NO production, were determined using Griess' reagent (Sigma-Aldrich, Saint Louis, MO, USA). The absorbance of the detected NO at 570 nm was used to calculate the percentage of inhibition of NO production.

### 2.5 Statistical analysis

The experiments were conducted in triplicate. The data are presented as means with corresponding standard deviations for each treatment. The results of proximate and physical properties were compared among samples using one-way analysis of variance (ANOVA) with Tukey's. The total phenolic and flavonoid content of sugarcane molasses was statistically analyzed using one-way ANOVA with the Duncan test

## 3. RESULTS AND DISCUSSION

Table 1 show the proximate analysis of sugarcane molasses, indicating the macronutrient composition, including moisture, fat, protein, ash, and carbohydrates. The moisture content results of sugarcane molasses (SM), ranging from 25.94±0.07% to 31.56±0.07%, exhibited significant differences ( $p < 0.05$ ). However, samples N1, N5, and N7 did not exhibit significant differences ( $p \geq 0.05$ ) when compared to all other samples. The results for fat content in SM, ranging from 0.03±0.00% to 0.50±0.01%, showed significant differences ( $p < 0.05$ ). Specifically, samples E4 and NE8 did not differ significantly ( $p \geq 0.05$ ) from the other SM samples. Similarly, the protein content of SM, spanning from 4.12±0.01% to 5.81±0.01%, demonstrated significant differences ( $p < 0.05$ ), with samples N5 and C8 not displaying significant differences ( $p \geq 0.05$ ). The ash content of SM, ranging from 5.03±0.03% to 8.77±0.05%, also exhibited significant differences ( $p < 0.05$ ), except for samples N1 and C1, which did not differ significantly ( $p \geq 0.05$ ) from the other SM samples.

**Table 1** Proximate contents of sugarcane molasses

Sample	Moisture (%)	Fat (%)	Protein (%)	Ash (%)	Carbohydrate (%)
N1	28.87±0.04 <sup>d</sup>	0.43±0.01 <sup>h</sup>	4.87±0.01 <sup>e</sup>	8.52±0.31 <sup>fg</sup>	57.16±0.01 <sup>c</sup>
N5	28.98±0.98 <sup>de</sup>	0.1±0.00 <sup>e</sup>	5.24±0.01 <sup>gh</sup>	6.36±0.01 <sup>c</sup>	59.31±0.01 <sup>h</sup>
N7	29.01±0.01 <sup>de</sup>	0.41±0.00 <sup>g</sup>	5.15±0.01 <sup>f</sup>	7.11±0.04 <sup>d</sup>	58.31±0.01 <sup>f</sup>
C1	27.21±0.04 <sup>c</sup>	0.35±0.00 <sup>f</sup>	5.22±0.02 <sup>g</sup>	8.77±0.05 <sup>g</sup>	58.41±0.02 <sup>g</sup>
C6	30.51±0.06 <sup>f</sup>	0.07±0.00 <sup>d</sup>	4.64±0.01 <sup>c</sup>	7.67±0.02 <sup>e</sup>	57.11±0.01 <sup>b</sup>
C8	27.00±0.01 <sup>b</sup>	0.50±0.01 <sup>i</sup>	5.27±0.02 <sup>h</sup>	6.63±0.01 <sup>c</sup>	60.58±0.01 <sup>j</sup>
C6	30.51±0.06 <sup>f</sup>	0.07±0.00 <sup>d</sup>	4.64±0.01 <sup>c</sup>	7.67±0.02 <sup>e</sup>	57.11±0.01 <sup>b</sup>
NE1	25.94±0.07 <sup>a</sup>	0.36±0.01 <sup>f</sup>	4.37±0.01 <sup>b</sup>	8.47±0.03 <sup>f</sup>	60.84±0.01 <sup>k</sup>
NE6	29.05±0.00 <sup>e</sup>	0.04±0.00 <sup>b</sup>	5.43±0.01 <sup>i</sup>	7.93±0.04 <sup>e</sup>	57.55±0.01 <sup>d</sup>
NE8	31.56±0.07 <sup>h</sup>	0.03±0.00 <sup>a</sup>	5.81±0.01 <sup>j</sup>	6.02±0.05 <sup>b</sup>	54.87±0.01 <sup>a</sup>
NE9	31.04±0.04 <sup>g</sup>	0.06±0.00 <sup>c</sup>	4.74±0.01 <sup>d</sup>	6.02±0.05 <sup>b</sup>	58.14±0.01 <sup>e</sup>
E4	30.57±0.07 <sup>f</sup>	0.04±0.01 <sup>ab</sup>	4.12±0.01 <sup>a</sup>	5.03±0.03 <sup>a</sup>	60.21±0.03 <sup>i</sup>

Values are presented as the mean ± SD. a, b, c, d, e, f, g, i, j, k followed by different letters in same of column are significantly difference ( $p < 0.05$ ), as a mean ± SD ( $n = 3$ ) as determined by the Turkey's multiple comparison test.

This study found that the main chemical composition is carbohydrate content. This result is related to [15] this study, which investigated the proximate composition of by-products from sugar production, found the highest carbohydrate content to be 75.10%. Our results are consistent with previous reports, which indicated that the carbohydrate content in sugarcane molasses (SM) is

primarily composed of sucrose, glucose, and fructose, accounting for 71.84% [16] highest moisture content observed in our study can be attributed to moisture originating from the fresh sugarcane and the processing involved in sugar production, resulting in a high the water content [17]. Ash content is used to describe the inorganic compounds resulting from the combustion of organic compounds [18], serving as a measure of the total mineral content within a food or other material.

Polyphenol compounds are present in the plant kingdom, and it is well-known that they commonly possess an aromatic ring bearing one or more hydroxyl groups. The study of polyphenol compounds indicated that the total phenolic content (TPC) and total flavonoid content (TFC) in sugarcane molasses (SM) are shown in figure 1. Among the samples, NE8 exhibited the highest TPC and TFC, which were significantly different ( $p < 0.05$ ) compared to the other samples of SM, with values of  $88.33 \pm 13.82$  mg GAE/g sample and  $1.36 \pm 0.08$  mg CE/g sample, respectively. The NE8 sample was identified as a polyphenol compound using the HPLC method, as shown in table 2. The analysis revealed the presence of polyphenol compounds including ferulic acid, quercetin, gallic acid, and rutin, with values of  $0.0064 \pm 0.0025$ ,  $0.0229 \pm 0.0112$ ,  $0.0288 \pm 0.0081$ , and  $0.0370 \pm 0.0049$  mg%, respectively. This study is consistent with a previous investigation of SM extract with ethanol, which found TPC and TFC contents to be 17.4 mg GAE/g and 5.2 mg CE/g, respectively [19]. Recent preclinical studies on polyphenols have demonstrated their potential health benefits, including anti-mutagenic effects in bacterial models and their ability to inhibit NO production, which is related to inflammatory activity [20].

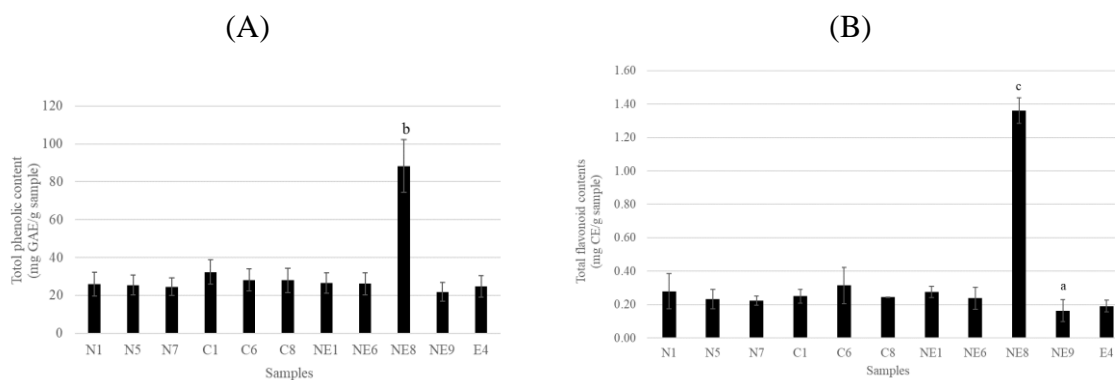


**Figure 1** Result of chemical compound of sugarcane molasses. (A) Total phenolic contents (GEA mg/g sample). (B) Total flavonoid contents (CE mg/g sample). Values are presented as the mean  $\pm$  SD. <sup>a,b,c</sup> Values followed by different letters in each sample are significantly ( $p < 0.05$ ), as determined by the Turkey's multiple comparison.

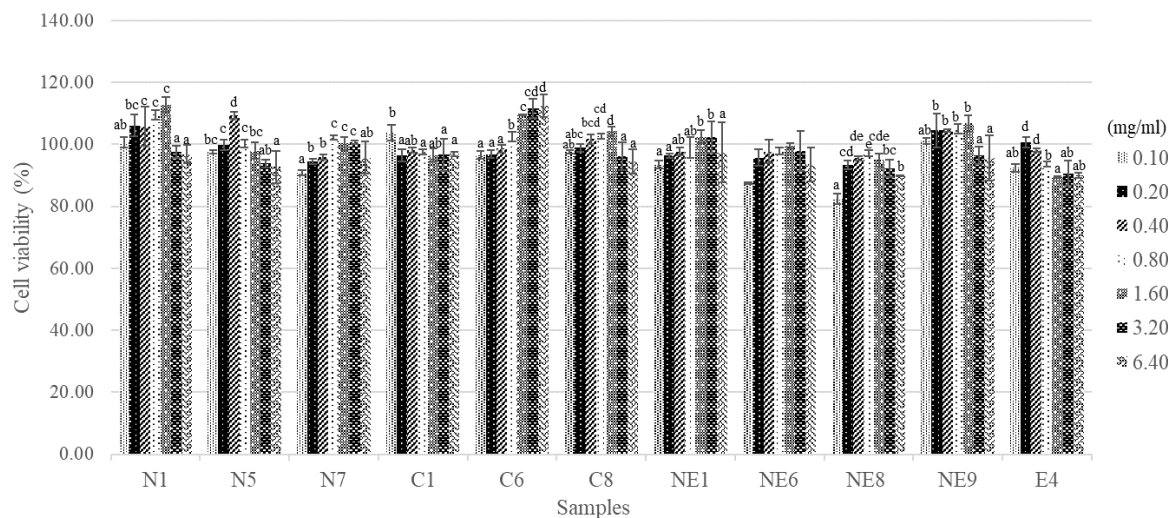
**Table 2** Phenolic and flavonoid profile of sugarcane molasses

Standard	Quantity % mg
Gallic acid	$0.0288 \pm 0.0081$
Ferulic acid	$0.0064 \pm 0.0025$
Quercetin	$0.0229 \pm 0.0112$
Rutin	$0.0370 \pm 0.0049$

The phenolics and flavonoids was identified with HPLC technique, all standard was used the 18C column for stationary phase. Values are presented as the mean  $\pm$  SD.

The investigation, nevertheless, was only focused on the bacteria model. Therefore, it is important to promote the anti-inflammatory properties impact of decreased NO generation in raw 264.7 macrophage cell were utilized. This our studied are investigated on cell viability and anti-inflammation. The cytotoxicity after treated with SM at the concentration of 0.1 – 6.4 mg/ml were measured through MTT assay. Figure 2 showed that all samples exhibited the ability to significantly lower the viability of raw 264.7 cells when SM was found in concentrations of 3.4 and 6.4 mg/ml. Although this activity went with, raw 264.7 macrophage cells were not harmed by SM at concentrations of 0.1 to 1.6 mg/ml. However, it was found all of the samples at all concentrations were over 80% cell viability, indicating that SM was thought to have a safe, non-toxic effect on raw 264.7 cells. The effect of SM on LPS induced NO production in raw 264.7 macrophage cell was showed in figure 3 SM and table 3 indicated its IC<sub>50</sub>.

**Figure 2** Effect of SM on cell viability in Raw 264.7 macrophage cell. Cells were treated with



sugarcane molasses at the concentration of 0.1 – 6.4 mg/ml for 24 hr. Values are presented as the mean ± SD. <sup>a, b, c, d, e</sup> followed by different letters in each of samples are significantly difference (p < 0.05).

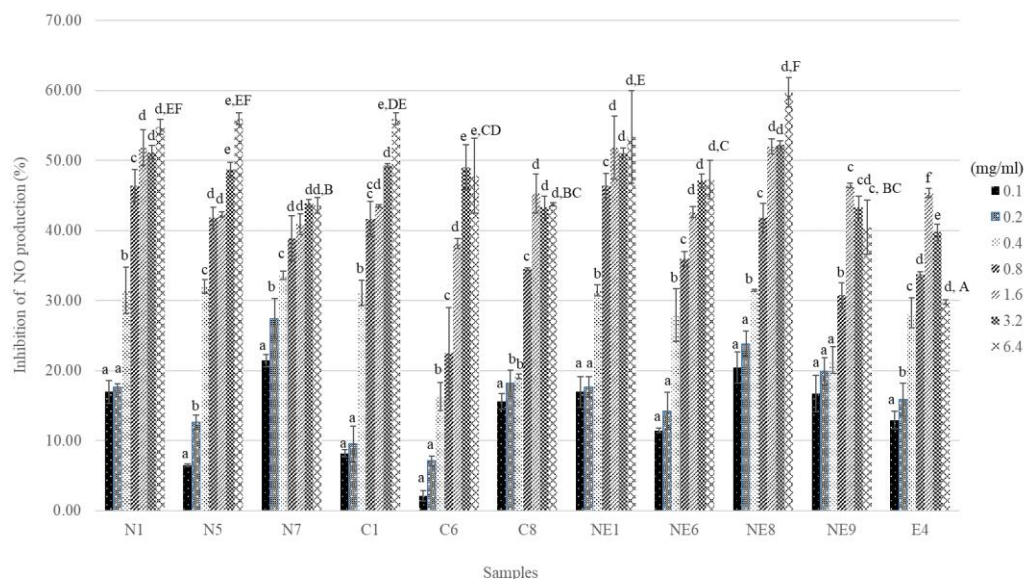


**Figure 3**  
Effect of SM on inhibition of NO production in Raw 264.7

macrophage cell. The LPS induced inflammatory at the concentration of 1  $\mu\text{g/ml}$ . Values are presented as the mean  $\pm$  SD. a, b, c, d, e followed by different letters in each of samples are significantly difference ( $p < 0.05$ ). A, B, C, D, E, F followed by different letters in each of samples at the highest of concentration of SM are significantly difference ( $p < 0.05$ ).

**Table 3** IC<sub>50</sub> value of sugarcane molasses in inhibition of NO production

Sample	IC <sub>50</sub> (mg/ml)
N1	4.03 $\pm$ 0.02
N5	4.33 $\pm$ 0.07
N7	> 6.40
C1	4.95 $\pm$ 0.01
C6	> 6.40
C8	> 6.40
NE1	4.13 $\pm$ 0.03
NE6	> 6.40
NE8	3.57 $\pm$ 0.07
NE9	> 6.40
E4	> 6.40

NO production was evaluated after LPS stimulation at a concentration of 1  $\mu\text{g/ml}$ , and SM was utilized as an inhibitor at a concentration of 0.1 - 6.4 mg/ml. At the highest SM concentration, the NE8 sample showed the highest inhibition of NO production, which was significantly different ( $p < 0.05$ ) from all other samples at 59.740.03%. IC<sub>50</sub> is 3.57 0.07 mg/ml. Through the synthesis of L-



arginine and the resulting inflammatory response in the mammalian immune system, LPS-induced macrophage cell stimulation enhanced NO overexpression. [21]. The NOS and COX synthesize NO, a mediator of the inflammatory response. When LPS was simulated, NO an inflammatory mediator was produced. [22]. Due to reports that flavonoids can reduce LPS-induced raw 264.7 cell via decreased NO, the beneficial biological compound can be used to prevent and treat diseases [23], this study found that rutin and quercetin were the richest flavonoid compounds, and that ferulic acid and gallic acid were the richest phenolic compounds. It also found that SM could decrease the LPS-stimulated inflammatory response on raw 264.7 macrophage cells. This finding was supported by other studies that identified phenolics and flavonoids as compounds that affect antioxidant activity. Oxidative stress, which is defined as an imbalance of increased reactive oxygen species generation, is a major contributor to several non-communicable conditions like inflammation. [24] Quercetin shows the potential to control inflammation and can decrease LPS-induced inflammation in cultured 264.7 macrophage cells, and its phenolic compounds exhibit antioxidant capacity. [25], recent research on rutin at amounts that ranged from 5 to 100  $\mu$ M all showed inhibitory effects on the production of NO in raw 264.7 macrophage cells when stimulated with LPS [26].

#### 4. CONCLUSIONS

It is probable that because this study revealed a favorable correlation with rutin antioxidant properties and a decrease of oxidative stress and NO generation, the phenolic compounds in molasses could promote the change of residues into useful molecule.

#### 5. ACKNOWLEDGEMENT

Thanks to all the advisors for their technical guidance and thorough review of the manuscript. This research is funded by the graduate school fellowship program in Agriculture and Agro-Industry from the Agricultural Research Development Agency (Public Organization) as fiscal year 2022

#### 6. REFERENCES

- [1] Zhang, K., Ding, Z., Mo, M., Duan, W., Bi, Y., and Kong, F. (2020). Essential Oils from Sugarcane Molasses: Chemical Composition, Optimization of Microwave Assisted Hydrodistillation by Response Surface Methodology and Evaluation of its Antioxidant and Antibacterial Activities. *Industrial Crops & Products*. 156: 112875.
- [2] Acosta-Piantini, E., Rodríguez-Díez, E., Chavarri, M., and López-de-Armentia, I. (2023). Preparation of Hydrolyzed Sugarcane Molasses as a Low-Cost Medium for the Mass Production of Probiotic *Lactobacillus paracasei ssp. paracasei* F19. *Separations*. 10: pp 33, Doi: <https://doi.org/10.3390/separations10010033>.
- [3] M. Carmen Villaran 3 and José Ignacio Lombraña Utilization of Molasses and Sugar Cane Bagasse for Production of Fungal Invertase in Solid state Fermentation using *Aspergillus niger* GH1. *Brazilian Journal of Microbiology*. 45(2): pp. 373 – 377.
- [4] Palmonari, A., Cavallini, D., Sniffen, C. J., Fernandes, L., Holder, P., Fagioli, L., Fusaro, I., Biagi, G., Formigoni, A., and Mamm, L. (2020). Short Communication: Characterization of Molasses Chemical Composition. *American Dairy Science Association*. 103: pp. 6244 – 6249.
- [5] Ali, B.; Qureshi, L.A.; Shah, S.H.A.; Rehman, S.U.; Hussain, I.; Iqbal, M. A Step Towards Durable, Ductile and Sustainable Concrete: Simultaneous Incorporation of Recycled Aggregates, Glass Fiber and Fly Ash. *Construction and Building Materials*. 251: 118980, Doi: <https://doi.org/10.1016/j.conbuildmat.2020.118980>.
- [6] Sineli, P.E., Maza, D.D., Aybar, M.J., Figueroa, L.I.C., and Vinarta, C.S. (2022). Bioconversion of Sugarcane Molasses and Waste Glycerol on Single Cell Oils for Biodiesel by the Red yeast *Rhodotorula glutinis* R4 from Antarctica. *Energy Conversion and Management*: X. 16: 100331.
- [7] Palmonari, A., Cavallini, D., Sniffen, C. J., Fernandes, L., Holder, P., Fagioli, L., Fusaro, I., Biagi, G., Formigoni, A., and Mamm, L. (2020). Short Communication: Characterization of Molasses Chemical Composition. *American Dairy Science Association*. 103: pp. 6244 – 6249.

- [8] Deseo, M.D., Elkins, A., Rochfort, S., and Kitchen, B. (2020). Antioxidant Activity and Polyphenol Composition of Sugarcane Molasses Extract. *Food Chemistry*. 314: pp. 126280, Doi: <https://doi.org/10.1016/j.foodchem.2020.126180>.
- [9] Esteban-Muñoz, A., Sánchez-Hernández, S., Samaniego-Sánchez, C., Giménez-Martínez, R., and Olalla-Herrera, M. (2021). Differences in the Phenolic Profile by UPLC Coupled to High Resolution Mass Spectrometry and Antioxidant Capacity of Two Diospyros kaki Varieties. *Antioxidants*.10(1): pp. 31, Doi: <https://doi.org/10.3390/antiox10010031>.
- [10] Deseo, M.D., Elkins, A., Rochfort, S., and Kitchen, B. (2020). Antioxidant Activity and Polyphenol Composition of Sugarcane Molasses Extract. *Food Chemistry*. 314: pp. 126280, Doi: <https://doi.org/10.1016/j.foodchem.2020.126180>.
- [11] Cheng, Y., Yu, Y., Wang, C., Zhu, Z., and Huang, M. (2021). Inhibitory Effect of Sugarcane (*Saccharum officinarum* L.) Molasses Extract on the Formation of Heterocyclic Amines in Deep-Fried Chicken Wings. *Food Control*. 119: pp. 107490.
- [12] Shafiqah-Atikah, M.K., Nor-Khaizura, M.A.R., Mahyudin, N.A., Abas, F. Nur-Syifa', J. and Ummul-Izzatul, Y. (2020). Evaluation of Phenolic Constituent, Antioxidant and Antibacterial Activities of Sugarcane Molasses Towards Foodborne Pathogens. *Food Research*. 4 (2): pp. 40 – 47.
- [13] Guan, Y., Tang, Q., Fu, X., Yu, S., Wu, S., and Chen, S. (2014). Preparation of Antioxidants from Sugarcane Molasses. *Food Chemistry*. 152: pp. 552 – 557.
- [14] Shalabi, O.M.A.K. (2022). Antioxidant, Antibacterial, and Antitumor Activities of Goat's Stirred Yoghurt Fortified with Carob Molasses. *Annals of Agricultural Sciences*. 67: pp. 119 – 126.
- [15] Mohd Khairul, S. A., Mahyudin, N. I., Abas, F., Jamaludin, N., and Mahmud AB Rashid, N. (2022). The Proximate Composition and Metabolite Profiling of Sugarcane (*Saccharum officinarum*) Molasses. *Malaysian Applied Biology*. 51(2): pp. 63 – 68.
- [16] Ogunwole, E., Kunle-Alabia, O, T., Akindele, O, O., and Rajia, Y. (2020). *Saccharum officinarum* Molasses Adversely Alters Reproductive Functions in Male Wistar Rats. *Toxicology Reports*. 7: pp. 345 – 352.
- [17] Hess, T. M., Sumberg, J., Biggs, T., Georgescu, M., Haro-Monteagudo, D., Jewitt, G., Ozdogan, M., Marshall, M., Thenkabail, P., Daccache, A. & Marin, F. (2016). A sweet deal? Sugarcane, Water and Agricultural Transformation in Sub-Saharan Africa. *Global Environmental Change*, 39: pp. 181 – 194.
- [18] Afify, A.S., Abdalla, A.A., Elsayed, A., Gamuhay, B., Abu-Khadra, A.S., Hassan, M. & Mohamed, A. (2017). Survey on the Moisture and Ash Contents in Agricultural Commodities in Al-Rass Governorate, Saudi Arabia in 2017. *Assiut Journal of Agricultural Sciences*, 48(6): pp. 55 – 62.
- [19] Deseo, M.D., Elkins, A., Rochfort, S., and Kitchen, B. (2020). Antioxidant Activity and Polyphenol Composition of Sugarcane Molasses Extract. *Food Chemistry*. 314: pp. 126280, Doi: <https://doi.org/10.1016/j.foodchem.2020.126180>.
- [20] Wang, Z., Wang, Q., Liu, S., Liu, X, F., Yu, X., and Jiang, Y, L. (2019). Efficient conversion of cane molasses towards high-purity isomaltulose and cellular lipid using an engineered *yarrowia lipolytica* strain in fed-batch fermentation. *Molecules*. 24: pp. 1228.
- [21] Baek, S., Park, T., Kang, M., and Park, D. (2020). Anti-Inflammatory Activity and ROS Regulation Effect of Sinapaldehyde in LPS-Stimulated RAW 264.7 Macrophages. *Molecules*. 25(18): pp. 4089, Doi: <http://dx.doi.org/10.3390/molecules25184089>.
- [22] Jang, M., Hwang, I., Hwang, B., and Kim, G. (2020). Anti-inflammatory Effect of *Antirrhinum majus* Extract in Lipopolysaccharide-stimulated RAW 264.7 macrophages. *Food Science and Nutrition*. 8: pp. 5063 – 5070.
- [23] Li, Y., Hao, N., Zou, S., Meng, T., Tao, H., Ming, P., Li, M., Ding, H., Li, J., Feng, S., Wang, X., and Wu, J. (2018). Immune Regulation of RAW264.7 Cells In Vitro by Flavonoids from *Astragalus complanatus* via Activating the NF-KB Signalling Pathway. *Journal of Immunology Research*. 7948068: pp. 9, Doi: <https://doi.org/10.1155/2018/7948068>.
- [24] Hong, S., Pangloli, P., Perumal, R., Cox, S., Noronha, L.E., Dia, V.P., and Smolensky, D. (2020). A Comparative Study on Phenolic Content, Antioxidant Activity and Anti-Inflammatory Capacity of Aqueous and Ethanolic Extracts of Sorghum in Lipopolysaccharide-Induced RAW 264.7 Macrophages. 9(12): pp. 1297, Doi: <https://doi.org/10.3390/antiox9121297>.
- [25] Ruangnoo, S., Jaiaree, N., Makchuchit, S., Panthong, S., Thongdeeying, P., and Itharat, A. (2012). An in vitro inhibitory effect on RAW 264.7 cells by antiinflammatory compounds from *Smilax corbularia* Kunth. *Asian Pacific J Allergy Immunology*. 30: pp. 268 – 274.
- [26] Tian, Y., Wei, C., He, J., Yan, Y., Pang, N., Fang, X., Liang, X., Fu, J. (2021). Superresolution Characterization of Core Centriole Architecture. *Journal of Cell Biology*. 220(4): e202005103, Doi: <http://dx.doi.org/10.1083/jcb.202005103>.

## Development of a low-cost cultivation medium for an industrial-scale spore production of *Priestia megaterium* RS91

Chaipat Chaemsuwankul<sup>1</sup>, Kanchalee Jetiyanon<sup>2</sup>, Peerada Prommeenate<sup>3</sup>, Weerayuth Kittichotirat<sup>4</sup> and Thunyarat Pongtharangkul<sup>1,\*</sup>

<sup>1</sup>*Department of Biotechnology, Faculty of Science, Mahidol university, Bangkok, 10400, Thailand.*

<sup>2</sup>*Department of Agricultural Science, Faculty of Agriculture, Natural Resources and Environment, Naresuan University, Phitsanulok, 65000, Thailand.*

<sup>3</sup>*Biochemical Engineering and Pilot Plant Research and Development Unit, National Center for Genetic Engineering and Biotechnology at King Mongkut's University of Technology Thonburi, Bangkok, 10150, Thailand.*

<sup>4</sup>*Systems Biology and Bioinformatics Research Group, Pilot Plant Development and Training Institute, King Mongkut's University of Technology Thonburi, Bangkok, 10150 Thailand.*

**\*Correspondence to:** *Department of Biotechnology, Faculty of Science, Mahidol University, Bangkok, 10400, Thailand. E-mail: thunyarat.pon@mahidol.edu*

**ABSTRACT:** The application of beneficial bacteria, such as Plant Growth-Promoting Rhizobacteria (PGPR), has shown immense potential in both plant growth enhancement and plant disease suppression. *Priestia megaterium* (formerly known as *Bacillus megaterium*) RS91 has been recognized as a highly efficient PGPR strain with several beneficial characteristics to plant including production of indole-3-acetic acid (IAA) and siderophore, as well as its ability to solubilize phosphate and fix nitrogen. Spores of RS91 can be formulated into a biofertilizer applicable for various plant varieties. Our research focuses on harnessing the potential of this bacterium in agriculture by developing a cost-effective cultivation medium suitable for commercial-scale spore production. To achieve this objective, we optimized the medium compositions and cultivation condition to maximize productivity while reducing the production cost. The newly developed medium 'omCCY91N' (3.59 THB/L) gave an average maximum spore count of  $8.8 \times 10^8$  spores/mL within 24 h in flask-scale cultivation. In a bioreactor-scale, cultivation of RS91 using omCCY91N did not require pH adjustment and gave an average maximum spore count of  $6.8 \times 10^8$  spores/mL within 18 h. The obtained spores were used for production of RS91 granular biofertilizer. The RS91 granular biofertilizer was stable and active for more than 6 months when stored in dry condition out of sunlight at a temperature of 37°C (a common on-farm storage condition for chemical fertilizers).

**Keyword:** PGPR, biofertilizer, rhizobacteria

## Inhibition of *C. gloeosporioides* growth using lemongrass crude extracts combined with pullulan film

Wanaree Suwannatrai<sup>1,2</sup>, Wichanee Bankeeree<sup>1,2</sup>, Kanogwan Seraypheap<sup>1,3</sup>  
and Sehanat Prasongsuk<sup>1,2\*</sup>

<sup>1</sup>Program in Biotechnology, Faculty of Science, Chulalongkorn University, Bangkok 10330, Thailand

<sup>2</sup>Plant Biomass Utilization Research Unit, Department of Botany, Faculty of Science, Chulalongkorn University, Bangkok 10330, Thailand

<sup>3</sup>Center of Excellence in Environment and Plant Physiology, Department of Botany, Faculty of Science, Chulalongkorn University, Bangkok 10330, Thailand

\*Corresponding Author: Plant Biomass Utilization Research Unit, Department of Botany, Faculty of Science, Chulalongkorn University, Bangkok 10330, Thailand E-mail: Sehanat.p@chula.ac.th

**ABSTRACT:** *Colletotrichum gloeosporioides* is the causative fungus of anthracnose, a post-harvest diseases in important fruits, leading to rapid fruit decay and shortened shelf life. While most farmers resort to chemical agents due to their convenience, speed, and high efficiency in controlling anthracnose, this practice has led to the accumulation of chemical residues in fruits and vegetables, posing a risk to consumers. This study focuses on inhibiting the growth of the *C. gloeosporioides* by utilizing herb extracts from lemongrass. Crude extract lemongrass of 1 g. was extracted by Soxhlet extraction that yielded crude extract for 140 mg. The investigation of the inhibitory effects of lemongrass crude extracts is conducted using the agar well diffusion method. The results show that a lemongrass extract with a concentration of 10 mg/ml dissolved in distilled water can effectively inhibit the growth of *C. gloeosporioides*. Subsequently, the minimum inhibitory concentration (MIC) of lemongrass crude extract against *C. gloeosporioides* was performed using the broth dilution method, revealing an MIC value of 2 mg/ml. In an effort to develop innovative surface coating, a biodegradable film was prepared by blending 3% (w/v) pullulan with lemongrass crude extract (6 mg/mL). This film exhibits promising inhibitory potential, leading to a 50% inhibition in the growth of *C. gloeosporioides*. Consequently, the utilization of lemongrass crude extracts with pullulan to form the film is a potentially promising strategy for inhibiting the growth of *C. gloeosporioides*, which can prevent post-harvest diseases of fruits and vegetables.

**Keyword:** *C. gloeosporioides*, Minimum inhibitory concentration, Crude extract, Pullulan film

## 1. INTRODUCTION

Fungi in the *Colletotrichum* sp., particularly *C. gloeosporioides*, are the causes of anthracnose, a post-harvest disease in important fruits such as mangoes, papayas, and sweet bananas, as well as various vegetables. This disease initially manifests as small black spots that progressively expand as the fruit ripens, eventually forming dark brown lesions. These conditions resulted in a reduced shelf life, compromised product quality, and an increased susceptibility to decay. Additionally, anthracnose can lead to shortened storage periods, affecting both domestic and international trade. [1] Consequently, farmers have increasingly relied on chemical agents for disease management [2]. The use of chemical agents has become a popular and expedient method for controlling plant diseases, often outperforming other approaches. However, the use of chemical agents has raised concerns due to the presence of pesticide residues exceeding the codex maximum residue limit value in vegetables and fruits. For instance, excessive residues of Mancozeb have been detected [3] highlighting the adverse effects of chemical control.

The utilization of plant extracts offers an alternative avenue and reduces chemical usage while effectively managing fungal diseases [4]. Numerous studies have investigated methods to extend the shelf life of fruits while inhibiting the growth of *Colletotrichum* sp. Plant extracts from widely accessible and cost-effective herbs such as ginger (*Zingiber officinale* Rosc.), galangal (*Alpinia galanga* Swartz.), lemongrass (*Cymbopogon citratus* Stapf.), garlic (*Allium sativum* L.), and betel leaf (*Piper chaba* Vahl.) have been considered as potential antifungal agents. These extracts exhibit the capability to inhibit *C. gloeosporioides* spore growth, with inhibition rates exceeding 80-100% in nutrient media [5]. The efficiency of these herbal extracts in combination with the bioactive polymer, pullulan produced from *Aureobasidium pullulans*, has been studied for surface coating of fruits to maintain their quality and freshness [6]. The reason behind is that pullulan is a versatile and non-toxic polymer with no color, odor, or taste [7]. It is commonly used in various industries including food film coating, food additives, cosmetics, and wound healing. [8] found that coating blueberries with pullulan preserved their freshness, weight, and sugar content by mitigating respiration and moisture loss. Additionally, coating apples with pullulan in combination with extracts from meadowsweet flowers, known for their antifungal and antibacterial properties, not only effectively controlled bacterial and fungal growth but also improved color retention and weight loss during storage.

Due to the advantages of herb extracts and pullulan, this work focuses on creating a pullulan film combined with lemongrass extracts that has the capacity to effectively inhibit the growth of *Colletotrichum* sp. These results provide valuable insights that could potentially be utilized in the future to impede fungi, especially *Colletotrichum* sp., in fruits or vegetables.

## 2. MATERIALS AND METHODS

### 2.1 Extraction of lemongrass crude

*Cymbopogon citratus* (lemongrass) leaves were obtained from local market [5] in Bangkok, Thailand. The sample was prepared by washing, cutting into small pieces, drying until a constant weight was reached, grinding, and then passing through a sieve. Subsequently, the sample powder was extracted using hot distilled water through a Soxhlet extraction at 60 °C for a duration of 3 hr, with a solid-to-liquid ratio of 1:20 (g/ml). Following extraction, the crude extract was filtrated through Whatman paper No.1 and concentrated using freeze-drying. The resulting crude extract was preserved under cryogenic condition at -20 °C, intended for further utilization in subsequent testing stages.

## 2.2 Agar well diffusion method

The spore germination inhibition test was conducted by utilizing the spore germination test method [9]. *C. gloeosporioides*, obtained from the Thailand Bioresource Research Center (TBRC), was cultured on potato dextrose agar (PDA) at room temperature for 14 days. This cultivation was carried out to generate spores for the preparation of a suspended spore solution at a density of  $1 \times 10^7$  spore/ml, as quantified using a hemacytometer. One hundred microliter of the spore solution was spread on a PDA plate and four wells (each of 0.5 cm diameter) were made on each PDA plate by a cork borer. Consequently, 100- $\mu$ l crude lemongrass extract solubilized in distilled water at concentrations of 10 and 20 mg/ml was added to the wells. The plates were incubated at room temperature ( $28 \pm 2^\circ\text{C}$ ) for 24 hr. Inhibition zones were subsequently observed and compared to a negative control utilizing distilled water and a positive control involving the fungicide Mancozeb 80% WP (Extraagro chemical LTD.), with a concentration of 0.16 mg/ml.

## 2.3 Determination of the half maximal inhibitory concentration (IC<sub>50</sub>) value

The crude lemongrass extract was prepared in the concentration range of 2 to 10 mg/ml by dissolving in distilled water. Each concentration (100  $\mu$ l) was then added into 20 ml of potato dextrose broth (PDB) containing a *C. gloeosporioides* spore density of  $1 \times 10^7$  CFU/ml. The inoculum was subjected to agitation at a speed of 150 rpm at room temperature for a duration of 16 hr. Subsequently, the growth of *C. gloeosporioides* was examined on PDA using the standard plate count technique. Incubation was conducted at room temperature for 16 hr, and the number of fungal colonies that developed on the agar was recorded. The percentage of growth inhibition was calculated using the following equation (1):

$$\text{Inhibition (\%)} = [(C-T)/C] \times 100 \quad (1)$$

where C and T are the number of fungal colonies in the negative control using distilled water and treatment, respectively. The assay was performed with triplicate and the positive control involved the use of fungicide Mancozeb 80% WP at a concentration of 0.16 mg/ml [3]. The IC<sub>50</sub> was calculated from the plots depicting the percentages of growth inhibition against the concentrations of the crude extract. The half maximal inhibitory concentration (IC<sub>50</sub>) was calculated using the following equation (2):

$$y = mx + c \quad (2)$$

where y is inhibition (in %), x is concentration (in mg/ml), c is the fitted constant value, and m is the slope of graph. Equation (2) can be obtained by fitting the plotted inhibition versus concentration. Consequently, the half maximal inhibitory concentration 50% or IC<sub>50</sub> can be determine by taking y = 50% in the fitted equation.

## 2.4 Formation of pullulan film containing lemongrass extract and its property in growth-inhibition of *C. gloeosporioides*

To preparing the film-forming solution, a 3% w/v pullulan solution (Hayashibara CO., LTD., Japan) was mixed with 0.2% v/v glycerol and crude lemongrass extract at a concentration capable of inhibiting *C. gloeosporioides* growth. Consequently, the solution was stirred with a magnetic bar until homogenous, poured into a film mold ( $15 \times 15 \text{ cm}^2$ ), and annealed for 24 hr. After that, the film was peeled and cut into circular shapes with a diameter of 10 Mm., then placed onto fungal culture plates. The inhibitory effects were compared against negative control plates that used distilled water as a negative control. The positive control plates were treated with the fungicide Mancozeb 80% WP at a concentration of 0.16 mg/ml. The experimental test was incubated at room temperature for 24 hr.

## 3. RESULTS AND DISCUSSION

### 3.1 Antifungal activity against *C. gloeosporioides* growth

In this study, the active compounds for using in fungal inhibition were extracted from lemongrass leaves using hot water through a Soxhlet apparatus. This technique offers several advantages that allows efficient yield extraction by continuously cycling the solvent through the sample and can effectively extract a wide range of bioactive compounds from plant materials. The yield of crude extract was determined to be 140 mg/g dry weight. It was found to be higher than those reported in previous studies of Khamklieng et al. [10] The yield of crude extract was determined to be 125 mg/g dry weight. Subsequently, the antifungal activity against *C. gloeosporioides* growth of the crude lemongrass extract was evaluated. It was observed that the a concentration of lemongrass extract as low as 10 mg/ml exhibited an inhibition zone in the growth of *C. gloeosporioides*, as shown in Fig. 1. The result was related with the report of Sutthisa et al. [11] that used 20 mg/ml.

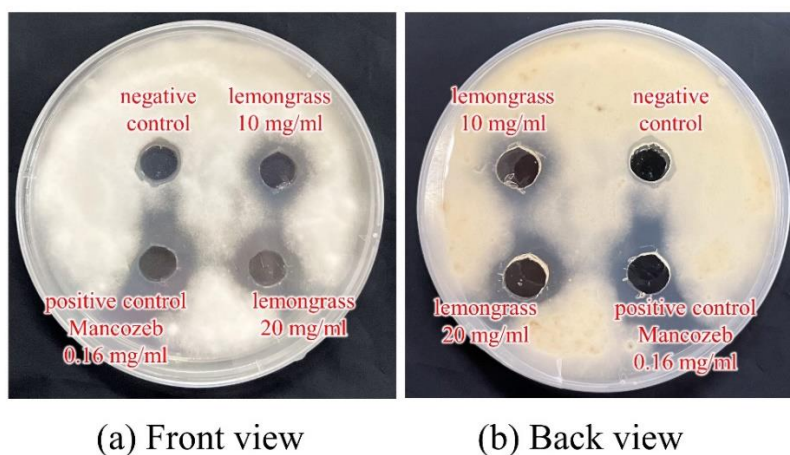


**Figure 1** (a) Front and (b) back view of inhibition zone of antifungal activity against *C. gloeosporioides* growth.

### 3.2 Determination of IC<sub>50</sub> value

The IC<sub>50</sub> value of the crude lemongrass extract with inhibitory effects against *C. gloeosporioides* growth was determined using the broth dilution method. As shown in Fig. 2, the minimum concentration of the lemongrass extract that continued to exhibit growth inhibition against *C. gloeosporioides* was 2 mg/ml. In addition, the calculated IC<sub>50</sub> value for the crude lemongrass extract was 6 mg/ml. This result was related with the previous study of Srinon et al. [5] that used 10 mg/ml. The concentration of crude extract at the IC<sub>50</sub> value was selected for subsequent incorporation into a pullulan film.

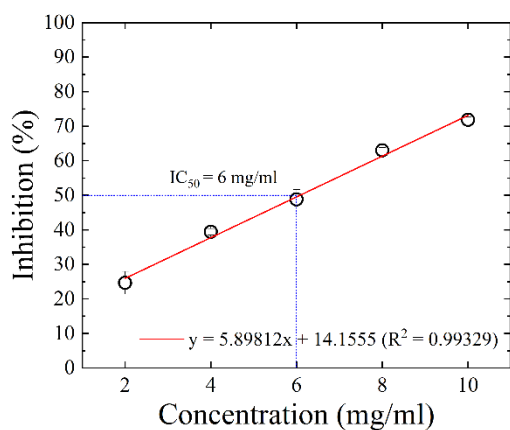


**Figure 2** Inhibition of *C. gloeosporioides* growth at versus concentration of crude lemongrass extract.

### 3.3 Pullulan film containing lemongrass extract and its property in growth-inhibition of *C. gloeosporioides*.

The biodegradable film was prepared by mixing 3% w/v pullulan with and without 6 mg/ml of crude lemongrass extract, while glycerol was used as a plasticizer in this study to enhance film flexibility. The antifungal activity of composite film against *C. gloeosporioides* was evaluated, and the results showed effective inhibition of *C. gloeosporioides* growth through the assessment of the inhibition zone, as illustrated in Fig. 3.

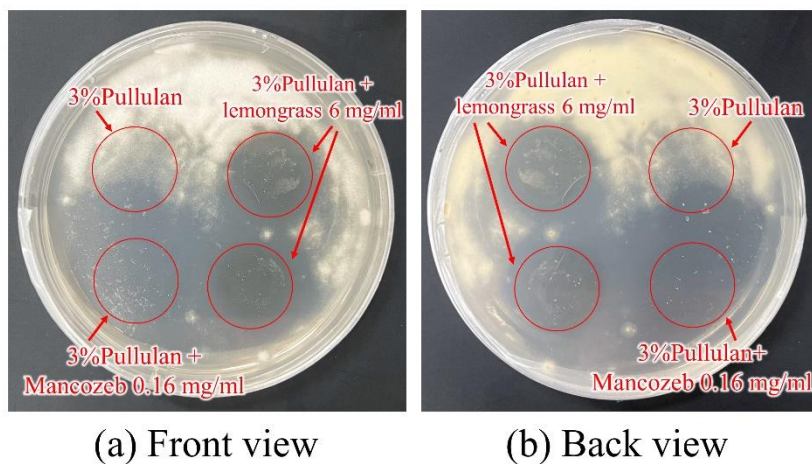


**Figure 3** (a) Front and (b) back view of inhibition zone of antifungal activity against *C. gloeosporioides* growth on pullulan film.

## 4. CONCLUSIONS

This study demonstrated the antifungal effectiveness of lemongrass crude extract against *C. gloeosporioides*, with a validated half maximal inhibitory concentration of 6 mg/ml. The presence of the extract in a pullulan film further substantiated its potency in inhibiting *C. gloeosporioides* growth. As such, this research emphasizes the potential of lemongrass extract, particularly when integrated into pullulan films, as a promising avenue for developing innovative surface coatings to combat post-harvest diseases in fruits and vegetables.



## 5. ACKNOWLEDGEMENT

This research was also supported by the Ratchadaphiseksomphot Endowment Fund from Chulalongkorn University.

## 6. REFERENCES

- [1] Ding, Z. S., Tian, S. P., Zheng, X. L., Zhou, Z. W., & Xu, Y. (2007). Responses of reactive oxygen metabolism and quality in mango fruit to exogenous oxalic acid or salicylic acid under chilling temperature stress. *Physiologia plantarum*, 130(1), pp. 112-121.
- [2] Meenakshi, S. & Saurabh, K. (2015). *Colletotrichum gloeosporioides*: An Anthracnose Causing Pathogen of Fruits and Vegetables. *Biosciences Biotechnology Research ASIA*, 12(2), pp. 1233-1246, DOI: 10.13005/bbra/1776
- [3] Nining, E., Sjarief, R., Mas' ud, Z. A., Sobir, S., & Machfud, M. (2020). Analysis of mancozeb and carbofuran pesticides residues in the production area of shallot (*Allium cepa* L. Var. *ascalonicum*). *Bulgarian Journal of Agricultural Science*, 26(5) pp. 974–981
- [4] Elaissi, A., Rouis, Z., Salem, N.A., Mabrouk, S., Bensalem, Y. & Salah, K.B. (2012). Chemical composition of 8 eucalyptus species essential oils and the evaluation of their antibacterial, antifungal and antiviral activities. *BMC Complementary Alternative Medicine*, 26 (5) pp. 974–981, DOI: 10.1186/1472-6882-12-81.
- [5] Srinon, W., Wuntid, T. and Soyong, K. (2009). Antifungal activities from Different Solvent Extracts of Medicinal Plants Against *Colletotrichum gloeosporioides* (Penz.) Causal Organism of Mango Anthracnose. In *Proceedings of Agricultural Sci. J.* pp. 75-78. January- April, 2009, Thailand
- [6] Leathers, T. D. (2003). Biotechnological production and applications of pullulan. *Applied microbiology and biotechnology*, 6(2) pp. 468-473. DOI 10.1007/s10295-002-0016-y
- [7] Yuen, S. (1974). Pullulan and its applications. *Process biochemistry*.
- [8] Kwasniewski, K., Cibisz, I., Gniewosz, M., Mitek, M., Pobiega, K., & Cendrowski, A. (2017). Effect of pullulan coating on postharvest quality and shelf-life of highbush blueberry (*Vaccinium corymbosum* L.). *Materials*, 10(8) pp. 965. DOI:10.3390/ma10080965
- [9] Jino, S., Chairat, S., Supakitthanakarn, S., and Ruangwong, O. (2022). *In vitro* efficiency of *Bacillus subtilis* S93 and *Bacillus siamensis* RFCD306 in controlling *Fusarium oxysporum* causing chrysanthemum wilt disease. In *Proceedings of Khon kaen agriculture jurnal.* pp. 1. 2022, Thailand
- [10] Khamklieng, U., Koonjaturut, A., Bundidpiboon, H., and Poomtien, J. (2021). Biofilm coating from garlic extracts plus biosurfactant against fungal pathogens on mangoes (Nam Dok Mai). In *Proceedings of Huachiew Chaiermprakiet Science and Technology Journal.* 113 pp. 1. January- June, 2021, Thailand
- [11] Sutthisa, W., Tapkhumram, P., Kanchanarat, W., and Arimastu P., (2014) Efficiency of Thai medicinal plant extract to control *Colletotrichum sp.*, a causal agent of mango anthracnose. In *Proceedings of Khon kaen AGR. J.* 42 pp. 1. 2014, Thailand

## Building a sustainable biomanufacturing business: solving human crises with bio-based solutions

Natthaporn Takpho

*Mojia Biotech, 048580, Singapore*

*\*Correspondence to: Mojia Biotech, 6 Raffles Quay #14-06, 048580, Singapore.  
Natt.t@mojiabio.com*

**ABSTRACT:** MojiaBio leads the biomanufacturing industry with a vision to create a sustainable future. Through cutting-edge advancements in genetic engineering, computational biology, and artificial intelligence, we develop transformative solutions that prioritize environmental sustainability. Our mission centers on pioneering green and economically viable biomanufacturing processes that rely on non-food sustainable feedstocks. With our innovative OrthBio™ platform, we overcome traditional biomanufacturing obstacles, streamlining production and optimizing carbon efficiency for cost-effective alternatives. At the core of MojiaBio's technology lies the proprietary C1+Bio™ platform, a pioneering game-changer that ensures exceptional environmental sustainability while delivering high-quality chemical products. The versatility and efficiency of the technology platform present a compelling alternative to conventional fermentation methods, delivering superior performance at a reduced cost. Our unwavering dedication to sustainability permeates every aspect of our operations. Through demand-driven innovation and global collaborations, we develop eco-friendly biomanufactured solutions, paving the way for a more sustainable future. Leveraging cutting-edge technology, our vision is to build a thriving society where renewable resources and energy-efficient processes coexist harmoniously, benefiting both humanity and the planet. Through the integration of OrthBio™ and the C1+Bio™ platforms, MojiaBio propels the biomanufacturing industry towards a greener and healthier tomorrow.

**Keyword:** Biomanufacturing technology, sustainability, green solutions, transformative innovation

## Characterization of flavin-containing Monooxygenase (FMO) from *Microbacterium esteraromaticum* SBS1-7

**Sathita Meeasa<sup>1</sup>, Wirakorn Pimpasida<sup>2</sup>, Peerada Prommeenat<sup>3</sup>, Weerayuth Kittichotirat<sup>4</sup> and Thunyarat Pongtharangkul<sup>1\*</sup>**

<sup>1</sup>*Department of Biotechnology, Faculty of Science, Mahidol University, Bangkok, 10400, Thailand.*

<sup>2</sup>*Bio-industrial Development Center, Mahidol University, Nakhon Pathom, 73170, Thailand.*

<sup>3</sup>*Biochemical Engineering and Pilot Plant Research and Development Unit, National Center for Genetic Engineering and Biotechnology at King Mongkut's University of Technology Thonburi, Bangkok, 10150, Thailand.*

<sup>4</sup>*Systems Biology and Bioinformatics Research Group, Pilot Plant Development and Training Institute, King Mongkut's University of Technology Thonburi, Bangkok, 10150 Thailand.*

**\*Correspondence to:** *Department of Biotechnology, Faculty of Science, Mahidol University, Bangkok, 10400, Thailand. E-mail: thunyarat.pon@mahidol.edu*

**ABSTRACT:** Flavin-containing monooxygenases (FMOs) can catalyze the oxygenation reaction by adding an oxygen atom to nucleophilic heteroatom-containing compounds such as nucleophilic S, N, O, and Se atom. Most FMOs are typically found in Eukaryotes, with fewer reports of their presence in Prokaryotes. This study focused on the type I FMO recently discovered in a BTEX-degrading bacterium *Microbacterium esteraromaticum* SBS1-7. Based on the sequence retrieved from the genome of SBS1-7, the codon optimized gene was successfully cloned and expressed in *E. coli* BL21 DE (3) with a high level of expression. The purified enzyme was evaluated for S-oxidation and N-oxidation using various types of substrates. The results were compared with those of their counterparts in eukaryotes. Further research is needed to uncover the diversity and functional significance of FMOs in prokaryotic organisms, as well as their potential roles in metabolism, adaptation, and other cellular processes.

**Keyword:** Type I FMOs, *Microbacterium* sp.

# Influence of culture media on biomass production and pigments of the freshwater alga *Chaetophora* sp. (Chlorophyta)

Narin Chansawang<sup>1\*</sup> and Benjawan Praprai<sup>1</sup>

<sup>1</sup>*Biodiversity Research Centre, Thailand Institute of Scientific and Technological Research, Pathum Thani 12120 THAILAND*

*\*Correspondence to: Biodiversity Research Centre, Thailand Institute of Scientific and Technological Research, Pathum Thani 12120 THAILAND. E-mail narin\_c@tistr.or.th*

**ABSTRACT** : Continuous progress in the fields of industrial biotechnology and agro-industrial wastewater treatment necessitates the development of new formulations of growing media based on novel sources of nutrients. The production of biomass, productivity, sustainability, and minimal environmental impact in the new formulations are essential, as well as ensuring the sustainability and minimal impact of their respective sources. The purpose of this study was to investigate the batch autotrophic growth of the fresh water alga *Chaetophora* sp. TISTR 9454 in the carboy photobioreactor that was grown in 4 different media. The results showed that after 6 days of incubation, the final algal biomass was higher in the urea+M medium ( $0.34 \pm 0.06$  g/L) than urea medium ( $0.31 \pm 0.03$  g/L). However, this difference was not statistically significant ( $p < 0.05$ ). Additionally, the highest algal biomass was found in BG-11+N ( $0.24 \pm 0.01$  g/L) and followed by NPM medium ( $0.21 \pm 0.03$  g/L). The highest aerial productivity was observed in the NPM medium, approximately  $27.37 \pm 5.37$  gDW/m<sup>2</sup>, followed by Urea+M ( $24.59 \pm 2.70$  gDW/m<sup>2</sup>), BG-11+N ( $19.30 \pm 0.40$  gDW/m<sup>2</sup>), and Urea ( $16.59 \pm 3.00$  gDW/m<sup>2</sup>). The pigments chlorophyll *a*, *b*, and total carotenoids were detected in the algal cells. The NPM medium exhibited the highest chlorophyll *a* level, productivity, and dry matter, approximately  $23.14 \pm 2.92$  mg/L,  $460.74 \pm 58.15$  mg/L/m<sup>2</sup>, and  $13.71 \pm 2.67\%$ , respectively. The NPM medium could be the best media and a cost-effective substitute for the BG-11+N medium (general media) and all so is suitable for the rapid growth of alga *Chaetophora*. Additionally, this medium can be easily prepared.

**Keyword:** Biomass, *Chaetophora* sp., freshwater alga, medium, pigment

## 1. INTRODUCTION

Algae are a diverse group of eukaryotic photosynthetic cells that can grow prolifically due to their simple structure. Their photosynthetic mechanism is similar to that of land plants, allowing efficient access to carbon source (CO<sub>2</sub>), water, and nutrients (mainly nitrogen and phosphorous) as well as light. Some algae species can utilize waste organic sources, such as brewery, food, municipal, and agro-industrial wastewater, as a carbon source through heterotrophic metabolism [1-2]. One of the essential requirements for algae growth is nutrients, which can be costly to produce due to the use of natural resources and energy. By optimizing the nutrients needed for algae growth, their production costs can be reduced, leading to a significant improvement in the economy of downstream processes.

Algae can be used in biosorption [3-4], whereby the cell wall plays a key role in metal binding [5-6]. This is due to the presence of groups in the cell wall polysaccharides or mucilage of algae that can act as binding sites for metals. Green algae have a cell wall matrix containing complex

heteropolysaccharides, which offer sulphate and carboxyl groups. Moreover, green algae are composed mainly of cellulose, with a high percentage of proteins (10-70%) bonded to polysaccharides, forming glycoproteins [7-8]. Biosorption refers to the rapid phenomenon of passive metal sequestration by the non-growing biomass/adsorbents [9]. It utilizes the ability of biological materials to accumulate heavy metals from water through physical-chemical pathways of uptake or metabolically mediated processes [10]. The complexation of elements in aqueous solutions depends on the concentration of functional groups and elements [3, 5-6].

*Chaetophora* is a large freshwater alga that exists in filamentous branching forms. Sometimes, it forms elongated or irregularly shaped clusters of internal cells with two-pointed branched filaments. These branched filaments are wrapped in soft or firm mucilage, forming macroscopic growths that appear spherical, hemispherical, tubercular, or shrub-like [11]. *Chaetophora* can be observed with the naked eye, resembling a piece of jelly, due to the mucus composed of macromolecule carbohydrate compounds or polysaccharides, which retain moisture for the cells and act as a viscosity agent [12]. It plays a vital role in ecosystems as it produces oxygen and serves as a primary producer in the freshwater food chain. *Chaetophora* can also be utilized to reduce contamination in wastewater, making it an environmentally friendly technique [13].

*Chaetophora* usually grows in water bodies such as flat water, canals, rivers, lakes and rice paddies. There are a few reports of growing this alga in the laboratory. In the development of biomass production, one of the major factors is selecting a suitable growth medium. The purpose of this research was to compare the efficacy of four different media on the growth of the alga *Chaetophora* sp. TISTR 9454. The media effect study was conducted to verify the suitability of the growth media suggested by the supplier for growing the alga *Chaetophora* sp. TISTR 9454. Since this growth media was a generalized nutrient formula (BG-11), specific nutrient compositions were obtained by evaluating the influence of the overall media concentration and comparing it with urea, a commercial fertilizer known for being a sustainable and cost-effective alternative nitrogen source. Algal cell growth was evaluated through biomass productivity.

## 2. MATERIALS AND METHODS

### Preparation of algal sample

*Chaetoceros* sp. TISTR 9454 received from Algal Excellent Center of Thailand Institute of Scientific and Technological Research. Cells were cultured in liquid medium BG-11 [14] in a 500 mL flask containing 150 mL medium with a light intensity of  $50 \pm 10 \mu\text{mol photons/m}^2\text{s}^{-1}$ , temperature  $28 \pm 1^\circ\text{C}$ , shaken continuously for 24 hours with a shaker at 100 rpm, cultured for 3-4 days, then inoculum was expanded to increase the volume by culturing algae in 10 liters carboys with working volume of 7 liters.

### Preparation of culture medium and cultivation

The experimental procedures were carried out utilizing transparent 5 liters capacity polyethylene terephthalate (PET) bottles. Each bottle was loaded with 4 liters of distinct culture media types (Table 1). The preparation of these media was performed meticulously, with each media being individually in the three PET bottles separately. The algal *Chaetophora* (10%) was inoculated in BG-11, NPM ( $\text{NaNO}_3 + \text{K}_2\text{HPO}_4 + \text{MgSO}_4 \cdot 7\text{H}_2\text{O}$ ), Urea, and UM (urea+  $\text{MgSO}_4 \cdot 7\text{H}_2\text{O}$ ). The culture was incubated for 6 days at  $28 \pm 1^\circ\text{C}$  and illuminated with cool white inflorescence lamps (POWER MAX, 4000K) at an intensity of  $50 \pm 10 \mu\text{mol photons/m}^2\text{s}^{-1}$  in a

12: 12 h light dark regime. The PET bottles were cotton plugged and gently air bubble through a sterile 0.2-micron filter for 24 h.

### Biomass harvesting

Algal cells were filtered with a 35-micron plankton net, rinsed with sterile distilled water 2-3 times, and then the samples were incubated at 50°C until dry. The dried algae are cooled down within a desiccator and then re-weighed. Essential metrics for analyzing the trials, including biomass yield, dry matter (%), moisture content (%), and aerial productivity, are calculated.

Biomass yield (mg/L) = Dry weight (mg)/Liter (L)

% Dry matter = [Dry sample weight (mg)/Wet sample weight (mg)] x100

% Moisture content = [Wet sample weight (mg)-Dry sample weight (mg)/Wet sample weight (mg)] x100

Aerial productivity= Biomass yield (mg/L)/Cultivation area (m<sup>2</sup>)

Table 1. Comparison of composition of media for growing of *Chaetophora* sp.

Composition	Recipe 1) BG-11+N	Recipe 2) NPM	Recipe 3) Urea	Recipe 4) Urea+M
NaNO <sub>3</sub> (g/L)	1.5	1.5		
NaCl (g/L)				
K <sub>2</sub> HPO <sub>4</sub> (g/L)		1.5		
K <sub>2</sub> HPO <sub>4</sub> •3H <sub>2</sub> O (g/L)	0.04			
Na <sub>2</sub> CO <sub>3</sub> (g/L)	0.02			
MgSO <sub>4</sub> •7H <sub>2</sub> O (g/L)	0.075	0.03		0.03
CaCl <sub>2</sub> (g/L)				
CaCl <sub>2</sub> •7H <sub>2</sub> O (g/L)	0.036			
Citric acid (g/L)	0.006			
Na <sub>2</sub> EDTA (g/L)	0.001			
Fe(SO <sub>4</sub> ) <sub>5</sub> •6H <sub>2</sub> O (g/L)				
Fe•Ammonium Citrate (g/L)	0.006			
CoCl <sub>2</sub> (mg/L)				
H <sub>3</sub> BO <sub>3</sub> (mg/L)	2.86			
MnCl <sub>2</sub> •4H <sub>2</sub> O (mg/L)	1.81			
MnSO <sub>4</sub> •4H <sub>2</sub> O (mg/L)				
ZnSO <sub>4</sub> •7H <sub>2</sub> O (mg/L)	0.222			
CuSO <sub>4</sub> •5H <sub>2</sub> O (mg/L)	0.0079			
Na <sub>2</sub> MoO <sub>4</sub> •2H <sub>2</sub> O (mg/L)	0.39			
Co(NO <sub>3</sub> ) <sub>2</sub> •6H <sub>2</sub> O (mg/L)	0.0494			
Urea (N:P:K=46:0:0) (g/L)			1.5	1.5
Approximately cost (US dollars/L)	0.028	0.013	0.019	0.024

N=Sodium nitrate, P= Dipotassium phosphate, M= Magnesium sulphate

### Pigment analysis

The dried algae powder (0.1 g) was mechanically disrupted using a homogenizer (IKA dispersion S18N-10G) at 8,000 rpm for 5 minutes in the presence of methanol (5 mL) as the extraction solvent. The experiment was conducted in a water bath to maintain the temperature of crude extract at 10±2 °C under dark condition since pigment is photosensitive. The extraction process was repeated, and each supernatant was pooled. Chlorophyll *a*, *b*, and total carotenoid content were determined using a spectrophotometer. The samples were placed in a glass cuvette and tested for the

absorption spectrum at 470, 652.4, and 665.2 nm. Measurements were performed in triplicate. Based on the absorption spectra, chlorophyll *a* and *b* content, as well as total carotenoid content, were determined according to the method described by Lichtenthaler and Buschmann [15]. The content of pigments was expressed as mg/L of extract and was calculated using the following equations:

$$\text{Chl } a = (16.72 \times A_{665.2}) - (9.16 \times A_{652.4})$$

$$\text{Chl } b = (34.09 \times A_{652.4}) - (15.28 \times A_{665.2})$$

$$\text{Total-Caro} = (1000 \times A_{470}) - (1.63 \times \text{Chl } a) - (104.96 \times \text{Chl } b) / 221$$

Where Chl *a*, Chl *b* are the concentrations of chlorophylls *a* and *b*; Total-Caro is the concentration of total carotenoids. The final concentration of values pigments was normalized to 1 L of cell and expressed in mg/L. The measurements were conducted in triplicate.

The chlorophyll *a* content per unit area or chlorophyll *a* (Chl *a*) productivity was estimated as following formula:

$$\text{Chlorophyll } a \text{ (Chl } a) \text{ productivity (mg/L/m}^2\text{)} = \text{Chl } a \text{ (mg/L)} / \text{cultivation area (m}^2\text{)}$$

### Statistical analysis

The experiential was performed with triplicate (n=3) and the data shows here are mean±standard error mean (SEM). The statistical analysis was done using IBM SPSS software version 19.0.

## 3. RESULTS AND DISCUSSION

### Growth of green algae

Green cell culture of *Chaetophora* sp. TISTR 9454 was prepared for optimized cultivation. Under our experimental conditions, *Chaetophora* was cultivated for 6 days using 4 different media to accumulate green biomass and estimate optimal growth. As we know, nitrogen can promote rapid algae growth and improve biomass yield and productivity, so sodium nitrate and urea were included in the medium for this study. At the end of the green phase cultivation, the highest final biomass of 0.34±0.06 gDW/L was observed in the Urea+M medium containing urea and magnesium (urea+MgSO<sub>4</sub>•7H<sub>2</sub>O), followed by the urea medium with a dry biomass of 0.31±0.03 gDW/L. However, this difference was not statistically significant (*p*<0.05). Moreover, algal biomass was found in BG-11+N (BG-11+NaNO<sub>3</sub>) and NPM medium (NaNO<sub>3</sub>+K<sub>2</sub>HPO<sub>4</sub>+MgSO<sub>4</sub>•7H<sub>2</sub>O) at approximately 0.24±0.01 gDW/L and 0.21±0.03 gDW/L, respectively (Figure 1A). The highest aerial productivity was observed in the NPM medium, around 27.37±5.37 gDW/m<sup>2</sup> (Figure 1B), followed by the UM medium (24.59±2.70 gDW/m<sup>2</sup>), BG-11+N (19.30±0.40 gDW/m<sup>2</sup>), and Urea (16.59±3.00 gDW/m<sup>2</sup>).

The NPM medium resulted in the highest dry matter biomass, approximately 13.71±2.67%, followed by Urea+M, BG-11+N, and Urea medium, which had approximately 12.32±1.34%, 9.68±0.21%, and 8.29±1.50%, respectively (Figure 2). In contrast, the NPM medium exhibited the lowest moisture content compared to the other three media. Most importantly, the feed price per liter of the NPM medium is the lowest at \$0.013 (Table 1). The results indicated a significant difference in dry biomass between the NPM medium and Urea+M medium, but no significant difference between BG-11+N and Urea medium. The results clearly show that the NPM medium can be a cost-effective substitute for the expensive BG-11+N medium. These results indicate that different sources of nitrogen may be important in structuring algal assemblages in environments with episodic nitrogen

supply. Similar results were observed in a study where the chlorophyte macroalgae *Ulva fenestrata* and *Enteromorpha intestinalis* were grown under various nutrient regimes in indoor semi-continuous and batch cultures [16]. Moreover, the natural alga *Cladophora vagabunda* from Waquoit Bay, Massachusetts, USA, grew well, possibly due to nitrogen (N) enrichment from anthropogenic inputs transported via groundwater [17]. The nitrogen sources responded well to enhance growth, but maximum growth was recorded for magnesium sulfate, indicating it as the favorable nitrogen source for the growth of the green alga *Chaetophora*. Nitrogen source and concentration in the growth media greatly influence algae biomass yield [18].

The NPM medium yielded higher algal biomass compared to BG-11+N, which contained trace metals. Similarly, Riley and Roth [19] reported that the concentrations of trace elements in algal cultures could be affected by the age and density of the culture. In a study conducted by Hayward [20] on the marine alga *Phaeodactylum tricorutum*, it was shown that the rapid initial uptake of iron and zinc decreased as cell numbers increased in a medium rich in these metals. The uptake of trace elements was not restricted to those with well-defined physiological functions.

The effects of magnesium on the dry biomass (dry weight; DW) of the green alga *Chaetophora* are shown in Figure 1B and 2A. Algal cells grew well in media containing magnesium (Mg) except urea. Its significance lies in its role as the central core of the chlorophyll molecule, which is a vital component responsible for photosynthesis in plant tissue. However, there have been few reports on the importance of magnesium in chlorophyll synthesis and the repercussions of its deficiency on plant growth [21]. Ishfaq et al. [22] reported that approximately 55% of arable lands in China are Mg-deficient and require subsidization of Mg fertilizers, especially in Mg-deficient regions. This can be beneficial in closing yield and quality gaps among different cultivated regions. Moreover, magnesium acts as an activator for key enzymes involved in various metabolic pathways. These enzymes include those responsible for DNA and RNA synthesis, nutrient absorption, and energy metabolism. Proper magnesium levels are necessary for maintaining optimal enzyme activity, facilitating efficient biochemical reactions that drive overall growth and development.

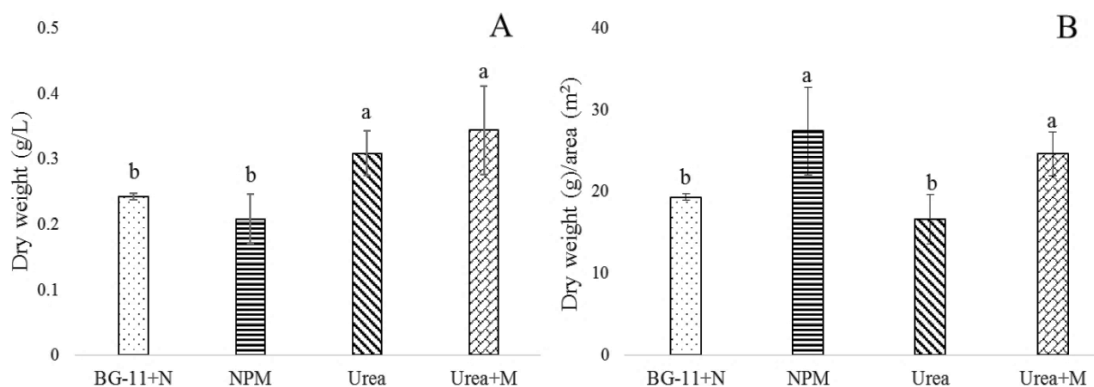


Figure 1. Biomass of *Chaetophora* sp. TISTR 9454 in unit gram dry weight per liter (A) and productivity in unit gram dry weight per area (B). The same letter is not significantly different.



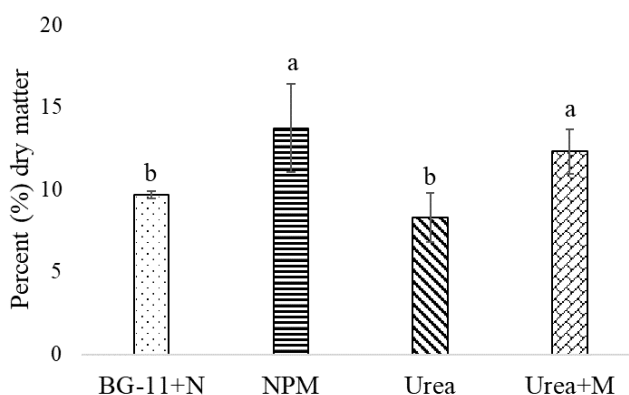


Figure 2. Percentage of dry algae *Cheaetophora* sp. TISTR 9454. The same letter is not significantly different.

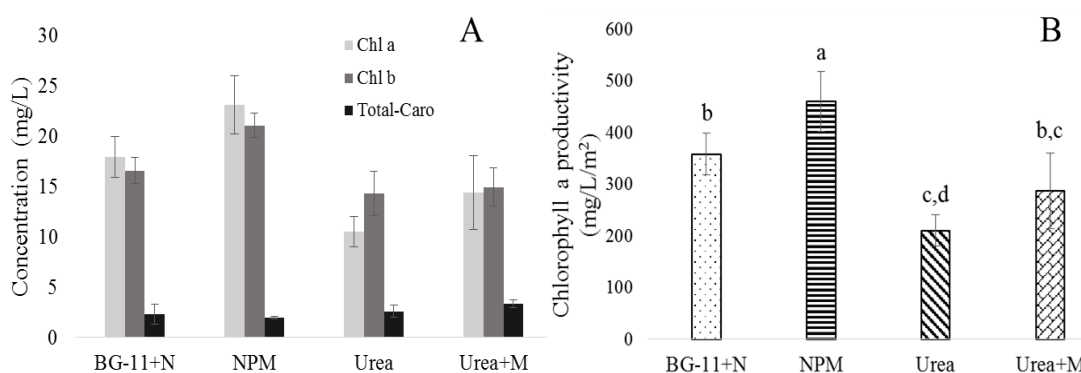


Figure 3. Pigments concentration of *Cheaetophora* sp. TISTR 9454 (A) and chlorophyll *a* productivity ( $\text{mg/L/m}^2$ ) (B). The same letter is not significantly different.

### Pigment content

*Chaetophora* sp. generally contains chlorophyll *a* (Chl *a*) and chlorophyll *b* (Chl *b*), which are responsible for its green color. The pigments chlorophyll *a*, *b*, and total carotenoids were found in algal cells. Based on Chl *a* content, Chl *a* is a reliable indicator for algal biomass. The NPM medium exhibited the highest levels of chlorophyll *a*, productivity, and dry matter (%DM), approximately  $23.14 \pm 2.92$  mg/L,  $460.74 \pm 58.15$  mg/L/m<sup>2</sup>, and  $13.71 \pm 2.67$  %DM, respectively (Figure 3 A-B, Figure 2). The algae *Chaetophora* grown in NPM and BG-11+N media containing 1.5 g/L NaNO<sub>3</sub> (Table 1.) exhibited higher chl *a* content compared to those grown in Urea and Urea+M media (Figure 3A). The chl *a* content (g/L) of algae cultivated in the NPM medium was approximately 2.19 times that of the chl *a* content from the urea medium, and around 1.60 times that of the chl *a* content from the urea+M medium. Nitrogen is one of the critical nutrients in the algal metabolic cycles. The first step cultivation was conducted to obtain algal biomass for the second phase cultivation, namely the stress phase cultivation. The green alga *Spirogyra varians* exhibited average Chl *a*, Chl *b*, total chlorophyll, and total carotenoid contents of approximately  $6.0 \pm 0.22$  μg/mL,  $3.0 \pm 0.03$  μg/mL,  $9.0 \pm 0.19$  μg/mL, and  $1.8 \pm 0.17$  μg/mL, respectively [23]. Moreover, Chl *a* has anti-inflammatory, anti-aging, and antimutagenic properties [24-26].

Chlorophyll *a* contains a magnesium ion (Mg<sup>2+</sup>) at its center, making it ionic and hydrophilic. It also has a ring that is hydrophobic in nature with a carbonyl group at its tail, making it polar [27].

Chlorophylls and carotenoids are essential pigments involved in the process of photosynthesis, playing complementary roles in capturing light energy. The quantitative determination of chlorophylls *a*, *b*, and carotenoids in a whole pigment extract of green plants is significantly influenced by the extraction method, including the choice of solvent, temperature, and duration of the extraction process. Since *Chaetophora* is an organism that can grow both autotrophically and heterotrophically, it can be easily cultivated in chemically defined media or sewage.

#### 4. CONCLUSIONS

This study compares the growth, dry matter, productivity, and pigments of freshwater macroalgae to select optimal media for intensive algal cultivation. Many efforts are currently underway to find and select new sources of nutrients or media for algal cultivation, with a particular focus on finding alternatives that are not expensive, easy to prepare, and take a short time for cultivation. The industry now demands alternative or new media formulations that can offer low cost, high yields, and minimal environmental impact. It is worth mentioning that green algae can accumulate high-value compounds and be produced in an ecological and sustainable way at a low cost if algae are used to treat industrial waste products and then remove CO<sub>2</sub> from the atmosphere. Future work involves producing high-productive biomass using flue-gas CO<sub>2</sub> from industrial waste in combination with using low-cost media to promote green technology and sustainability. Furthermore, producing valuable compounds, including pigment contents generated from algal biomass, could also help reduce the cost of wastewater management using algae.

#### 5. ACKNOWLEDGEMENT

This work was one part of a research program supported by the Thailand Science Research and Innovation (TSRI), Ministry of Higher Education, Science, Research, and Innovation. The authors are grateful to the staff at the Algal Excellence Centre (ALEC) for providing the laboratory facilities.

#### 6. REFERENCES

- [1]Amenor fenyó, D. K., Huang, X., Zhang, Y., Zeng, Q., Zhang, N., Ren, J., & Huang, Q. (.2019)Microalgae brewery wastewater treatment: potentials, benefits and the challenges. International journal of environmental research and public health, (11)16, .1910 <https://doi.org/10.3390/ijerph16111910>
- [2]Pardilhó, S., Cotas, J., Pereira, L., Oliveira, M. B., & Dias, J. M. (.2022)Marine macroalgae in a circular economy context: A comprehensive analysis focused on residual biomass. Biotechnology Advances, 60, .107987 <https://doi.org/10.1016/j.biotechadv.2022.107987>
- [3]Kumar, K. V., Ramamurthi, V., & Sivanesan, S. (.2006)Biosorption of malachite green, a cationic dye onto Pithophora sp., a fresh water algae. Dyes and Pigments, (2-1)69, .107-102 <https://doi.org/10.1016/j.dyepig.2005.02.005>
- [4]Dönmez, G. Ç., Aksu, Z., Öztürk, A., & Kutsal, T. (.1999)A comparative study on heavy metal biosorption characteristics of some algae. Process Biochemistry, (9)34, .892-885 [https://doi.org/10.1016/S0032-9592\(99\)00005-9](https://doi.org/10.1016/S0032-9592(99)00005-9)
- [5]Moenne, A., González, A., & Sáez, C. A. (.2016)Mechanisms of metal tolerance in marine macroalgae, with emphasis on copper tolerance in Chlorophyta and Rhodophyta. Aquatic Toxicology, 176, .37-30 <https://doi.org/10.1016/j.aquatox.2016.04.015>
- [6]Godlewska-Żyłkiewicz, B. (.2001)Analytical applications of living organisms for preconcentration of trace metals and their speciation. Critical Reviews in Analytical Chemistry, (3)31, .189-175DOI: 20014091076730/10.1080
- [7]Ivánová, D., Kaduková, J., Kavuličová, J., & Horváthová, H. (.2012)Determination of the functional groups in algae *Parachlorella kessleri* by potentiometric titrations. Nova Biotechnologica et Chimica, (2)11, .99-93DOI: <https://doi.org/10.2478/v3-0010-012-10296>
- [8]Romera, E., González, F., Ballester, A., Blázquez, M. L., & Munoz, J. A. (.2007)Comparative study of biosorption

of heavy metals using different types of algae. *Bioresource Technology*, (17)98, .3353-3344

<https://doi.org/10.1016/j.biortech.2006.09.026>

[9] Ismail, I., & Moustafa, T. (2016). Biosorption of heavy metals. Heavy metals: sources, toxicity and remediation techniques, 3, 131-174. In book: Heavy Metals: Sources, Toxicity and Remediation Techniques Publisher: Nova Science Publishers, Inc. Editors: Deepak Pathania.

[10] Andrade, A. D., Rollemberg, M. C. E., & Nóbrega, J. A. (2005) Proton and metal binding capacity of the green freshwater alga *Chaetophora elegans*. *Process Biochemistry*, (5)40, .1936-1931

<https://doi.org/10.1016/j.procbio.2004.07.007>

[11] Liu, B., Xiong, Q., Liu, X., Liu, G., & Hu, Z. (2019). Molecular phylogeny and taxonomy of the genus *Chaetophora* (Chlorophyceae, Chlorophyta), including descriptions of *Chaetophoropsis aershanensis* gen. et sp. nov. *Journal of Phycology*, 55(1), 74-83. <https://doi.org/10.1111/jpy.12803>

[12] Caisová, L. (2020). Freytet, P., & Verrecchia, E. P. (1998). Freshwater organisms that build stromatolites: a synopsis of biocrystallization by prokaryotic and eukaryotic algae. *Sedimentology*, 45(3), 535-563.

<https://doi.org/10.1046/j.1365-3091.1998.00155.x>

[13] Agrawal, S. C., & Sharma, U. K. (1996). Chemical and biological properties of culture filtrates of *Westiellopsis prolifica* and *Chaetophora attenuata*. *Israel Journal of Plant Sciences*, 44(1), 43-48. DOI:

<https://doi.org/10.1080/07929978.1996.10676632>

[14] Allen, M. M., & Stanier, R. Y. (1968). Growth and division of some unicellular blue-green algae. *Microbiology*, 51(2), 199-202. <https://doi.org/10.1099/00221287-51-2-199>

[15] Lichtenthaler, H. K., & Buschmann, C. (2001). Chlorophylls and carotenoids: Measurement and characterization by UV-VIS spectroscopy. *Current Protocols in Food Analytical Chemistry*, 1(1), F4-3.

<https://doi.org/10.1002/0471142913.faf0403s01>

[16] Björnsäter, B. R., & Wheeler, P. A. (1990). Effect of nitrogen and phosphorus supply on growth and tissue composition of *Ulva fenestrata* and *Enteromorpha intestinalis* (ulvales, chlorophyta). *Journal of Phycology*, 26(4), 603-611. <https://doi.org/10.1111/j.0022-3646.1990.00603.x>

[17] Peckol, P., DeMeo-Anderson, B., Rivers, J., Valiela, I., Maldonado, M., & Yates, J. (1994). Growth, nutrient uptake capacities and tissue constituents of the macroalgae *Cladophora vagabunda* and *Gracilaria tikvahiae* related to site-specific nitrogen loading rates. *Marine Biology*, 121, 175-185. <https://doi.org/10.1007/BF00349487>

[18] Fujita, R. M. (1985). The role of nitrogen status in regulating transient ammonium uptake and nitrogen storage by macroalgae. *Journal of Experimental Marine Biology and Ecology*, 92(2-3), 283-301. [https://doi.org/10.1016/0022-0981\(85\)90100-5](https://doi.org/10.1016/0022-0981(85)90100-5)

[19] Riley, J. P., & Roth, I. (1971). The distribution of trace elements in some species of phytoplankton grown in culture. *Journal of the Marine Biological Association of the United Kingdom*, 51(1), 63-72. DOI:

<https://doi.org/10.1017/S0025315400006457>

[20] Hayward, J. (1969). Studies on the growth of *Phaeodactylum tricornutum* V. the relationship to iron, manganese and zinc. *Journal of the Marine Biological Association of the United Kingdom*, 49(2), 439-446. DOI:

<https://doi.org/10.1017/S0025315400036018>

[21] Maguire, M. E., & Cowan, J. A. (2002). Magnesium chemistry and biochemistry. *Biomaterials*, 15, 203-210.

<https://doi.org/10.1023/A:1016058229972>

[22] Ishfaq, M., Wang, Y., Yan, M., Wang, Z., Wu, L., Li, C., & Li, X. (2022). Physiological essence of magnesium in plants and its widespread deficiency in the farming system of China. *Frontiers in plant science*, 13, 802274.

<https://doi.org/10.3389/fpls.2022.802274>

[23] Tipnee, S., Ramaraj, R., & Unpaprom, Y. (2015). Nutritional evaluation of edible freshwater green macroalga *Spirogyra varians*. *Emergent Life Sciences Research*, 1(2), 1-7.

[24] Hosikian, A., Lim, S., Halim, R., & Danquah, M. K. (2010). Chlorophyll extraction from microalgae: A review on the process engineering aspects. *Bioprocess Development for Biofuels and Bioproducts*, 2010.

<https://doi.org/10.1155/2010/391632>

[25] Subramoniam, A., Asha, V. V., Nair, S. A., Sasidharan, S. P., Sureshkumar, P. K., Rajendran, K. N., ... & Ramalingam, K. (2012). Chlorophyll revisited: anti-inflammatory activities of chlorophyll a and inhibition of expression of TNF- $\alpha$  gene by the same. *Inflammation*, 35, 959-966. <https://doi.org/10.1007/s10753-011-9399-0>

[26] Cho, S. (2014). The role of functional foods in cutaneous anti-aging. *Journal of Lifestyle Medicine*, 4(1), 8. doi: 10.15280/jlm.2014.4.1.8

[27] Sumanta, N., Haque, C. I., Nishika, J., & Suprakash, R. (2014). Spectrophotometric analysis of chlorophylls and carotenoids from commonly grown fern species by using various extracting solvents. *Research Journal of Chemical Sciences*, 4(9), 63-69.

# Effects of an organic nitrogen supplement on production of recombinant HPV52 L1 capsid protein in *Hansenula polymorpha*

Wichitra Phimsen<sup>1</sup>, Natsima Kopitak<sup>1</sup>, Thantawat Theeranan<sup>1</sup>,  
Chuenchit Boonchird<sup>1</sup>, Manop Suphantharika<sup>1</sup> and Thunyarat Pongtharangkul<sup>1,\*</sup>

<sup>1</sup>Department of Biotechnology, Faculty of Science, Mahidol University,  
Bangkok, 10400, Thailand.

\*Correspondence to: Department of Biotechnology, Faculty of Science, Mahidol University, Bangkok,  
10400, Thailand, E-mail: thunyarat.pon@mahidol.edu

**ABSTRACT:** Human papillomavirus (HPV) 52 is the most common high-risk HPV subtype in Southeast Asia and the 4<sup>th</sup> most common subtype in Thailand. The L1 capsid protein HPV52 subtype is produced by a recombinant yeast in the form virus-like particle (VLP) as one valent of HPV vaccine development. Previously, a defined medium SYN6 was designed for cultivation of a methylotrophic yeast *Hansenula polymorpha*. In this study, effects of complex, non-animal derived nitrogen source supplementation into SYN6 on growth and HPV52 L1 protein production by a recombinant *H. polymorpha* were investigated. Although both nitrogen sources evaluated in this study (Hy-Express<sup>TM</sup> System II and Hy-Express<sup>TM</sup> System IV) did not significantly affect growth of a recombinant *H. polymorpha*, supplementation of Hy-Express<sup>TM</sup> System IV resulted in a significant increase (1.45-folds) in volumetric L1 protein yield (mg-L1 protein/L-culture). Moreover, the inclusion of both complex nitrogen sources had a significant impact on stabilizing the culture's pH, leading to a lower requirement for pH adjustment.

**Keyword:** Human papilloma virus, Virus-like particle, VLP

## 1. INTRODUCTION

Cervical cancer is the 4<sup>th</sup> most common cancer and the 2<sup>nd</sup> largest cause of cancer death in women worldwide [1-2]. Human papillomavirus (HPV) infection was identified as the cause of cervical cancer with more than 150 different types of HPV have been reported thus far. HPV52 is the most common high-risk HPV subtype in Southeast Asia and the 4<sup>th</sup> most common subtype in Thailand. Prophylactic vaccines to prevent HPV infections are mostly based on virus-like particle (VLP) derived from HPV L1 capsid proteins. VLP vaccines can be produced from the bacterial and yeast expression systems, which are easily to be scaled up into a cost-effective manufacturing system [3]. VLPs of HPV L1 protein have been produced in yeast expression systems including *Saccharomyces cerevisiae*, *Pichia pastoris* and *Hansenula polymorpha* [4].

*H. polymorpha* has been used for production of recombinant proteins, vaccines, and biopharmaceuticals due to several unique characteristics. A defined medium called SYN6, previously developed for cultivation of *H. polymorpha* [5], is used most frequently for cultivation of *H. polymorpha*. Despite a wide-spread use of SYN6, a few studies [6-7] reported an enhancing effect of complex organic nitrogen source (e.g., yeast extract and wheat peptone) on recombinant protein production in *H. polymorpha*. The effects, however, are strain-specific and therefore the optimal medium must be optimized specifically for each production strain. In this study, commercial non-animal derived complex nitrogen sources were supplemented into to evaluate their effects on growth and L1 protein production. The use of components with non-animal origin from well-known manufacturers would facilitate the safety and qualify checks by related regulators. The knowledge obtained from this study can be used further for bioreactor-scale production of HPV 52 L1 protein as well as other recombinant proteins in *H. polymorpha*.

## 2. MATERIALS AND METHODS

**Strain verification:** Recombinant *Hansenula polymorpha* strain HPV52 used in this research was previously constructed based on *H. polymorpha* NCYC495 (SH4330) *ura3* (Ura<sup>-</sup>) (provided by Yeast Genetic Resource Center (YGRC), Osaka University, Japan) [8]. Strain HPV52 harbored a chromosome integrated plasmid pTB8 (L1 HPV52), constructed based on a backbone of plasmid pUC57 (derivative of pUC19), as shown in Figure 1.

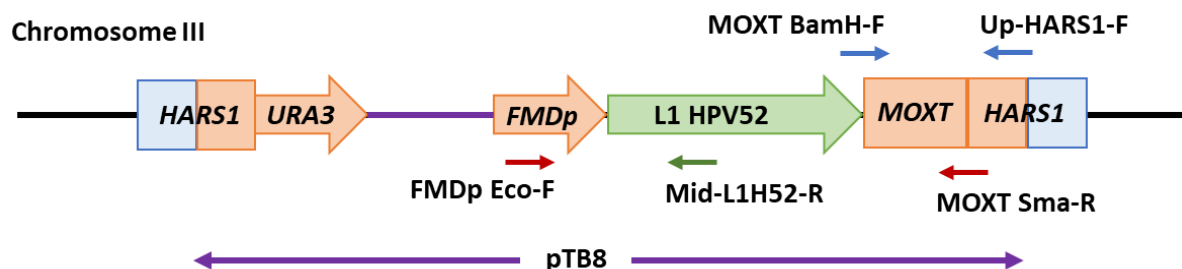


Figure 1 Diagram of a pTB8 plasmid integration in the chromosome of *H. polymorpha* NCYC495 *ura3* at HARS1 site. PCR primer positions for verification of the plasmid existence are presented as arrows [8].

The recombinant yeast *H. polymorpha* harboring HPV52 L1 gene was verified by PCR using 3 different pairs of primers. The presence of L1 HPV 52 gene was verified using primer FMDp Eco-F and Mid-L1H52-R (expected PCR product of 800 bp), while an integration location was confirmed using primer Up-HARS1-F and MOXT BamH-F (expected PCR product of 900 bp). Lastly, the presence of a complete expression cassette was confirmed using primer FMDp Eco-F and MOXT Sma-R (expected PCR product of 2500 bp). After amplification, the PCR products were analyzed by an agarose gel electrophoresis with  $\lambda$  DNA HindIII Digest or 2-Log DNA ladder (NEB, Massachusetts, USA) as a DNA marker.

**Inoculum preparation:** Recombinant *H. polymorpha* was maintained as a frozen working stock culture (at  $-80^{\circ}\text{C}$ ) in Synthetic complete (SC) medium containing uracil dropout mix (SC-ura) and 20% (w/v) glycerol. For pre-inoculum preparation, 500  $\mu\text{L}$  of frozen stock was added into 5 mL of SC-ura broth. The culture was incubated at  $30^{\circ}\text{C}$ , 200 rpm for 16 h. Then, 500  $\mu\text{L}$  of the pre-inoculum was added into 25 mL of SYN6 medium [5] (with ferrous in a form of ammonium iron (II) sulfate hexahydrate) supplemented with 1% glycerol and the culture was incubated at  $30^{\circ}\text{C}$ , 200 rpm for 18-20 h before being used as an inoculum for flask-scale cultivation.

**Flask-scale cultivation:** Flask-scale cultivation was performed using 100 mL of SYN6 supplemented with 1% glycerol. The culture with an initial  $\text{OD}_{660}$  of 0.1 was incubated at  $30^{\circ}\text{C}$ , 200 rpm for 36 h ('growth phase'). After that, the culture was centrifuged (at 10,000 rpm,  $4^{\circ}\text{C}$  for 10 min) and the cell pellet was collected and resuspended in an equal volume of SYN6 medium supplemented with 1% methanol. The culture was incubated at  $30^{\circ}\text{C}$ , 200 rpm for 24 h ('induction phase'). During cultivation, samples were taken and analyzed for  $\text{OD}_{660}$ , pH and L1 protein using Western blot and ELISA according to the protocol described elsewhere [9]. Total protein was determined using Bradford assay and specific L1 yield (mg-L1 protein/mg-total protein) was calculated accordingly. While an original SYN6 medium was serving as a control, 2 different non-animal derived nitrogen sources (Hy-Express<sup>TM</sup> System II and Hy-Express<sup>TM</sup> System IV; Kerry,

Ireland) were supplemented into SYN6 medium at 10 g/L (in both phases) to evaluate their effects on growth and L1 protein production. Nitrogen source that gives high growth and L1 protein production would be selected and evaluated further.

### 3. RESULTS AND DISCUSSION

**Strain verification:** Recombinant *H. polymorpha* strain HPV52 was verified using 3 different primer pairs as mentioned previously in Materials and Methods. The result revealed the expected sizes of PCR products (Figure 2).

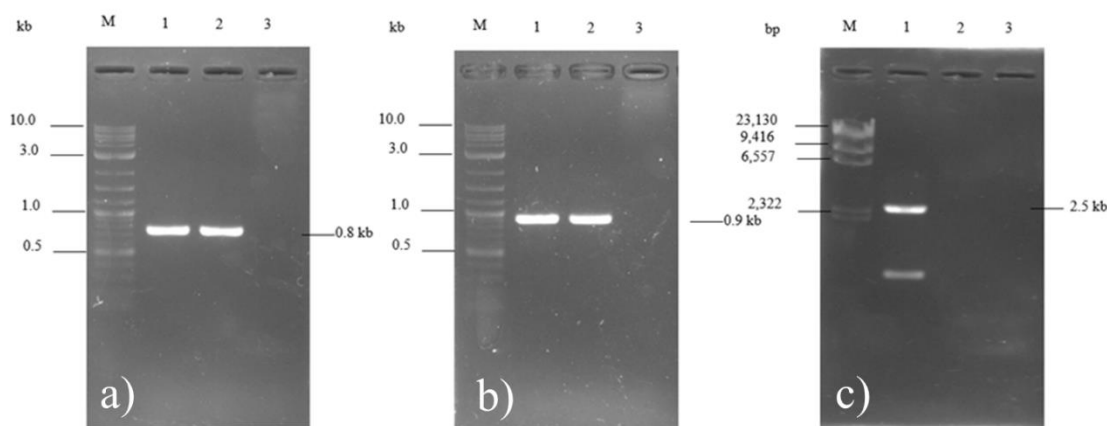


Figure 2 PCR products of the recombinant *H. polymorpha* harboring pTB8 revealing a) presence of HPV 52 L1 gene, b) integration at HARS1 site, and c) a complete expression cassette for L1 protein. Lane M: 2-Log DNA Ladder in (A) and (B), λ DNA HindIII Digest marker in (C); Lane 1 and 2: PCR product from the recombinant yeast harboring plasmid pTB8; Lane 3: Negative control.

**Effects of complex nitrogen source supplementation:** SYN6 medium was supplemented with 2 different non-animal derived nitrogen sources (at 10 g/L) expected to promote growth and recombinant protein expression. The nitrogen sources evaluated include Hy-Express™ System II and Hy-Express™ System IV. Growth (as OD<sub>660</sub>) and pH before and after a methanol induction are summarized in Figure 3a and 3b, respectively. Overall, supplementation of complex nitrogen sources did not affect growth of the recombinant *H. polymorpha* (Figure 3a). This observation agreed with the previous report in which supplementation of several peptones rarely affected growth of *H. polymorpha* used for production of the recombinant parathyroid hormone (rPTH) fragment 1-34 [7]. During a cultivation of *H. polymorpha* in SYN6, the medium was acidified by an ammonia uptake via an ammonia/H<sup>+</sup> antiport (Jenzelewski 2002), therefore, the culture pH normally decreased from 5.5 to 3.5-4 (Figure 3b). With supplementation of organic nitrogen source, the stabilization of pH before and after methanol induction was possible because of higher buffering capacity offered by peptones [10]. As the difference in pH control is one of the factors contributing to the difference responses observed when scaling up, an ability to control pH in flask-scale cultivation (in which pH adjustment is difficult) is considered highly beneficial. Even though growth (Figure 3a) and specific L1 protein yield in terms of mg-L1 protein per mg-total protein (Figure 3c) were not enhanced significantly, supplementation of Hy-Express™ System IV resulted in a significant increase in a volumetric L1 yield in terms of mg-L1 protein per liter of culture (Figure 3d). Higher biomass density (as indicated by OD<sub>660</sub>) and expression of L1 protein (as indicated by the specific L1 protein yield) both contributed to the higher volumetric yield observed.

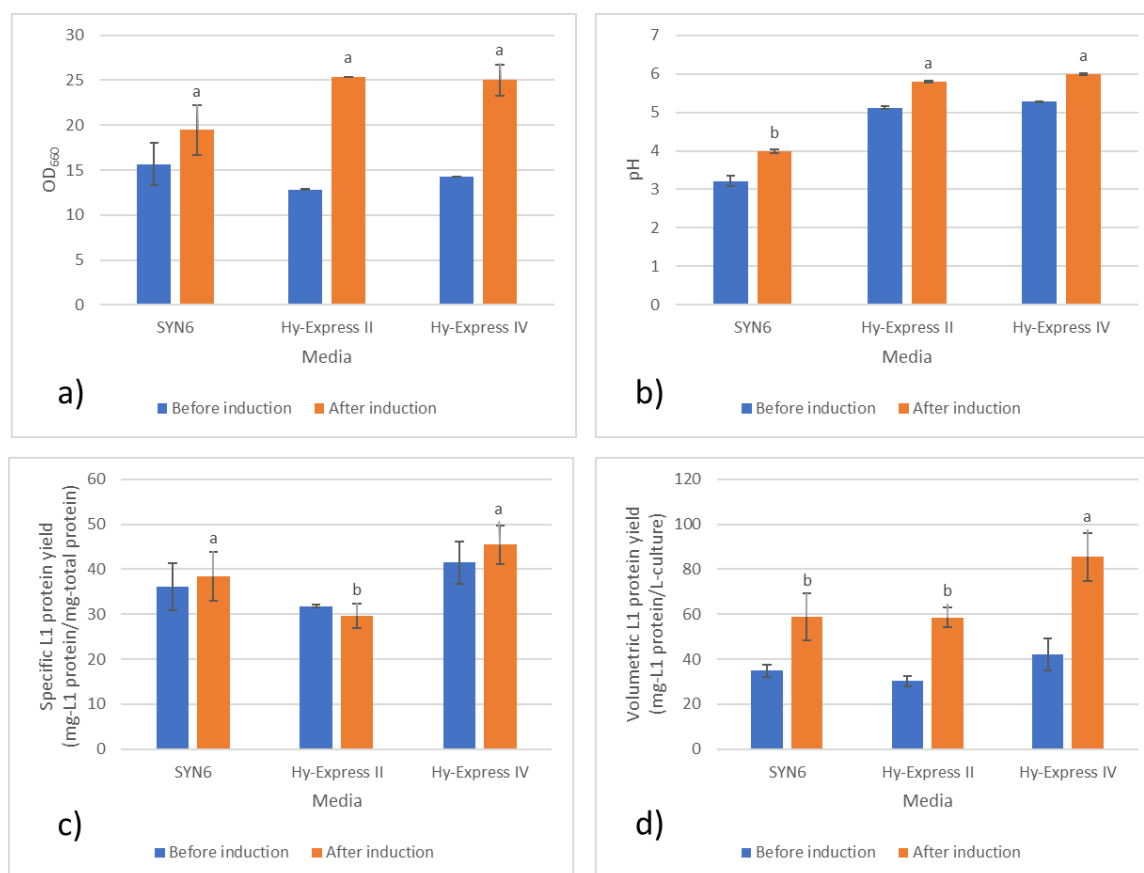


Figure 3 Growth (as OD<sub>660</sub>; a), pH (b), specific L1 protein yield (as mg-L1 protein/mg-total protein; c), and volumetric L1 protein yield (as mg-L1 protein/L-culture) before and after methanol induction of recombinant *H. polymorpha* harboring HPV 52 L1 gene when cultivated in SYN6 supplemented with different nitrogen sources. Different alphabet superscripts above the bar indicate a statistically significant difference ( $p$ -value  $\leq 0.05$ ).

#### 4. CONCLUSIONS

Although both nitrogen sources evaluated in this study (Hy-Express<sup>TM</sup> System II and Hy-Express<sup>TM</sup> System IV) did not significantly affect growth of a recombinant *H. polymorpha* HPV52, supplementation of Hy-Express<sup>TM</sup> System IV resulted in a significant increase (1.45-folds) in volumetric L1 protein yield (mg-L1 protein/L-culture). Such enhancement was suspected as a result of a slight increase in biomass density and specific L1 protein yield observed. Moreover, both complex nitrogen sources clearly stabilized the pH of the culture, a beneficial feature for a flask-scale cultivation in which pH adjustment was not practicable.

#### 5. ACKNOWLEDGEMENTS

This research project is supported by Mahidol University (Fundamental Fund: fiscal year 2023 by National Science Research and Innovation Fund (NSRF)). We are deeply grateful to BioNet-Asia Co. Ltd. for their invaluable suggestions, as well as to Kerry and A.N.H. Scientific Marketing Co., Ltd. for providing the samples of Hy-Express<sup>TM</sup> System II and Hy-Express<sup>TM</sup> System IV used in this study.

## 6. REFERENCES

- [12] Moody, C.A. and Laimins, L.A. (2010). Human papillomavirus oncoproteins: pathways to transformation. *Nature Reviews Cancer*, 10(8), pp. 550-560, DOI: 10.1038/nrc2886.
- [13] Bruni, L., Albero, G., Serrano, B., Mena, M., Collado, J.J., Gómez, D., Muñoz, J., Bosch, F.X. and de Sanjosé, S. (2021). Human Papillomavirus and Related Diseases in Thailand. Summary Report ICO/IARC Information center on HPV and cancer (HPV information center). 166 p. [Updated 2021 Oct 22; cited 2022 Oct 22] Available from: <https://www.hpvcentre.net/statistics/reports/THA.pdf>.
- [14] Fuenmayor, J., Gòdia, F. and Cervera, L. (2017). Production of virus-like particles for vaccines. *New Biotechnology*, 39, pp. 174-180, DOI: 10.1016/j.nbt.2017.07.010.
- [15] Bredell, H., Smith, J.J., Görgens, J.F. and van Zyl, W.H. (2018). Expression of unique chimeric human papilloma virus type 16 (HPV-16) L1-L2 proteins in *Pichia pastoris* and *Hansenula polymorpha*. *Yeast*, 35(9), pp. 519-529, DOI: 10.1002/yea.3318.
- [16] Jenzelewski, V. (2002). Fermentation and primary product recovery. In G. Gellissen, (Ed), *Hansenula polymorpha – biology and applications*. Weinheim: Wiley-VCH, 156–174.
- [17] Moussa, M., Ibrahim, M., El Ghazaly, M., Rohde, J., Gnoth, S., Anton, A., Kensy, F., Mueller, F. (2012) Expression of recombinant staphylokinase in the methylotrophic yeast *Hansenula polymorpha*. *BMC Biotechnology*, 12:96, DOI: 10.1186/1472-6750-12-96.
- [18] Mueller, F., Moussa, M., El Ghazaly, M., Rohde, J., Bartsch, N., Parthier, A., et al. (2013). Efficient production of recombinant parathyroid hormone (rPTH) fragment 1-34 in the methylotrophic yeast *Hansenula polymorpha*. *Generics and Biosimilars Initiative Journal*, 2(3), pp. 114-122, DOI: 10.5639/gabij.2013.0203.035.
- [19] Boontawon, T. (2017). Expression of the L1 major capsid protein of human papilloma virus type 52 and 58 in *Hansenula polymorpha* [master's thesis]. Faculty of Graduated Studies. Mahidol University.
- [20] Kopitak, N., Thitithanyanont, A., Payongsri, P. and Boonchird, C. (2018). Construction of recombinant yeast *Hansenula polymorpha* expressing of human papillomavirus type 33 and 45 major capsid protein L1. In *Proceedings of the 30<sup>th</sup> Annual Meeting of the Thai Society for Biotechnology and International Conference*. November 22-23, 2018, Bangkok, Thailand.
- [21] Atilola, O.A., Gyawali, R., Aljaloud, S.O. and Ibrahim, S.A. (2015). Use of phytone peptone to optimize growth and cell density of *Lactobacillus reuteri*. *Foods*, 4, pp. 318-327, DOI: 10.3390/foods4030318.



# Formulating *Thunbergia laurifolia* Lindl. cream with nanostructured lipid carriers for bacterial skin infection treatment

Esther Thongaram<sup>1</sup>, Worawat Surarit<sup>1</sup>, and Pariya Na Nakorn<sup>1\*</sup>

<sup>1</sup>Department of Biotechnology, Thammasat University, Pathum Thani, 12120, Thailand

\*Correspondence to: Department of Biotechnology, Faculty of Science and Technology, Thammasat University, Rangsit Campus, Phahonyothin Road, Khlong Luang, Pathumthani, 12120, Thailand.

E-mail: pariya\_n@sci.tu.ac.th, esthers.tho@gmail.com

**ABSTRACT:** *Thunbergia laurifolia* Lindl. (Rang Jeud) is a Thai herbal medicinal plant used in traditional medicine to treat pruritus, skin diseases, and herpes. Previous studies have reported its ability to inhibit bacterial growth. This research aimed to develop a dermatological cream formulation utilizing *T. laurifolia* extract, known for its phytochemical and pharmaceutical properties, particularly antibacterial activity. The objective of this study is to investigate as well as develop Rang Jeud cream utilizing nanostructured lipid carriers for eczema skin problem treatment. The study exhibited no cytotoxic effects on the HaCaT cell line. In terms of cream formulation, the F2 formula demonstrated excellent sensory properties, a skin-compatible pH, and the desired viscosity. It also exhibited good physical and physicochemical stability over a period of six months and even under accelerated stability tests. By combining the *T. laurifolia* extract with the best cream base and incorporating 10% NLC, the researchers developed the RJ-DL-NLC cream. This cream successfully addressed skin water loss and exhibited a clear zone of inhibition in evaluating antimicrobial activity. The final product demonstrated favorable sensory qualities, and the addition of NLC significantly improved its efficiency. The solution effectively hydrated the skin, targeting the underlying cause of skin infections, and served as a comparable treatment option for bacterial skin infections when compared to commercial medications. This research not only contributes to the value of Thai medicinal plants but also provides a safe, effective, and cost-efficient alternative for improving the health of the Thai population.

**Keyword:** *Thunbergia laurifolia*, Rang Jeud cream, Evaluation of cream, Bacterial skin infection, Nanostructured lipid carriers

## 1. INTRODUCTION

*Thunbergia laurifolia* Lindl, commonly known as Rang Jeud, belongs to the Acanthaceae family and is widely distributed in Southeast Asian countries [1], including Thailand [2–3]. This plant has been utilized in Thailand for centuries as a natural medicine due to its detoxifying properties and folk remedy status [4–5]. Numerous pharmacological activities of *T. laurifolia* have been reported, including the reduction of blood glucose levels in diabetic rats, antimutagenic and antimicrobial effects, hepatoprotective properties, antinociceptive and anti-inflammatory actions, antioxidant activities, and detoxification capabilities [6–8]. One application of these natural compounds is in the form of cream formulations for therapeutic purposes, particularly in treating skin problems.

Creams are semi-solid dosage forms that are safe for use on the skin, as it is the most accessible organ of the human body with a large surface area. Creams typically consist of multiple ingredients dispersed in a suitable base material and are categorized into various types [9]. There is an increasing demand for creams containing herbal components, and medicated creams with active ingredients are used for therapeutic purposes such as treating infections [10–11]. The effectiveness of formulations relies on the ability of the active components to penetrate the epidermis. The stratum corneum, the outermost layer of the skin, acts as a barrier to prevent the penetration of

drugs and cosmetic ingredients [12]. However, the use of nanosystems, such as lipid nanoparticles, shows promise in facilitating the transport of molecules through the stratum corneum due to their lipophilicity [13].

Nanostructured lipid carriers (NLC) represent the second generation of lipid nanoparticles. They are gaining attention as new colloidal drug carriers for topical use, overcoming the limitations of first-generation solid lipid nanoparticles (SLN) [14–16]. Incorporating liquid lipids produces structural defects in solid lipids, resulting in a less ordered crystalline arrangement that prevents drug leakage and allows for a high drug load. The small size of NLC ensures close proximity to the stratum corneum, facilitating better drug delivery into the skin [17]. Moreover, the ability of lipid nanoparticles to prevent water loss from the skin contributes to improved skin hydration [18–19]. Therefore, this study aims to investigate a suitable herbal cream formula with nanostructured lipid carriers for treating bacterial skin infections or eczema skin problem.

## 2. MATERIALS AND METHODS

### 2.1 The cytotoxicity activity of *T. laurifolia* extracts

The cytotoxic effects of *T. laurifolia* extracts were assessed by the MTT assay. Briefly, HaCaT cells were seeded into a well of a 96-well plate at the density of 20,000 cells/well and then incubated at 37 °C in a CO<sub>2</sub> incubator for 24 h. The extract was dissolved in DMEM. Then, the cells were incubated with different concentrations of the *T. laurifolia* extract in a CO<sub>2</sub> incubator for 72 h. After the incubation, the extract and DMEM were removed, and MTT at a final concentration of 0.25 mg/mL was added into the cells. After the incubation for 1 h, the MTT was removed, and 100 µl of DMSO was added to dissolve the formazan crystals in the cells. Finally, the absorbance was measured at 570 nm using the microplate reader (sunrise, Austria), and the viability was calculated.

### 2.2 Formulation of Rang Jeud cream

A cream based on an oil-in-water (O/W) emulsion prepared in this study was modified from [20–22]. The cream's formula is shown in Table 1. The oil-soluble components and emulsifying agent (stearic acid, cetyl alcohol, glyceryl monostearate, isopropyl myristate, propylene glycol, olive oil, KF-995, and emulium delta) were heated to 75 °C, and the water-soluble components and active ingredients (disodium EDTA, glycerin, and RJ-NLC) were also heated to 75 °C. Next, the aqueous phase was added in portions to the oil phase with continuous stirring for 10 min. After that, the heating was stopped, and the emulsion was homogenized using an overhead stirrer (WB2000-M, WIGGENS, Germany) until it cooled down to 45°C. The prepared RJ-NLC was added and stirred for another 10 min. Finally, the Rang Jeud cream was poured into a cream jar.

### 2.3 Efficacy test of Rang Jeud cream

#### 2.3.1 Occlusive test [23-24]

The in vitro occlusion test was modified from De Vriger *et al.* [25] to evaluate the occlusive effect of the formulation. Firstly, a flask (50 ml) was filled with 25 g of distilled water, and a piece of filter paper (Whatman No.1) was used to cover the top of the flask. Next, 350 mg of samples were spread homogeneously on the filter surface. The sample was not applied to a group of flasks and was used as a control group. Then, flasks were kept at 32 °C for 24 h to mimic the skin's surface temperature, and they were weighed at 6, 12, and 24 h to determine the water loss. Each sample was measured in triplicate (n = 3), and the occlusion factor (F) was

**Table 1.** Composition of the cream formulation\*

Components	F2	RJ-NLC	F2+ 10%NLC
Disodium EDTA	0.1	-	0.1
Glycerin	1	-	1
Isopropyl myristate	5	0.5	5
Propylene glycol	3	-	3
Emulium Delta	5	-	5
Tween 80	-	6	-
Oleic acid	-	2.5	-
Stearic acid	1.5	7	1.5
Cetyl Alcohol	1.5	-	1.5
Glyceryl Monostearate	3	-	3
Olive Oil	1	-	1
KF-995	1	-	1
Phenoxyethanol	1	-	1
Dicloxacillin	-	0.13	-
<i>T. laurifolia</i>	-	10.08	-
RJ-DL-NLC	-	-	10
Distilled water (100 ml)	qs	qs	qs

\*(as noted in petty patent application 2303001762)

calculated according to the following equation:

$$F = 100 \times [(A-B)/A]$$

A = The water loss without an NLC sample (control)

B = The water loss with an NLC sample

When compared to the reference, an occlusion factor of 0 means that there is no occlusive effect, while an occlusion factor of 100 means that there is the most occlusive effect.

### 2.3.2 Antibacterial activity [26]

This method used a pathogenic bacterial species to inoculate an agar plate using the spread plate technique. This involves spreading 100 ul of the microbial solution onto the agar surface using a glass spreader. Subsequently, a filter paper disc containing a known concentration of the sample was placed on the agar medium. The plates were then inverted and incubated at 37°C for 24 h to facilitate bacterial growth. During incubation, the antimicrobial extract solution gradually diffuses through the agar medium, thereby inhibiting the growth of the tested bacterial species. Finally, the antibacterial activity was assessed by measuring the diameter of the resulting inhibition zone against the microorganisms under investigation. All disc diffusion experiments were conducted in three independent trials, and the antibacterial activity was reported as the mean ± standard error mean.

## 2.4 Stability Test [27]

### 2.4.1 Thermal stability

The thermal stability of Rang Jeud cream was determined by storing 50g at 4 °C for 48 h and at 45 °C for 48 h. Repeat the test for a total of 6–8 cycles. After that, the physical and physiochemical properties were assessed.

### 2.4.2 Light stability

The Rang Jeud cream was stored in a transparent container and placed in the sun for one week. The others were placed by the window for 3 months, and the control was kept out of the light at room temperature.

### 2.4.3 Gravity stability

The gravity stability of the Rang Jeud cream was determined by centrifuging at a reasonable speed, for example, 3750 rpm with a radius of 10 cm, for 5 h. It would be comparable to setting it aside for a year.

### 2.5 Statistical analysis

The statistical analysis was carried out using Microsoft Excel 365 and GraphPad Prism 5. The results were presented as the mean  $\pm$  standard deviation (SD). An ANOVA was applied to assess significant differences in the means of the evaluated parameters. Differences were considered statistically significant when the p-value was less than 0.05.

## 3. RESULTS AND DISCUSSION

The previous study showed that the aqueous leaf extract of *T. laurifolia* had a total phenolic content (TPC) of  $192.228 \pm 0.004$  mg GAE/g extract and a total flavonoid content (TFC) of  $564.297 \pm 0.003$  mg QE/g extract and contained a half-maximal inhibitory concentration (IC<sub>50</sub>) of 0.015 mg/ml. All results were corresponding to Posridee *et al.*'s research [28]. Then this *T. laurifolia* extract was used for the following investigation.

### 3.1 The cytotoxicity activity of *T. laurifolia* extracts

In the MTT assay, incubation with *T. laurifolia* extract at final concentrations of 0.05, 0.1, 0.5, and 1 mg/mL revealed no detectable change in the MTT conversion rates of HaCaT cells. This result indicated that the extract did not cause cytotoxic effects on the HaCaT cell line. This is in agreement with the findings in [29], namely that the aqueous extract of *T. laurifolia* had only low cytotoxicity. After that, the suitable concentration of *T. laurifolia* extract was encapsulated in NLC and best Rang Jeud cream formulation (F2) as described in table 1 (as noted in petty patent application 2303001762).

### 3.2 Efficacy test of Rang Jeud cream

#### 3.2.1 Occlusive test

An *in vitro* study was conducted to evaluate the occlusivity of NLC using the 'occlusion factor' as a parameter. The results demonstrated that the combination of NLC with the best cream-based formulations led to a significant increase in skin coverage. The measured occlusive value increased from the baseline value of 65.2950% for the normal base cream to 71.7317% after incorporating NLC. This highlights the enhanced ability of the NLC-based formulation to protect against water evaporation from the skin. Moreover, the use of oleic acid as the liquid lipid in NLC systems was found to be a promising technique. It synergistically improved skin hydration by forming an adhesive lipid film layer on the skin's surface, enhancing the occlusive effect. These findings support the conclusion that the application of oleic acid-based NLC systems holds the potential to improve skin hydration and overall skin health.

#### 3.2.2 Antibacterial activity

The antibacterial activity of the Rang Jeud cream, containing *T. laurifolia* aqueous leaf extract incorporated with NLC and base cream, was evaluated using the agar disc diffusion method. The diameters of inhibition zones were measured to assess the antimicrobial potency of the samples. The results showed that the Rang Jeud cream (RJ-DL-NLC-cream, 0.010, 0.001 g/g) exhibited a clear zone of inhibition measuring  $26.13 \pm 0.103$  mm, which is comparable to standard drugs available on the market at the same concentration. The inhibition zones increased with the

concentration of *T. laurifolia* and dicloxacillin. The formulated cream demonstrated the potential for treating bacterial skin infections, particularly those caused by *S. aureus*, a common pathogen. The results also supported the synergistic activity of *T. laurifolia* extract and dicloxacillin, as evidenced by the larger inhibition zones. This aligns with previous research conducted by Liu *et al.* [30] and Sato *et al.* [31], suggesting that certain flavonoids can complement antibiotics and effectively inhibit bacterial growth. No activity against *E. coli* was observed for any of the samples or the positive control, and the negative control (base cream formulation) showed no zone of inhibition.

### 3.3 Stability Test

#### 3.3.1 Thermal stability

The results indicated that the product displayed exceptional stability, with no alterations in its physical characteristics or physicochemical properties observed throughout the temperature variations. This outcome highlights the product's ability to maintain its integrity, consistency, and overall quality under challenging conditions. The stability of the Rang Jeud cream is crucial as it ensures long-term effectiveness, reliability, and an extended shelf life.

#### 3.3.2 Light stability

The results demonstrated excellent light stability, as the product retained its original greenish color derived from the herbal extract. Even after being exposed to outdoor light for 7 days and indoor light for 1 month, the product showed no significant color alteration, indicating its ability to resist fading or discoloration. This light stability is vital as it ensures the product maintains its desired appearance and aesthetic appeal over time, guaranteeing visual consistency and quality throughout its shelf life.

#### 3.3.3 Gravity stability

The results revealed excellent stability, with no observed changes throughout the test period. The product demonstrated its ability to withstand centrifugal force without experiencing phase separation, sedimentation, or other undesirable alterations in its physical properties or formulation.

## 4. CONCLUSIONS

Based on the experimental results obtained in this study, it can be concluded that all objectives have been successfully met. The extract testing revealed that *T. laurifolia* aqueous leaf extract contains phytochemicals from the phenolic compound group, which can effectively inhibit the growth of pathogenic bacteria by targeting the bacterial cell wall. This aligns with the final product's antibacterial activity test, where adding the extract to the cream base formula resulted in significant inhibition of *S. aureus* bacteria. Furthermore, comparison with standard drugs in the market demonstrated comparable antibacterial efficacy at the same concentration, indicating the potential of this dark trough cream as a replacement for existing market drugs. Moreover, the cream formulation exhibited favorable tactile characteristics, resembling non-greasy creams and ointments commonly used to treat skin infections, because incorporating nanotechnology and structured lipid carriers allowed for a light and comfortable application, eliminating the need for viscous wax while effectively covering and moisturizing the skin. This product helps maintain skin moisture, promotes a healthy skin barrier, and balances the microbiome ecosystem, reducing the risk of bacterial infections. The cream's pH, which falls within the range of skincare oils with mild acidic properties, contributes to strengthening the skin's protective barrier. Overall, this study presents a promising product that treats bacterial skin infections or eczema skin problem, delivers superior sensory qualities, and supports skin health.

## 5. ACKNOWLEDGEMENT

The authors gratefully acknowledge the financial support provided by Faculty of Science and Technology, Contract No. SciGR 20/2565 and research fund of year 2022 from Department of Biotechnology, Faculty of Science and Technology, Thammasat University.

## 6. REFERENCES

- [22] Chaiyana W, Chansakaow S, Intasai N, Kiattisin K, Lee KH, Lin WC, Lue SC, Leelapornpisid P. (2020). Chemical Constituents, Antioxidant, Anti-MMPs, and Anti-Hyaluronidase Activities of *Thunbergia laurifolia* Lindl. Leaf Extracts for Skin Aging and Skin Damage Prevention. *Molecules*, 25(8), pp. 1923, DOI: 10.3390/molecules25081923.
- [23] Junsri M, Siripongvutikorn S. (2016). *Thunbergia laurifolia*, a traditional herbal tea of Thailand: botanical, chemical composition, biological properties and processing influence. *International Food Research Journal*, 23(3), pp. 923-927.
- [24] Nanna U, Chiruntanat N, Jaijoy K, Rojsanga P, Sireeratawong S. (2017). Effect of *Thunbergia laurifolia* Lindl. Extract on Anti-Inflammatory, Analgesic and Antipyretic Activity. *J Med Assoc Thai*, 100(5), pp. 98-106.
- [25] Chan EWC, Lim YY. (2006). Antioxidant activity of *Thunbergia laurifolia* tea. *Journal of Tropical Forest Science*, 18(2), pp. 130-136.
- [26] Junsri M, Siripongvutikorn S, Yupanqui CT, Usawakesmanee W. (2017). Phenolic and Flavonoid Compounds in Aqueous Extracts of *Thunbergia laurifolia* Leaves and Their Effect on the Toxicity of the Carbamate Insecticide Methomyl to Murine Macrophage Cells. *Functional Foods in Health and Disease*, 7(7), pp. 529-544, DOI: 10.31989/ffhd.v7i7.336.
- [27] Oh HKF, Siow LF, Lim YY. (2019). Approach to preserve phenolics in *Thunbergia laurifolia* leaves by different drying treatments. *J Food Biochem*, 43(7), pp. e12856, DOI: 10.1111/jfbc.12856.
- [28] Wonkchalee O, Boonmars T, Aromdee C, Laummaunwai P, Khunkitti W, Vaeteewoottacharn K, Sriraj P, Aukkanimart R, Loilome W, Chamgramol Y, Pairojkul C, Wu Z, Juasook A, Sudsarn P. (2012). Anti-inflammatory, antioxidant and hepatoprotective effects of *Thunbergia laurifolia* Linn. on experimental opisthorchiasis. *Parasitol Res*, 111(1), pp. 353-9, DOI: 10.1007/s00436-012-2846-5.
- [29] Chan EWC, Eng SY, Tan YP, Wong ZC. (2011). Phytochemistry and Pharmacological Properties of *Thunbergia laurifolia*: A Review. *Pharmacognosy Journal*, 3(24), pp. 1-6, DOI: 10.5530/pj.2011.24.1.
- [30] Mohiuddin AK. (2019). Skin Care Creams: Formulation and Use. *OSP J Clin Trials*, 1(1).
- [31] Chen MX, Alexander KS, Baki G. (2016). Formulation and Evaluation of Antibacterial Creams and Gels Containing Metal Ions for Topical Application. *J Pharm (Cairo)*, 2016, pp. 5754349, DOI: 10.1155/2016/5754349.
- [32] Bhide MM, Nitave SA. (2016). Formulation and evaluation of polyherbal cosmetic cream. *World J. Pharm. Pharm. Sci*, 5(1), pp. 1527-1536.
- [33] Akbari S, Nour AH. (2018). Emulsion types, stability mechanisms and rheology: A review. *International Journal of Innovative Research and Scientific Studies*, 1(1), pp. 14-21.
- [34] Khan BA, Akhtar N, Shoaib Khan HB, Waseem K, Mahmood T, Rasul A, Lqbal M, Khan H. (2011). Basics of pharmaceutical emulsions: A review. *Afr. J. Pharm. Pharmacol*, 5(25), pp. 2715-2725, DOI: 10.5897/AJPP11.698.
- [35] Souza IDL de, Saez V, Campos VEB de, Mansur CRE. (2019). Size and vitamin E release of nanostructured lipid carriers with different liquid lipids, surfactants and preparation methods. *Macromolecular Symposia*, 383(1), DOI: 10.1002/masy.201800011.
- [36] Ghasemiyeh P, Mohammadi-Samani S. (2018). Solid lipid nanoparticles and nanostructured lipid carriers as novel drug delivery systems: applications, advantages and disadvantages. *Res Pharm Sci*, 13(4), pp. 288-303, DOI: 10.4103/1735-5362.235156.
- [37] Garcês A, Amaral MH, Sousa Lobo JM, Silva AC. (2018). Formulations based on solid lipid nanoparticles (SLN) and nanostructured lipid carriers (NLC) for cutaneous use: A review. *Eur J Pharm Sci*, 112, pp. 159-167, DOI: 10.1016/j.ejps.2017.11.023
- [38] Chauhan I, Yasir M, Verma M, Singh AP. (2020). Nanostructured Lipid Carriers: A Groundbreaking Approach for Transdermal Drug Delivery. *Adv Pharm Bull*, 10(2), pp. 150-165, DOI: 10.34172/apb.2020.021.
- [39] Khosa A, Reddi S, Saha RN. (2018). Nanostructured lipid carriers for site-specific drug delivery. *Biomed Pharmacother*, 103, pp. 598-613, DOI: 10.1016/j.biopha.2018.04.055.
- [40] Purohit DK, Nandgude TD, Poddar SS. (2016). Nano-lipid carriers for topical application: Current scenario. *Asian J. Pharm*, 9(5), pp. 1-9, DOI: 10.22377/ajp.v10i1.544.
- [41] Arti P, Mianish S, Kalpana P. (2014). Formulation and Evaluation of Poly Herbal Cream. *International Journal of Pharmaceutical & Biological Archives*, 5(4), pp. 67-71.

- [42] Bhide MM, Nitave SA. (2015). Formulation and evaluation of polyherbal cosmetic cream. *World Journal of Pharmacy and Pharmaceutical Sciences*, 5(1), pp. 1527-1536.
- [43] Bharat P, Pankaj S, Atul K, Pankaj S. (2013). Formulation and evaluation of polyherbal face cream. *Internationale Pharmaceutica Scientia*, 3(3), pp. 63-68.
- [44] Choi WS, Cho HI, Lee HY, Lee SH, Choi WY. (2010) Enhanced Occlusiveness of Nanostructured Lipid Carrier (NLC)-based Carbogel as a Skin Moisturizing Vehicle. *J Pharm Inves*, (6)40, pp. 378-373, DOI: /10.4333/KPS.2010.40.6.373
- [45] Amasya G, Aksu B, Badilli U, Onay-Besikci A, Tarimci N. (2019). QbD guided early pharmaceutical development study: Production of lipid nanoparticles by high pressure homogenization for skin cancer treatment. *Int J Pharm*, 563, pp. 110-121, DOI: 10.1016/j.ijpharm.2019.03.056.
- [46] De Vringer, T. (1992). Topical preparation containing a suspension of solid lipid particles. European Patent No..91200664
- [47] Sekar M, Halim FH. (2017). Formulation and Evaluation of Natural Anti-Acne Cream Containing *Syzygium samarangense* Fruits Extract. *Annual Research & Review in Biology*, 17(3), pp. 1-7, DOI: 10.9734/ARRB/2017/36467
- [48] Priyadarsini SS, Kumar PR, Thirumal M. (2018). Formulation and evaluation of a herbal antibacterial cream from ethyl acetate extract of leaves of *Spinacia oleracea* Linn. against *Aeromonas* skin and soft tissue infections, 12(3), pp. 537-542.
- [49] Posridee K, Oonsivilai A, Oonsivilai R. (2022). Acute and sub-chronic toxicity study of Rang Chuet (*Thunbergia laurifolia* Lindl.) extracts and its antioxidant activities. *Toxicol Rep*, 9, pp. 2000-2017, DOI: 10.1016/j.toxrep.2022.11.002.
- [50] Junsu M, Takahashi Yupanqui C, Usawakesmanee W, Slusarenko A, Siripongvutikorn S. (2020) *Thunbergia laurifolia* Leaf Extract Increased Levels of Antioxidant Enzymes and Protected Human Cell-Lines In Vitro Against Cadmium. *Antioxidants (Basel)*, (1)9, pp. 47, DOI: /10.3390/antiox.9010047
- [51] Liu, I. X., Durham, D. G., and Richards, R. M. E. (2000). Baicalin synergy with  $\beta$ -lactam antibiotics against methicillin-resistant *Staphylococcus aureus* and other  $\beta$ -lactam-resistant strains of *S. aureus*. *J. Pharm. Pharmacol.* 52: 361-366.
- [52] Sato, Y., Shibata, H., Arakaki, N., and Higuti, T. (2004). 6,7-Dihydroxyflavone dramatically intensifies the susceptibility of methicillin-resistant or  $\beta$ -sensitive *Staphylococcus aureus* to beta-lactams. *Antimicrob. Agents Chemother.* 48: 1357- 1360.

# Marine actinomycetes isolation from mangrove sediment and partial purification of their anticancer activity

Tepakorn Kongsaya<sup>1</sup> and Bungonsiri Intra<sup>1,2\*</sup>

<sup>1</sup>Department of Biotechnology, Mahidol University, Bangkok, 10400, Thailand

<sup>2</sup>Mahidol University-Osaka University Collaborative Research Center for Bioscience and Biotechnology (MU-OU: CRC), Mahidol University, Bangkok, 10400, Thailand

\*Correspondence to: Department of Biotechnology, Mahidol University, Address, Bangkok, 10400, Thailand. Bungonsiri.int@mahidol.edu

**ABSTRACT:** Cancer is a major leading cause of morbidity and mortality worldwide, affecting people on a global scale. Marine actinomycetes are a promising source for discovering novel therapeutic agents due to their diverse chemical structures and biological functions. This study aims to isolate and partially purify an anticancer compound from marine actinomycetes. A total of forty-three actinomycetes-like colonies were successfully isolated derived from the sediment of the mangrove forest. All the isolated strains were tested for antagonistic activity against *S. cerevisiae* IFO 10725. The results showed that only 3 strains (MTK11, MTK26, and MTK30) exhibited strong anti-yeast activity and were selected for additional evaluation anticancer activity against human breast (MCF-7) and colorectal (HCT-116) cell lines. The crude extract of *Streptomyces* sp. strain MTK26 displayed promising activity against both cancer cell lines. Doxorubicin (Positive controls) had activity against MCF-7 and HCT-116 with 79.88 and 93.84%, respectively. This crude extract was partial purification through a Sep-Pak C18 Plus short cartridge using a water and acetonitrile system. Fractions with 40% acetonitrile (ACN) and 60%ACN demonstrated inhibitory activity against breast cancer cells, with inhibitory percentages of 93.72% and 93.96%, respectively. Additionally, these two fractions along with the 80%ACN, exhibited potent anticancer activity with more than 90% inhibitory activity against colorectal cancer cells. Consequently, fractions 40%ACN and 60%ACN were chosen for further purification and structural elucidation.

**Keyword:** Anticancer activity, Marine actinomycetes, Secondary Metabolite

## 1. INTRODUCTION

Cancer is a life-threatening disease that has become a major concern for human health in the 21<sup>st</sup> century [1]. In Thailand, there were 190,636 reported new cancer cases and 124,866 cancer-related deaths in 2020. The common types of cancer in Thailand are liver, lung, breast, and colorectal cancer (data reported from GLOBOCAN). Chemotherapy is standard cancer treatment in most cases [2], but it often faces drug resistance due to DNA mutation and drug degradation mechanisms [3]. However, this treatment comes with various side effects by affect DNA and protein expression in both cancer and normal cells, leading to problems such as nausea, vomiting, mucositis, and diarrhea [4]. Therefore, the search for effective anticancer agents remains a major goal in cancer therapy [5].

Natural products are an important source of cancer treatments, with over 48% of drugs approved between January 1981 to September 2019 being anticancer or anti-infection agents based on natural products and their derivatives [6]. Actinomycetes are potential sources of natural products with broad biological properties and are commonly found in terrestrial and marine environments. While the metabolites from terrestrial bacteria are well-known, researchers have increasingly turned their focus to the marine environment for discovering secondary metabolites due to its extreme conditions. Marine actinomycetes that survive in such extreme environments may produce unique compounds that hold promise for natural product research [7]. Therefore, this research aims to isolate marine actinomycetes with potent anticancer activity from mangrove forest in Thailand and partially purify the anticancer compounds from the crude extraction.



## 2. MATERIALS AND METHODS

### Isolation and identification of actinomycetes from mangrove sediment

Mangrove sediment was collected from Chanthaburi province in Thailand (12°31'51.6"N; 102°03'00.9"E) and stored in a polyethylene bag at 4°C. The collected sediment was pretreated by air-drying at room temperature for a week. To begin the isolation process, one gram of sample was suspended in 9 ml of sterile normal saline, and then 100 µL of each dilution was spread on various media: water proline (WP) agar (proline 10 g, agar 15 g and tap water to 1 l), water proline with 10% seawater (WP10%) agar, water proline with 20% seawater (WP20%), starch casein nitrate (SCA) agar (soluble starch 10 g, casein (vitamin free) 0.3 g, KNO<sub>3</sub> 2 g, MgSO<sub>4</sub>·7H<sub>2</sub>O 0.05 g, K<sub>2</sub>HPO<sub>4</sub> 2 g, NaCl 2 g, CaCO<sub>3</sub> 0.02 g, FeSO<sub>4</sub>·7H<sub>2</sub>O 0.01 g, agar 15g and reverse osmosis water to 1 l), starch casein nitrate with 10% seawater (SCA10%) agar (soluble starch 10 g, casein 1 g, agar 15 g and made up with 10% seawater) and starch casein nitrate with 20% seawater (SCA20%) agar. The isolation plates were supplemented with cycloheximide (50 µg/mL) and nalidixic acid (25 µg/mL) to inhibit the growth of fungi and Gram-negative bacteria, respectively. The plates were then incubated at 30°C for 14 days. After the incubation period, actinomycetes-like colonies were selected and streaked on the same agar medium. Pure cultures were preserved in tryptic soy broth (TSB) with 20% glycerol at -20°C.

The actinomycetes with potential activity were cultivated in 301 medium for 3 days to produce cell biomass. The DNA template's concentration and purity were determined using a µdrop (Thermo Scientific Multiskan GO microplate Spectrophotometer). Amplification of the 16S rRNA gene sequences from the DNA template was performed using universal primers 27F (5'-AGAGTTTGATCCTGGCTCAG-3') and 1492R (5'-TACGGCTACCTTGTTACGACTT-3'). The PCR reaction consisted of an initial denaturation at 95°C for 5 min, followed by 30 cycles of amplification (95°C for 30 sec, 52°C for 30 sec, 72°C for 2 min) and a final extension at 72°C for 5 min. The 16S rRNA sequences were then compared with available sequences in the EZbioCloud database (<https://www.ezbiocloud.net>) for species identification. To construct the phylogenetic tree, MEGA11 software was used with the neighbor-joining algorithm to align the homologous regions in the sequences.

### Screening for antagonistic activity

The primary screening involved the agar well diffusion method. Pure cultures of isolated strains were cultivated in 301 medium for 7 days. The culture broths were then centrifuged to collect the supernatant. Next, 100 µl (1×10<sup>6</sup> CFU/ml) of *Saccharomyces cerevisiae* IFO 10725 was swabbed with sterile cotton on yeast extract peptone dextrose (YPD) agar (yeast extract 10 g, peptone 20 g, dextrose 20 g, agar 15g, and reverse osmosis water to 1 l). Wells with a diameter of 6 mm were created using a cork borer and 200 µl of each supernatant was dispensed into the wells. The plates were incubated at 30°C overnight, and the inhibition zones were observed.

For the secondary screening, the crude extract of isolated strains was dissolved with methanol and dropped onto sterile 6 mm blank paper disks. After the crude extract was dried, the disks were transferred on the surface of YPD agar swabbed with *S. cerevisiae* IFO 10725. After incubating the plates for 24 hours, the zone of inhibition was measured.

### Production and extraction of secondary metabolites

The isolated strains were precultured in 301 medium on an incubator shaker (200 rpm) for 3 days. The seed culture was then transferred into a baffled flask containing 100 ml of 301 medium and incubated for 7 days. Then, the culture broth was centrifuged at 4°C, 8000 rpm for 10 minutes to obtain cell-free the supernatant, which was filtrated using Kimwipes paper. Ethyl acetate extraction was performed using a separatory funnel to collect the organic layer, which was subsequently evaporated using a rotary evaporator. Intracellular metabolites were obtained using ethanol and concentrated into a dry extract. The supernatant was combined with the intracellular extract to yield the crude extract.

### Anticancer activity test

The anticancer activity of crude extracts or fractions was investigated using the MTT (3-(4,5-dimethylthiazol-2-yl)-2,5-diphenyltetrazolium bromide) assay conducted by the Excellent Center for Drug Discovery (ECDD) in Thailand. Human breast cancer (MCF-7) and human colorectal cancer (HCT-116) cell lines were seeded into 96-well microtiter plates at a concentration of  $2 \times 10^3$  cell/ml and incubated for 24 hours. The dried extracts were dissolved in dimethyl sulfoxide (DMSO) to a final concentration of 10 µg/ml and then treated with the cell for 72 hours. Doxorubicin was used as a positive control, while DMSO served as the negative control. After the treatment period, the cells were incubated with MTT solution for 3 hours, and the formazan crystals were solubilized in DMSO and the absorbance was measured at 570 nm.

### Bioassay-guide fractionation

The crude extract with high inhibitory activity was fractionated using a Sep-Pak® C18 Plus short cartridge (Water, Milford, MA, USA). The soluble extract was loaded into the column and eluted with an acetonitrile-water system ranging from 20% to 100% (v/v) acetonitrile, resulting in 5 fractions. Each fraction was then evaporated using rotary evaporator, and their activity against cancer cell lines.

### High performance liquid chromatography

The Fraction was investigated the metabolic profiles using HPLC (Agilent HP1100 system) with a photodiode array UV-Vis detector (200-600 nm) and a reverse phase column (Cadenza CD-C18 reverse phase symmetry column, 2.1×150 mm, 3.5 µm pore size). The mobile phase consisted of a gradient from 5% to 100% CH<sub>3</sub>CN with 0.1% CH<sub>2</sub>O<sub>2</sub> at a column temperature at 40°C. The flow rate was set at 1 ml/min and the UV wavelength detected at 254 nm.

## 3. RESULTS AND DISCUSSION

### Isolation of marine actinomycetes

A total of 43 actinomycete-like colonies (as shown in Figure 1) were successfully isolated from the sediment of the mangrove forest using various media, as detailed in Table 1. Among the media used, starch casein nitrate agar (SCA) demonstrated the highest number of isolated strains, followed by water proline agar (WP) with 10% seawater. However, only 2 isolates were obtained from SCA with 10% seawater. SCA medium has been reported as a specific selective medium for isolating actinomycetes [8] because it provides complex substrates such as starch, casein, and nitrate, which can reduce the growth of other microbes. Additionally, WP agar is recommended for isolating antibiotic-producing actinomycetes [9], making it conducive for increasing the ratio of seawater and providing complex ions. This creates an opportunity to isolate marine microorganism especially rare actinomycetes [10].



Figure 1 Examples of isolated marine actinomycete-like colonies.

Table 1. The number of isolated actinomycete-like colonies from different cultivation media.

Number of isolated strains					
Isolation medium					
SCA	SCA10%	SCA20%	WP	WP10%	WP20%
13 (MTK01-13)	2 (MTK14-15)	8 (MTK16-23)	6 (MTK24-29)	10 (MTK30-39)	4 (MTK40-43)

### Antagonistic activity

All isolated strains were evaluated for antagonistic activity using the agar well diffusion method. Fourteen strains exhibited activity against *S. cerevisiae* IFO 10752, as shown in Table 2. Among them, strain MTK11 showed the maximum inhibition zone of 41.0 mm. However, all active strains with antagonistic activity were selected for disk diffusion test.

The crude extract of three strains (MTK11, MTK26, and MTK30) exhibited strong anti-yeast activity. Notably, MTK11 still showed the largest zone of inhibition, approximately 20.0 mm against the indicator strain. These promising strains were chosen for the anticancer activity test. The results indicated that the zone of inhibition in the secondary screening dramatically decreased compared to the primary screening. This decrease can be attributed to the fact that the supernatant contained a mixture of metabolites [11] that were active against the indicator strain. During the process of ethyl acetate extraction, compounds with semi-polar and non-polar characteristics were obtained [12]. Additionally, there is possibility that some compound degradation might have occurred which potentially influenced the observed activity in the secondary screening. Nonetheless *S. cerevisiae* has been reported as a model for screening potential compounds for cancer therapy. Yeast cells contained 30% of conserved genes similar to humans which are related to cancer pathways such as DNA replication checkpoint, DNA damage checkpoint and mitogen stimulation [13]. This biological similarity makes yeast cells an ideal candidate for the primary screening of anticancer compounds in this experiment.

Table 2. Antagonistic activity of isolated marine actinomycetes against *S. cerevisiae* IFO 10752 by agar well diffusion & Disk diffusion methods.

Isolated name	Inhibition zone (mm)	
	Agar well diffusion method	Disk diffusion method
MTK4	26.5	-
MTK5	20.0	-
MTK7	21.0	-

\* The diameter of inhibition zones including the diameter of well and paper (6 mm), - = No activity.

Table 2. Antagonistic activity of isolated marine actinomycetes against *S. cerevisiae* IFO 10752 by agar well diffusion & Disk diffusion methods. (continued)

Isolated name	Inhibition zone (mm)	
	Agar well diffusion method	Disk diffusion method
MTK10	19.5	-
MTK11	41.0	20.0
MTK14	17.0	-
MTK16	19.5	-
MTK22	24.0	-
MTK26	20.0	13.0
MTK30	20.5	11.0
MTK32	18.0	-
MTK35	18.5	-
MTK36	9.0	-
MTK39	16.5	-

\* The diameter of inhibition zones including the diameter of well and paper (6 mm), - = No activity.

### Anticancer activity

Anticancer activity was assessed against two cancer cell lines, MCF-7 and HCT-116, as shown in Figure 2. The crude extract of MTK26 demonstrated potential anticancer activity against both cancer cell lines, with more than 80% inhibitory activity comparable to the positive control (Figure 1). As a result, the crude extract of this strain was partially purified into fractions, which were then evaluated for their anticancer activity. All three selected strains displayed distinct morphology, suggesting the presence of different species. This variance in species could potentially lead to the production of various compounds.

Activity against breast cancer cell lines (37.19-93.96%) and colorectal cancer cells (75.71–96.43%) was exhibited by all fractions, as depicted in Table 3. Specifically, significant growth inhibition of MCF-7 cells at 96.43% and 96.36% inhibition was observed in fractions 40%ACN and 60%ACN, respectively. Conversely, strong inhibitory activity against HCT-116 cells was demonstrated by three fractions: 40%ACN, 60%ACN, and 80%ACN. In contrast, the lowest activity against both cancer cell lines were shown by 100%ACN. These results suggest that fractions 40% and 60% are potential candidates for further purification. The target compounds were assumed to have retention time between 16-18 minutes, indicating less polarity based on the HPLC chromatogram (Table 3). Based on partial purification method, the compounds were eluted with distinct characteristics across various fractions. These distinct characteristics have an impact on the observed anticancer activity within each respective fraction.

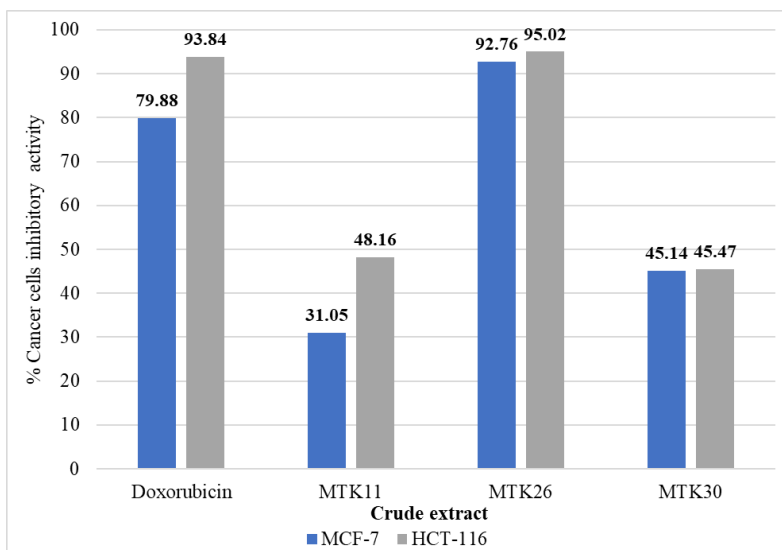
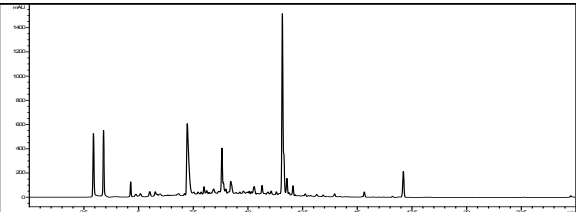
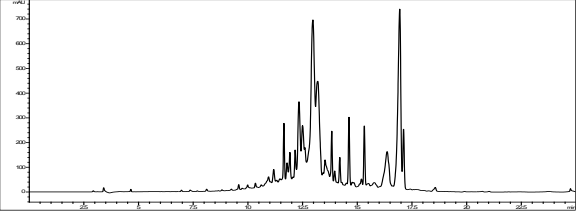
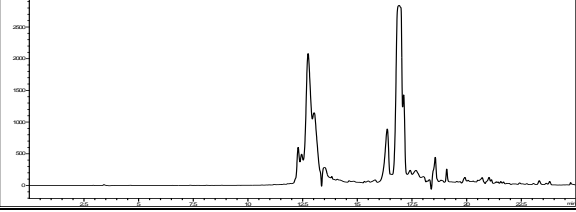


Figure 2 The percentage inhibitory activity of crude extract against MCF-7 and HCT-116 cancer cell lines.

Table 3 Percent inhibitory activity and chromatogram profile of each fraction from MTK26 against human breast cancer (MCF-7) and human colorectal cancer (HCT-116) cell lines

Fraction Name	HPLC chromatogram profile	% Inhibitory activity against cancer cell lines	
		MCF-7	HCT-116
Doxorubicin (Positive controls)	-	79.88	93.84
20%Acetonitrile (20%ACN)		58.29	81.31
40%Acetonitrile (40%ACN)		<b>93.72*</b>	<b>96.43*</b>
60%Acetonitrile (60%ACN)		<b>93.96*</b>	<b>96.36*</b>

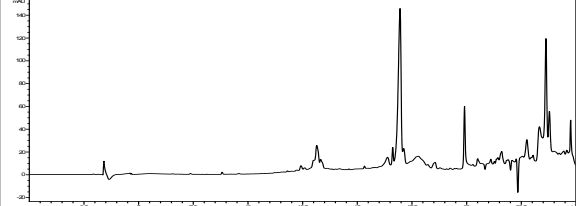
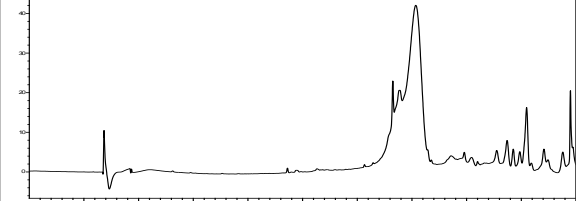
80%Acetonitrile (80%ACN)		78.20	<b>90.91*</b>
-----------------------------	--	-------	---------------

Table 3 Percent inhibitory activity and chromatogram profile of each fraction from MTK26 against human breast cancer (MCF-7) and human colorectal cancer (HCT-116) cell lines

Fraction Name	HPLC chromatogram profile	% Inhibitory activity against cancer cell lines	
		MCF-7	HCT-116
100%Acetonitrile (100%ACN)		37.19	75.71

\*The inhibitory activity against cancer cell line is greater than that of the positive control.

### Identification of marine actinomycetes with potential anticancer activity

The almost complete 16S rRNA gene sequence (1,499 bp) of MTK26 was found to be closely related to *Streptomyces albiflaviniger* NRRL B-1356<sup>T</sup> and *Streptomyces yogyakartensis* NBRC 100779<sup>T</sup>, with 99.08% and 99.03% sequence similarity, respectively. The phylogenetic tree (Figure 3) shows that MTK26 formed an independent branch in cluster I with a bootstrap value of less than 50%. A suggested cutoff for species-level identification is a 16S rRNA gene sequence similarity ranging from 98.2% to 99.0% [14]. Thus, MTK26 exhibits potential as a novel species based on criteria for species identification should further investigation through genome sequencing and taxonomic studies is necessary to confirm the novelty of this strain.



Figure 3 The Neighbor-Joining tree based on 16S rRNA sequences of MTK26 with 1000 bootstrap values. Cluster I comprise a group of *Streptomyces* species that cluster together in both the Neighbor-Joining and Minimum-evolution algorithms.

#### 4. CONCLUSIONS

Forty-six actinomycete-like colonies were successfully isolated from the mangrove forest sediment. Among them, three strains (MTK11, MTK26, and MTK30) demonstrated potential antagonistic activity against *S. cerevisiae* IFO 10752. Notably, the crude extract of *Streptomyces* sp. strain MTK26 exhibited strong anticancer activity against both human breast (MCF-7) and human colorectal cancer (HCT-116) cell lines. Moreover, fraction 40%ACN and 60%ACN showed promise as candidates for further purification of target compounds, which will be subjected cytotoxicity test with normal cells and for elucidating their structure.

#### 5. ACKNOWLEDGEMENT

This research project is supported by Mahidol University (Fundamental Fund: fiscal year 2023 by National Science Research and Innovation Fund (NSRF)). Additionally, it is partially supported by CIF and CNI, faculty of science, Mahidol University. The authors are thankful for financial support from the Scholarship for Young Scientist 2023.

## 6. REFERENCES

1. Baidara, P. and S.M. Mandal, *Bacteria and bacterial anticancer agents as a promising alternative for cancer therapeutics*. Biochimie, 2020. **177**: p. 164-189.
2. Zaigham, A. and R. Sakina, *An Overview of Cancer Treatment Modalities*, in *Neoplasm*, S. Hafiz Naveed, Editor. 2018, IntechOpen: Rijeka. p. Ch. 6.
3. Housman, G., et al., *Drug Resistance in Cancer: An Overview*. Cancers (Basel), 2014. **6**(3): p. 1769-1792.
4. Amjad, M.T., A. Chidharla, and A. Kasi, *Cancer Chemotherapy*, in *StatPearls*. 2023, StatPearls Publishing Copyright © 2023, StatPearls Publishing LLC.: Treasure Island (FL) ineligible companies. Disclosure: Anusha Chidharla declares no relevant financial relationships with ineligible companies. Disclosure: Anup Kasi declares no relevant financial relationships with ineligible companies.
5. Law, J.W.-F., et al., *Anticancer Drug Discovery from Microbial Sources: The Unique Mangrove Streptomyces*. 2020. **25**(22): p. 5365.
6. Newman, D.J. and G.M. Cragg, *Natural Products as Sources of New Drugs over the Nearly Four Decades from 01/1981 to 09/2019*. Journal of Natural Products, 2020. **83**(3): p. 770-803.
7. Jagannathan, S.V., et al., *Marine Actinomycetes, New Sources of Biotechnological Products*. 2021. **19**(7): p. 365.
8. KÜster, E. and S.T. Williams, *Selection of Media for Isolation of Streptomyces*. Nature, 1964. **202**(4935): p. 928-929.
9. Huck, T.A., N. Porter, and M.E. Bushell, *Positive selection of antibiotic-producing soil isolates*. 1991. **137**(10): p. 2321-2329.
10. Subramani, R. and W. Aalbersberg, *Marine actinomycetes: An ongoing source of novel bioactive metabolites*. Microbiological Research, 2012. **167**(10): p. 571-580.
11. Mani-López, E., D. Arrijoja-Bretón, and A. López-Malo, *The impacts of antimicrobial and antifungal activity of cell-free supernatants from lactic acid bacteria in vitro and foods*. Compr Rev Food Sci Food Saf, 2022. **21**(1): p. 604-641.
12. Ariel, D., et al., *Optimization of Combination of N-Hexane Solution and Ethyle Acetate on Secondary Metabolite Compounds Profile of Streptomyces hygrosopicus*. Jurnal Kedokteran Brawijaya, 2021. **31**: p. 186.
13. Gao, G., L. Chen, and C. Huang, *Anti-cancer drug discovery: update and comparisons in yeast, Drosophila, and zebrafish*. Curr Mol Pharmacol, 2014. **7**(1): p. 44-51.
14. Kim, M., et al., *Towards a taxonomic coherence between average nucleotide identity and 16S rRNA gene sequence similarity for species demarcation of prokaryotes*. 2014. **64**(Pt\_2): p. 346-351.



## Phosphatidylserine production via a two-stage carbon dioxide utilization technology

Zhong-Lin Li<sup>1</sup>, Jian-Yu Lin<sup>1</sup> and Liang-Jung Chien<sup>1\*</sup>

<sup>1</sup>Department of Chemical Engineering, Ming Chi University of Technology, New Taipei City, 243303, Taiwan

\*Correspondence to: Department of Chemical Engineering, Ming Chi University of Technology, New Taipei City, 243303, Taiwan. LJCHIEN@mail.mcut.edu.tw

**ABSTRACT:** Phosphatidylserine (PS), a fatty substance that protects the nerve cells in your brain and enables them to communicate with each other, is extensively used in functional food, health, chemical, and pharmaceutical industries. In this research, we constructed a tri-gene cyanobacterium integrative vector, pSerACB, encoding 3-phosphoglycerate dehydrogenase (SerA), phosphoserine aminotransferase (serC), and phosphoserine phosphatase (SerB), and linear fragments of pSerACB were inserted into neutral-site NS1 to allow *Synechococcus elongates* PCC7942 strain metabolize carbon dioxide synthesis L-serine. The maximum L-serine reaches 2.78 g/L in genetically modified *Synechococcus elongates* Cs23 strain under 34°C and 3% CO<sub>2</sub> for 56h. We used a phospholipase D-immobilized magnetic catalyst to catalyze L-serine and soybean lecithin for further PS synthesis. The PLD-catalyzed PS synthesis process showed an 83.2% conversion rate and 1.86 g/L of accumulated PS concentration under a substrate (soybean lecithin: L-serine) concentration ratio of 1: 5, 10 mM Ca<sup>2+</sup> ion, 45°C, and 12h reaction time. This research provides a novel green approach to carbon dioxide utilization.

**Keywords:** Phosphatidylserine, *Synechococcus elongates*, carbon dioxide, phospholipase D.

# Minocycline encapsulation in PEG-PLGA nanoparticles

Monthira Rattanatayaron<sup>1</sup> and Nisa Patikarnmonthon<sup>1,2\*</sup>

<sup>1</sup>Department of Biotechnology, Faculty of Science, Mahidol University, Bangkok, 10400, Thailand

<sup>2</sup>Mahidol University-Osaka University Collaborative Research Center for Bioscience and Biotechnology, Faculty of Science, Mahidol University, Bangkok, 10400, Thailand

\*Correspondence to: Department of Biotechnology, Faculty of Science, Mahidol University, Bangkok, 10400, Thailand. nisa.pat@mahidol.edu

**ABSTRACT:** Minocycline (MIN) is one of the three antibiotics for dental pulp infection treatment, with broad-spectrum antimicrobial and bacteriostatic activities. However, it can be rapidly removed from the body due to its hydrophilic property. To overcome the problem, the encapsulation of the MIN into the PEG-PLGA nanoparticles can be applied for efficient treatment. Hence, this study aims to find suitable conditions for preparing PEG-PLGA nanoparticles and to enhance the encapsulation efficiency of MIN-loaded PEG-PLGA nanoparticles. The nanoparticles were formed using the solid-in-oil-in-water (S/O/W) method. Then, a further step was done to remove the organic solvent from the nanoparticle solution either by dialysis or vacuum. The data from dynamic light scattering showed that the dialysis method provided particles size of  $116.3 \pm 1.1$  d.nm with lower PDI ( $0.209 \pm 0.004$ ). On the other hand, the vacuum method gave the bigger particles ( $136.2 \pm 2.7$  d.nm) with higher PDI ( $0.348 \pm 0.013$ ). Thus, MIN-loaded PEG-PLGA nanoparticles were formed with good size ( $103.1 \pm 0.6$  d.nm) and PDI ( $0.113 \pm 0.011$ ), but with low encapsulation efficiency (%EE) of 1.66%. Therefore, to enhance the %EE, the ion-pairing agents including dextran sulfate (DS), deoxycholic acid (DOC), oleic acid (OA), and tripolyphosphate (TPP) were added to precipitate the MIN molecule in the MIN-loaded PEG-PLGA nanoparticles formation. The mass ratios which provided the highest precipitation were 1:2 for DS, 1:1 for DOC, 1:2 for OA, and 1:5 for TPP, resulting in %EE of 26.58%, 3.20%, 9.39%, and 2.86%, respectively. The results showed that the presence of an ion-pairing agent provides a higher %EE compared to the MIN-loaded PEG-PLGA nanoparticles without the addition of an ion-pairing agent. This may conclude that DS seems to be the most suitable ion-pairing agent to help enhance MIN encapsulation for PEG-PLGA nanoparticle formation.

**Keyword:** Nanoparticle, Encapsulation, Minocycline, Ion-pairing agents

## 1. INTRODUCTION

Dental pulp infection is associated with polymicrobial, mainly bacteria, in the pulp of the tooth. It can be caused by small factors such as aging, smoking, mistreating dental cavities, and periodontal problems. Those factors can cause damage to the tooth and further damage the pulp, giving a chance for the microbes to infect the pulp [1]. Once the infection occurs, antibiotics will be used to eliminate the possible infection along with the dental pulp regeneration treatment [2]. Hence, the commonly used antibiotics are called 3Mix consisting of ciprofloxacin (CIP), metronidazole (MET), and minocycline (MIN). MIN is a tetracycline antibiotic with a bacteriostatic effect as its activity causes inhibition of protein synthesis in bacteria. It is considered a broad-spectrum antibiotic with efficient activity against both gram-positive and gram-negative pathogens [3]. Minocycline in the market is the hydrophilic derivative, it has been reported to be rapidly removed from the body

according to its hydrophilic property [4]. Hence, MIN needed to be added regularly with high concentration to obtain an efficient treatment, which comes along with various effects. Thus, encapsulating MIN into nanoparticles to prolong the presence of MIN can be applied to overcome the drawback. Poly (ethylene glycol) methyl ether-*block*-poly(lactide-*co*-glycolide) or PEG-PLGA is one of the most used polymers with FDA-approved materials with self-assemble, biodegradable, and biocompatible abilities [5]. Using PEG-PLGA as a polymer to encapsulate MIN seems to be a good choice. However, the encapsulation method and condition must be determined to obtain the desired size with high encapsulation efficiency. Therefore, this study aims to find suitable conditions for preparing PEG-PLGA nanoparticles and to enhance the encapsulation efficiency of MIN-loaded PEG-PLGA nanoparticles.

## 2. MATERIALS AND METHODS

### Materials

Poly (ethylene glycol) methyl ether-*block*-poly(lactide-*co*-glycolide) (PEG average  $M_n$  2,000, PLGA average  $M_n$  11,500), minocycline HCl (MIN), oleic acid, and sodium tripolyphosphate were purchased from Sigma-Aldrich Corp., St. Louis, MO, USA. Dextran sulfate sodium salt from *Leuconostoc* spp. with a molecular weight more than 500,000 g/mol was purchased from Sigma-Aldrich Chemie GmbH, Riedstr, Steinheim, Germany. Deoxycholic acid, sodium salt was purchased from Merck KGaA, Frankfurter Str., Darmstadt, Germany. Acetone was purchased from RCI Labscan, Bangkok, Thailand. Dialysis membrane with MWCO-6-8000 was purchased from Spectra/Por, Thomas Scientific, Swedesboro, New Jersey, USA.

### Methods

#### PEG-PLGA nanoparticles preparation

The nanoparticles were formed using solid-in-oil-in-water (S/O/W) with and without an ion-pairing agent added as described by Kashi and Watcharadulyarat [6-7]. PEG-PLGA was dissolved with 1 ml of acetone in the concentration of 20 mg/ml. 0.07 ml of distilled water or MIN was added to the polymer solution. For condition with ion-pairing, 0.03 ml of ion-pairing agent (IP) was also added into the solution. Then the solution was injected into 6 ml of distilled water, forming nanoparticles. After the formation, the nanoparticles solution was further dialysis or vacuum to remove the acetone. For the dialysis method, the nanoparticles solution was dialyzed against distilled water at room temperature under magnetic stirring for 6 hours and changed the water every 2 hours. For the vacuum approach, the nanoparticle solution was left in the vacuum oven at room temperature overnight. The nanoparticles were characterized by size and PDI using dynamic light scattering (DLS) technique.

#### Suitable ratio of IP and MIN for nanoparticle formation

With equivalent volume in the formation of the nanoparticles, each IP including dextran sulfate (DS), deoxycholic acid (DOC), tripolyphosphate (TPP), and oleic acid (OA) was mixed with a fixed amount of MIN. The amount of the IP was varied to have the mass ratio of IP:MIN as 1:10, 1:5, 1:2, 1:1, and 2:1 (hereinafter referred to as 0.1, 0.2, 0.5, 1, and 2). Then the turbidity of the mixture was measured with a microplate reader (MULTISKAN GO, Thermo Scientific) at an absorbance of 600 nm, in order to determine the suitable IP:MIN ratio for each IP.

### Encapsulation efficiency of MIN-loaded PEG-PLGA nanoparticles

The mass ratio with the most turbidity for each ion-pairing agent was further used in the MIN-loaded PEG-PLGA nanoparticles formation as mentioned earlier. For the encapsulation efficiency (%EE) of MIN-loaded PEG-PLGA nanoparticle, the sample was lyophilized prior to resuspend back in DMSO with the equivalent volume sample before lyophilization. The absorbance of MIN at 367 nm was measured by a microplate reader. Then, the %EE was determined by the following equation (1).

$$\text{Encapsulation efficiency (\%EE)} = \frac{\text{Weight of drug in nanoparticles}}{\text{Initial weight of drug}} \times 100 \quad (1)$$

### Statistical analysis

The statistical analysis was performed, and the results were shown as mean  $\pm$  standard deviation. The difference between the two groups was evaluated using a two-sided, unpaired *t*-test. With more than three groups, an analysis of variance (ANOVA) followed by Tukey's multiple comparisons test was performed. Significant differences are represented as \*\*, \*\*\*, \*\*\*\* for  $P < 0.01$ , 0.001, and 0.0001, respectively.

## 3. RESULTS AND DISCUSSION

### PEG-PLGA nanoparticles preparation

The PEG-PLGA nanoparticles were formed using the S/O/W method, after that the acetone was removed by dialysis and vacuum. The size distribution of nanoparticles was further characterized by the DLS technique. As shown in Table 1, the nanoparticles obtained after dialysis were smaller in size with low PDI values when compared to vacuum. However, both techniques provided the size of nanoparticles in the acceptable range. According to the previous study [8], nanoparticles with a size between 10-200 d.nm tend to provide an acceptable drug prolongation property; otherwise, they will be rapidly removed. The size distribution of the vacuumed nanoparticles (Figure 1) showed the presence of large particles of around 5000 d.nm, which can be confirmed by a high number of PDI ( $0.348 \pm 0.010$ ). The acceptable PDI values of polymeric nanoparticles are less than or equal to 0.2, as suggested in the previous report [9]. The dialysis method provided nanoparticles with a closer PDI value to 0.2 ( $0.209 \pm 0.004$ ) is a more desirable approach. Hence, with the smaller size and PDI value, dialysis was chosen in this work as a method for removing the organic solvent after the formation of the nanoparticles.

Table 1 The effect of the organic solvent removal method on Z-Average (d.nm.) and PDI of PEG-PLGA nanoparticles

Organic solvent removal method	Z-Average (d.nm)	PDI
Dialysis	116.3 $\pm$ 1.1	0.209 $\pm$ 0.004
Vacuum	136.2 $\pm$ 2.7	0.348 $\pm$ 0.013

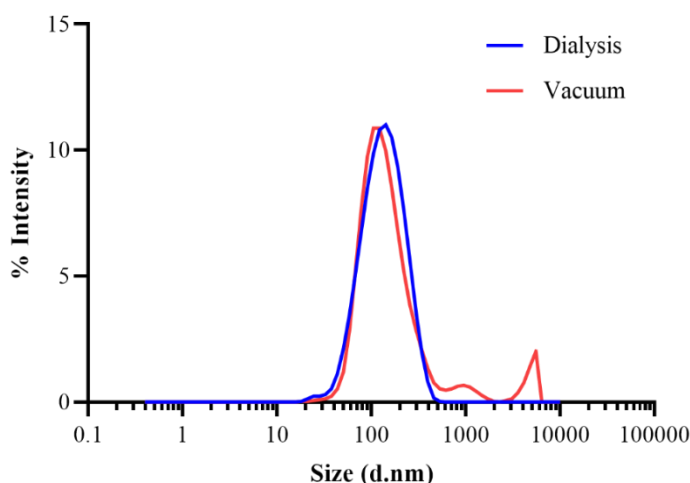


Figure 1 The size distribution plot of PEG-PLGA nanoparticles prepared by dialysis and vacuum methods to remove the organic solvent.

#### MIN-loaded PEG-PLGA nanoparticles preparation

The hydrophilic property of MIN affects not only the efficiency of the treatment but also the difficulty of encapsulation. The %EE of MIN-loaded PEG-PLGA nanoparticles was 1.66% which is considered as low encapsulation. Hence, the ion-pairing (IP) agents were introduced to help precipitate MIN to improve the encapsulation. DS, DOC, TPP, and OA were chosen to be representatives of potent ion-pairing agents reported previously [10]. However, the suitable ratio between ion-pairing and MIN should be determined before the actual MIN-loaded PEG-PLGA nanoparticles formation. The mass ratio of each IP to MIN was varied to be 0.1, 0.2, 0.5, 1, and 2 and then the turbidity of the sample was measured to find the most precipitate ratio. DS, DOC, TPP, and OA showed the most precipitating ability with a mass ratio of 0.5, 1, 0.2, and 0.5, respectively as shown in Figure 2. TPP and OA appeared to provide low and similar turbidity throughout all tested ratios, which indicated the low precipitation of MIN. On the other hand, the absorbance of the sample was sharply increased as the mass ratio of IP: MIN increased from 0.1 to 0.5 for DS and 0.1 to 1 for DOC, then decreased afterward. A bell-like curve was not expected as the precipitation was expected to be saturated, not decreased. According to Jain [11], the bell-like curve suggested that the IP was saturated and preferred to aggregate into micelles that are completely soluble. This could be a possible explanation for the decrease in the turbidity of the sample with high IP.

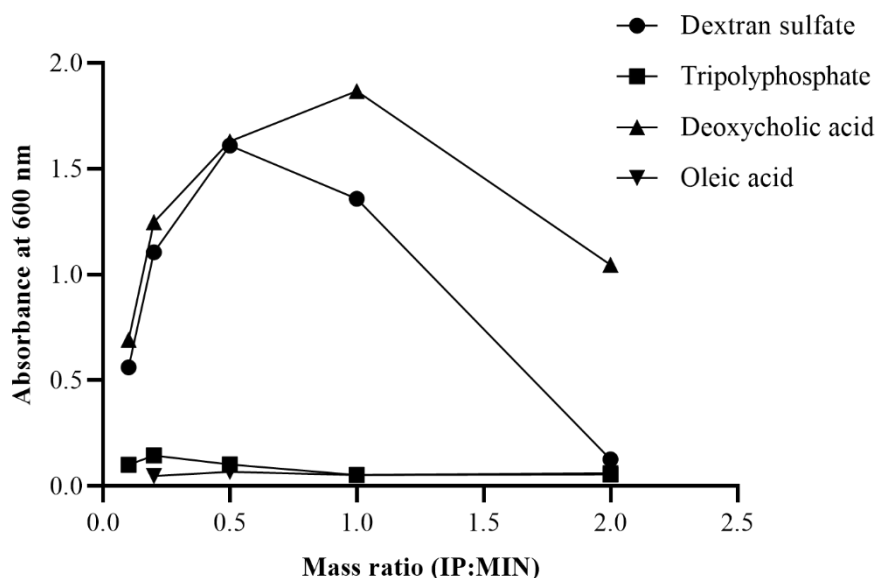


Figure 2

Effect of ion-pairing agents to minocycline mass ratio to the turbidity at 600 nm

Those mass ratios with the highest MIN precipitation were further used in MIN-loaded PEG-PLGA nanoparticle formation. The size and PDI of the nanoparticles were characterized, as shown in Table 2. The size of the MIN-loaded PEG-PLGA nanoparticles are all in the suitable range (10-200 d.nm). When considering the PDI value, all IP provided PDI values in the acceptable range except for OA ( $0.222\pm 0.035$ ). To observe the effect of IP on the encapsulation ability, the %EE was determined. DS showed the highest %EE ( $26.58\pm 0.28$ ), followed by OA ( $9.39\pm 0.44$ ), DOC ( $3.20\pm 0.17$ ), and TPP ( $2.86\pm 0.07$ ). Compared with the %EE of MIN-loaded PEG-PLGA without IP added ( $1.66\pm 0.29$ ), the %EE was higher with the addition of IP (Table 2). The enhancement was confirmed by statistical analysis (Figure 3), which suggests that the presence of IP can significantly enhance the encapsulation. This can be concluded that DS can be chosen as it showed the most desirable characteristics of nanoparticles in terms of size, PDI, and %EE. However, the %EE can be further improved for more efficient treatment of MIN when applied in nanoparticle form.

Table 1 MIN-loaded PEG-PLGA characteristics when formed with different ion-pairing agents.

Ion-pairing agent	Mass ratio (IP: MIN)	Z-Average (d.nm.)	PDI	%EE
Without ion-pairing	-	$103.1\pm 0.6$	$0.113\pm 0.011$	$1.66\pm 0.29$
Dextran sulfate	0.5	$103.8\pm 0.6$	$0.118\pm 0.018$	$26.58\pm 0.28$
Deoxycholic acid	1	$98.4\pm 1.1$	$0.124\pm 0.024$	$3.20\pm 0.17$
Oleic acid	0.5	$144.2\pm 1.4$	$0.222\pm 0.035$	$9.39\pm 0.44$
Tripolyphosphate	0.2	$120.2\pm 1.4$	$0.095\pm 0.032$	$2.86\pm 0.07$

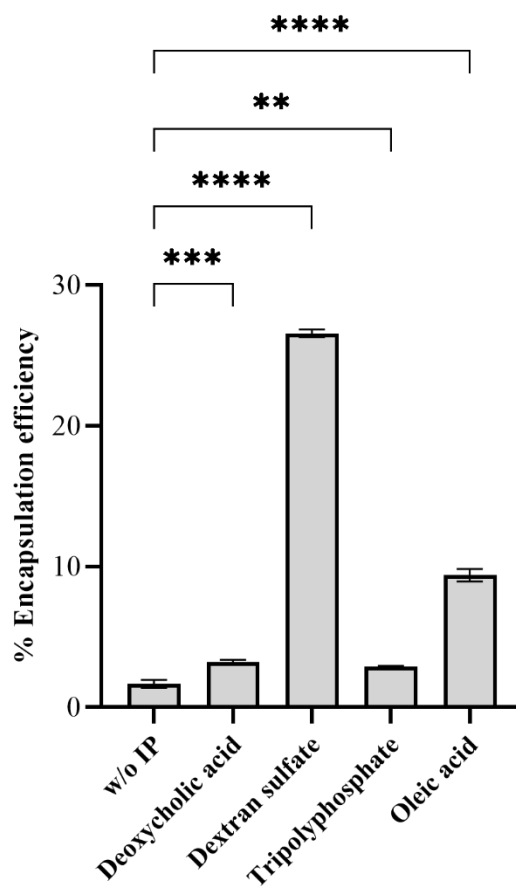


Figure 3 Effect of ion-pairing agents on the encapsulation efficiency of MIN-loaded PEG-PLGA nanoparticles. The analysis of variance (ANOVA) was performed followed by Tukey's multiple comparisons test, where \*\*, \*\*\*, and \*\*\*\* indicated significant difference at  $P < 0.01$ ,  $0.001$ , and  $0.0001$ , respectively.

#### 4. CONCLUSIONS

To remove the organic solvent after the PEG-PLGA nanoparticles formation, the dialysis method was chosen as it provided the small size and PDI of nanoparticles. For the MIN-loaded PEG-PLGA nanoparticles formation, the presence of ion-pairing agents provides a significantly higher %EE compared to the MIN-loaded PEG-PLGA nanoparticles without the ion-pairing agent being added. Dextran sulfate (DS) at a mass ratio of 1:2 is the most suitable ion-pairing agent to help enhance encapsulation. With the improvement of the encapsulation presented in this work, we hope that the MIN-loaded PEG-PLGA nanoparticle can be applied in pulp regeneration to prolong the presence of MIN and enhance the effectiveness of treatment.

#### 5. ACKNOWLEDGEMENT

This work has been partially supported by the Scholarship for Young Scientists, Faculty of Science, Mahidol University. We also would like to express our gratitude to the MU-OU: CRC, the Faculty of Science, Mahidol University, and Associate Professor Dr. Nuttawee Niamsiri, for providing the instruments, facilities, and support.

## 6. REFERENCES

- [1] Nair, P. N. (2004). Pathogenesis of apical periodontitis and the causes of endodontic failures. *Crit Rev Oral Biol Med*, 15(6), 348-381. doi:10.1177/154411130401500604
- [2] Bottino, M. C., Pankajakshan, D., and Nor, J. E. (2017). Advanced Scaffolds for Dental Pulp and Periodontal Regeneration. *Dent Clin North Am*, 61(4), 689-711. doi:10.1016/j.cden.2017.06.009
- [3] Segura-Egea, J. J., Gould, K., Sen, B. H., Jonasson, P., Cotti, E., Mazzoni, A., Sunay, H., Tjäderhane, L., and Dimmer, P. M. H. (2017). Antibiotics in Endodontics: a review. *Int Endod J*, 50(12), 1169-1184. doi:10.1111/iej.12741
- [4] Garza, A. Z., Park, S. B., and Kocz, R. (2022). Drug Elimination. In *StatPearls*. Treasure Island (FL): StatPearls Publishing, Copyright © 2022, StatPearls Publishing LLC.
- [5] Makadia, H. K., and Siegel, S. J. (2011). Poly Lactic-co-Glycolic Acid (PLGA) as Biodegradable Controlled Drug Delivery Carrier. *Polymers*, 3(3), 1377-1397. doi:10.3390/polym3031377
- [6] Kashi, T. S., Eskandarion, S., Esfandyari-Manesh, M., Marashi, S. M., Samadi, N., Fatemi, S. M., Atyabi, F., Eshraghi, S., and Dinarvand, R. (2012). Improved drug loading and antibacterial activity of minocycline-loaded PLGA nanoparticles prepared by solid/oil/water ion pairing method. *International journal of nanomedicine*, 7, pp 221-234. doi:10.2147/IJN.S27709
- [7] Watcharadulyarat, N., Rattanatayarom, M., Ruangsawasdi, N., and Patikarnmonthon, N. (2023). PEG-PLGA nanoparticles for encapsulating ciprofloxacin. *Sci Rep*, 13(1), 266. doi:10.1038/s41598-023-27500-y
- [8] Ahmed, O. A. A., and Badr-Eldin, S. M. (2020). Biodegradable self-assembled nanoparticles of PEG-PLGA amphiphilic diblock copolymer as a promising stealth system for augmented vinpocetine brain delivery. *Int J Pharm*, 588, 119778. doi:10.1016/j.ijpharm.2020.119778
- [9] Danaei, M., Dehghankhold, M., Ataei, S., Hasanzadeh Davarani, F., Javanmard, R., Dokhani, A., Khorasani, S., and Mozafari, M. R. (2018). Impact of Particle Size and Polydispersity Index on the Clinical Applications of Lipidic Nanocarrier Systems. *Pharmaceutics*, 10(2). doi:10.3390/pharmaceutics10020057
- [10] Ristroph, K. D., and Prud'homme, R. K. (2019). Hydrophobic ion pairing: encapsulating small molecules, peptides, and proteins into nanocarriers. *Nanoscale Adv*, 1(11), 4207-4237. doi:10.1039/c9na00308h
- [11] Jain, V., Singodia, D., Gupta, G. K., Garg, D., Keshava, G. B., Shukla, R., Shukla, P. K., and Mishra, P. R. (2011). Ciprofloxacin surf-plexes in sub-micron emulsions: a novel approach to improve payload efficiency and antimicrobial efficacy. *Int J Pharm*, 409(1-2), 237-244. doi:10.1016/j.ijpharm.2011.02.020



# Encapsulation of anti-DENV E mAbs in polymeric nanoparticle for intracellular delivery

Nutthanicha Intrarakasem<sup>1</sup>, Romchat Kraivong<sup>3,4,5</sup>, and Nisa Patikarnmonthon<sup>1,2\*</sup>

<sup>1</sup>Department of Biotechnology, Faculty of Science, Mahidol University, Bangkok 10400, Thailand

<sup>2</sup>Mahidol University-Osaka University Collaborative Research Center for Bioscience and Biotechnology (MU-OU:CRC), Faculty of Science, Mahidol University, Bangkok, 10400, Thailand

<sup>3</sup>Molecular Biology of Dengue and Flaviviruses Research Team, National Center for Genetic Engineering and Biotechnology, National Science and Technology Development Agency, Pathum Thani, Thailand

<sup>4</sup>Medical Biotechnology Research Unit, National Center for Genetic Engineering and Biotechnology, Siriraj Hospital, Bangkok, Thailand.

<sup>5</sup>Faculty of Medicine Siriraj Hospital, Siriraj Center of Research Excellent in Dengue and Emerging Pathogens, Mahidol University, Bangkok, Thailand.

\*Correspondence to: Department of Biotechnology, Faculty of Science, Mahidol University, Bangkok, 10400, Thailand. [nisa.pat@mahidol.edu](mailto:nisa.pat@mahidol.edu)

**ABSTRACT:** Dengue infection is a major public health problem causing acute febrile illness, muscle aches, pains, and fever, especially in the tropics and subtropics worldwide. Dengue vaccines are now available in the market as live attenuated vaccines but with some controversy. Antibody therapy might be an alternative approach to reduce the severity of dengue infection. With the specific binding to the viral protein, this approach might be able to reduce the viral assembly inside the cell and lower the number of viruses. Meanwhile, the extracellular antibody-virus complex has adverse effects as it has been reported to enhance the infectivity of the virus. Therefore, the nanoparticle might be used to minimize such problems using the encapsulation technique. This work aims to develop the antibody-loaded nanoparticle for the intracellular delivery of monoclonal antibodies against dengue envelope protein (anti-DENV E mAbs). Poly (ethylene glycol)-*block*-poly(d,l-lactide-*co*-glycolide) (PEG-PLGA) was used in this work, it is well-known for biomedical applications due to its biocompatibility and has been approved by US FDA. In this work, the compatibility of various organic solvents; including acetone, acetonitrile, DMSO, and dichloromethane, against mAbs has been examined using sodium dodecyl-sulfate polyacrylamide gel electrophoresis (SDS-PAGE). The results showed that acetone, acetonitrile, and DMSO did not damage the disulfide bond. The solid-in-oil-in-water (S/O/W) method was developed for the formation and encapsulation of anti-DENV E mAbs-loaded PEG-PLGA nanoparticles. The nanoparticles were characterized by Dynamic Light Scattering (DLS), and the size of both empty and mAb-loaded nanoparticles obtained were around 100 nm in diameter. The binding activity was confirmed by the antigen dot assay. The results suggested the S/O/W be able to be used for encapsulating the mAbs with the desired size and retain their binding activity.

**Keyword:** nanoparticle, PEG-PLGA, monoclonal antibodies, dengue virus

## 1. INTRODUCTION

Dengue infection is a mosquito-borne, acute febrile illness causing muscle aches, pains, and fever. It is a major public health problem in the tropics and subtropics worldwide. According to the World Health Organization (WHO), there is no specific treatment for dengue fever. The best option is to treat the patient according to the symptoms using acetaminophen or paracetamol. Dengue virus (DENV) is a single-stranded RNA virus belonging to the genus *Flavivirus* of the *Flaviviridae* family.

DENV has four distinct serotypes, the genome of each serotype comprises approximately 11 kb of single-stranded RNA. The genome encodes three structural proteins; including the membrane (M) protein, envelope (E) protein, and capsid (C) protein; and the non-structural (NS) protein. This research focuses on the E protein [1], which plays essential roles during endosomal-mediated virus internalization, by promoting attachment of virus to the host cell and fusion to the cell membrane. The E protein is a major antigen against host protective immunity, which could induce neutralizing antibodies. Furthermore, E-protein is known as the most important target for immune response in humans to generate the protective antibody. In this research, the antibody received from a collaborative laboratory contains a hydrophilic sequence and is water soluble. Its size is approximately 150 kDa, composed of four polypeptide chains forming a flexible Y-shaped structure. Generally, mAbs interact with the extracellular target (cell-surface or secreted) protein but not the intracellular protein because of their limitation of cell penetration. Thus, the action of mAbs might not come from the suppression of viral infection at the intracellular stages [2]. Therefore, we aim to intracellularly deliver the anti-DENV E mAbs into living cells by encapsulating them in polymeric nanoparticles. The poly (ethylene glycol)-*block*-poly(d,l-lactide-*co*-glycolide) (PEG-PLGA) was applied in this work. The PEG-PLGA is a block co-polymer, consisting of the hydrophilic segment (PEG) and hydrophobic segment (PLGA). PEG and PLGA are used widely for biomedical applications because of their excellent biodegradability, and biocompatibility, and are approved by the US Food and Drug Administration (FDA) [3], [4]. PEG-PLGA nanoparticles have been reported to encapsulate the BSA [5] and ovalbumin [6]. Therefore, we expected that they are also able to encapsulate the antibody and can provide intracellular delivery of the antibody. The objectives of this work are to test the compatibility of organic solvents with antibodies, to develop of suitable conditions for antibody encapsulation using PEG-PLGA, to characterize the nanoparticles, in terms of size and encapsulation efficiency, and finally to investigate the binding activity of mAbs-loaded nanoparticle to the antigen via antigen dot assay.

## 2. MATERIALS AND METHODS

### MATERIALS

PEG average Mn 2,000 PLGA average Mn 11,500 (Sigma-Aldrich, USA). The anti-DENV E mAbs were developed by the collaborator, Dr. Romchat Kraivong, (BIOTEC, NSTDA, Thailand). Acetone, chloroform, methanol, and glacial acetic acid were purchased from RCI Labscan™. Sodium dodecyl sulfate (SDS) was obtained from Bio-Rad, USA. Sepharose 4B was purchased from Cytiva, Sweden. Coomassie Brilliant Blue R-250 was obtained from PanReac Applichem, Germany. Goat anti-Human IgG (H+L) Secondary Antibody, HRP, Pierce™ ECL Western Blotting Substrate, and Pierce™ BCA Protein Assay Kit were purchased from Thermo Fisher Scientific Inc, USA.

### METHODS

#### Compatibility testing of organic solvents with antibodies by SDS-PAGE

Antibodies were diluted to the final protein concentration of 50 µg/ml in various solvents including acetone, acetonitrile, DMSO, dichloromethane, type I water (as a control), and non-reducing sample buffer. After that, 10 µL of each sample was loaded into an individual well of 10% acrylamide gel of SDS-PAGE. Typically, SDS-PAGE is used for separate proteins based on their molecular weight. Pre-stained molecular weight marker (PageRuler™) was used as a reference. The SDS-PAGE was performed at a constant voltage, 100 V for 1.5 h until the bromophenol blue tracking dye reaches the gel's bottom. The gel was stained with Coomassie blue for 30-60 min and destained in 60% (v/v) methanol in DW water with 10% (v/v) glacial acetic acid for 4–24 h prior to analysis.

### Preparing the anti-DENV E mAb loaded-PEG-PLGA nanoparticles

20 mg of PEG-PLGA was dissolved in 1 ml of acetone. Then, the initial amount of anti-DENV E mAb (160 µg) was added dropwise into the PEG-PLGA solution under stirring condition for at least 1 min. For the negative control, Phosphate Buffered Saline (PBS) was used instead of an antibody. Then, the resulting dispersion was added to 6 ml of type I water and stirred further for 5 mins. After that, the nanoparticle was dialyzed in water to eliminate acetone for 8 h, and water was changed every 2 h. The three batches of samples were pooled before purification. The nanoparticles were purified via gel permeation chromatography (GPC), using a size exclusion column containing Sepharose 4B and using type I water to elute the particle. The fraction that contains nanoparticles was determined by measuring the absorbance at 600 nm via a microplate reader (Thermo Scientific™ Multiskan™ GO Microplate Spectrophotometer). The sample was then concentrated by Amicon Ultra Centrifugal Filter 30kDa MWCO, and the supernatant was filtered by Ultrafiltration Spin-Columns, 0.45 µm cutoff. The following step was performed under the biological safety cabinet to maintain the sterile condition of the sample.

### Size distribution measurement by dynamic light scattering

The size distribution or Z-average size and polydispersity index (PDI) of PEG-PLGA nanoparticles were determined by dynamic light scattering using a particle size analyzer (Malvern Zeta nanosizer ZS, Malvern Instruments Ltd, US). The sample was placed in the cuvette 1ml for size measurement. If the sample was diluted in a ratio of 1:9 (V/V) of the sample to filtered RO water.

### Encapsulation efficiency

To investigate the amount of antibody loaded inside the nanoparticle, the PEG-PLGA nanoparticle was lyophilized and dissolved in 0.05 N NaOH and 1% sodium dodecyl sulfate [7]. The amount of mAb was estimated using the micro bicinchoninic acid protein assay according to the procedure provided by the manufacturer. The concentration of mAb-loaded in nanoparticles was calculated according to the standard curve. The slope of the standard curve was obtained by linear regression for the mAb concentration range between 2-40 µg/ml. The percentage of encapsulation efficiency was calculated using the below equation;

$$\text{Encapsulation efficiency (EE\%)} = \frac{W_f}{W_i} \times 100$$

where  $W_f$  is the final amount of mAbs encapsulated in the nanoparticle, and  $W_i$  is the initial amount of mAb added.

### Dot blot assay

A dot blot was used to detect whether nanoparticles contain antibodies or not. 2 µl sample (or containing 152 ng of mAb) was dotted onto the nitrocellulose membrane and left until dry. Then, the sample was blocked with skim milk for 30 min on a rock. After that, the membrane was washed with 0.05% PBST (Phosphate-Buffered Saline/Tween) and followed by incubating with goat anti-human IgG-HRP at a dilution of 1:2000 v/v for 1 h at room temperature in the dark. Then, the membrane was washed three-time for 5 min before staining with ECL (Enhanced chemiluminescence) for 5 min. The membrane was exposed to an imaging tool with chemiluminescent detection capabilities. Free mAbs and BSA encapsulation were applied as positive and negative control, respectively.

### Antigen dot assay

An antigen dot was used to detect whether mAb-loaded nanoparticles able to bind the antigen. The supernatant that contains viral antigens was dotted on the nitrocellulose membrane. Then the membrane was blocked with skim milk for 30 min on the rocker, and washed with 0.05% PBST. The membrane was incubated with the antibody-loaded nanoparticle in skim milk at 4°C overnight. After that, the membrane was washed three times with 0.05% PBST for 5 min followed by incubating with a goat anti-human IgG-HRP at a dilution of 1:2000 for 1 h at room temperature in the dark. Then,

the membrane was washed three times with 0.05% PBST for 5 min before staining with ECL for 5 min. The membrane was exposed to an image with chemiluminescent detection capabilities. Free antibodies mixed with the acetone were also tested. Free mAbs and BSA encapsulation were applied as positive and negative control, respectively.

## RESULTS AND DISCUSSION

### Effect of solvent on the antibodies

The S/O/W method used acetone as an organic phase to dissolve the PEG-PLGA. Therefore, the concern of using acetone was raised since it might be able to damage the disulfide bond of the mAb. If the disulfide bond of the mAb was damaged, the antigen binding might be interfered. If the organic solvents do not affect the disulfide bond, the presence of mAb on the SDS-PAGE should be in a single band similar to the native form at 180 kDa. The result was shown in **Figure 1a**, with the mAb dissolved in type I water as a control. The result showed a single band with little shift upward over 180 kDa. Similarly, the mAbs dissolved in acetonitrile, DMSO, and acetone were in the same pattern when compared to the control. Note that, acetone was not performed in the same experiment since it was too volatile to be loaded in the well at the beginning. Therefore, after the mAb was dissolved in acetone, the sample was evaporated and resuspended with type I water prior to being loaded. However, the result from **Figure 1b** showed a similar pattern. The results ensured that these organic solvents do not break disulfide bonds. Therefore, encapsulation of the mAbs with the presence of organic solvent can be performed using the S/O/W method.

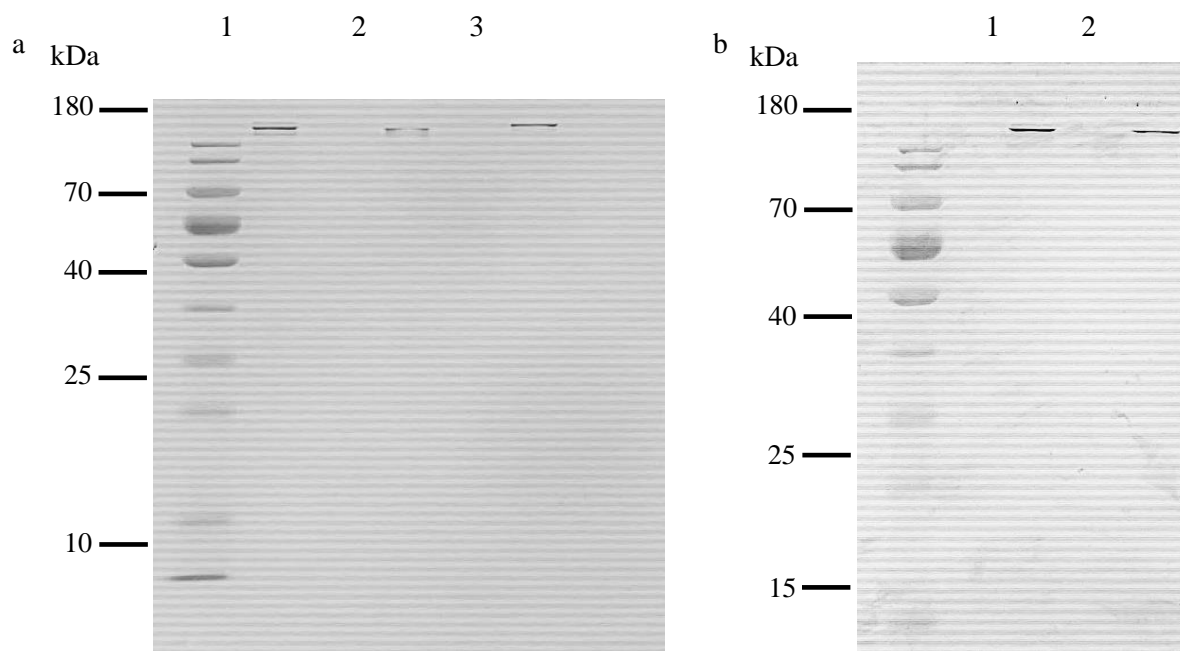


Figure 1: The SDS-PAGE patterns of mAb dissolved in different solvents including type I water (a1, b1), acetonitrile (a2), DMSO (a3), and acetone (b2). PageRuler™ was used as protein marker ranging from 10-180 kDa.

### mAb-loaded PEG-PLGA nanoparticles

The antibodies were encapsulated via the S/O/W method. In this experiment, 160  $\mu\text{g}$  of mAb was added to form nanoparticles or the same volume of PBS for an empty nanoparticle. The result was shown in **Table 1**. The empty PEG-PLGA nanoparticles showed a diameter size of approximately  $101.29 \pm 3.42$  nm with PDI of  $0.151 \pm 0.015$  whereas the diameter size of mAb-loaded PEG-PLGA nanoparticles was  $98.33 \pm 8.01$  nm with PDI of  $0.172 \pm 0.052$ . Both samples are not different in size and PDIs were acceptable range below 0.2 which refers to the homogeneity of nanoparticles. The encapsulation efficiency (%EE) was  $58.97 \pm 12.801$ , thus the final antibodies content obtained was 283.056  $\mu\text{g}$ .

Table 1: Size of PEG-PLGA nanoparticle with and without mAb.

Sample	Diameter size (nm.)	PDI	%EE
Empty NPs	$101.29 \pm 3.42$	$0.151 \pm 0.015$	-
mAb-loaded NPs	$98.33 \pm 8.01$	$0.172 \pm 0.052$	$58.97 \pm 12.801$

### Dot blot assay

This technique is used to further confirm whether the sample contains mAb with antigen-binding activity but does not inform the quantitative data. This assay used mAb-loaded nanoparticles as primary antibodies and Hu(H+L) IgG-HRP was used for secondary antibodies. If the sample contains mAbs, it should bind with secondary antibodies and show the dot on the membrane. The result was shown in **Figure 2**, where a) is the free mAbs as a positive control, b) the mAb-load PEG-PLGA nanoparticle, and c) BSA-loaded PEG-PLGA nanoparticles as a negative control. The result confirmed that the mAb-load PEG-PLGA nanoparticle can bind to the secondary antibodies similarly to the control without breaking process. It could be that the secondary antibodies can permeate the nanoparticle membrane and bind the mAbs within the nanoparticle, or the mAbs within the nanoparticle leak out, or there were some mAbs on the surface of the nanoparticles. However, this experiment suggested that the mAb-loaded PEG-PLGA NPs contained the mAb of interest.

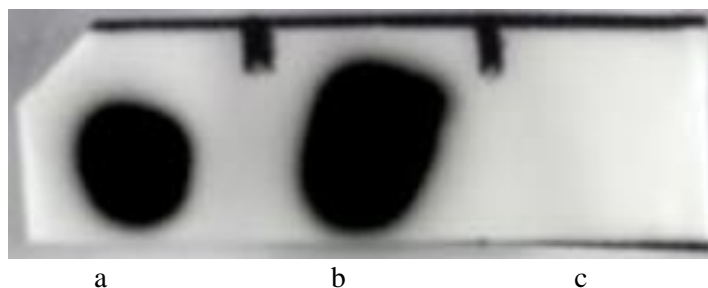
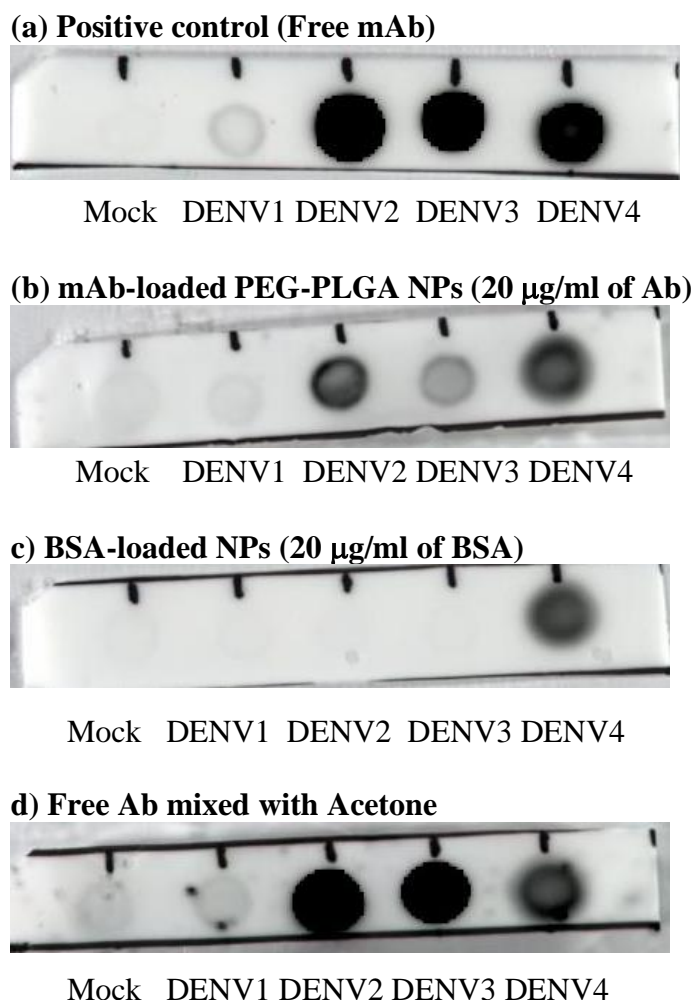


Figure 2: Dot blot assay a) control b) mAb-loaded PEG-PLGA NPs and c) BSA-loaded PEG-PLGA NPs.

### Antigen blot assay

Antigens dot assay is used for detecting whether mAb-loaded nanoparticles can bind the antigen. The sample was examined with mock culture media of noninfected cells without viral antigens. DENV1-4 were dengue antigens of serotypes 1-4. The free mAbs were mixed in the organic solvent before dotting on the membrane to check the effect of the organic solvent on the conformation of the antibodies. The results were shown in **Figure 3**, the free mAbs and BSA-loaded PEG-PLGA NPs are used as positive control and negative control, respectively. The free mAbs showed the dot on a

membrane with DENV serotypes 1, 2, 3, and 4 antigens (**Figure 3a**). The BSA-loaded PEG-PLGA showed the dot on the membrane with DENV 4 (**Figure 3c**), this may be due to the contaminant that interfered with the test as the antigens used in this experiment were not purified. However, mAb-loaded PEG-PLGA NPs show a dot on a membrane with the DENV1, 2, 3, and 4 antigens without background (**Figure 3b**). Free mAbs mixed with the acetone showed the dot on a membrane with the DENV1, 2, 3, and 4 (**Figure 3d**). The low binding signal of DENV1 in every condition might be due to the low titers of the virus. Therefore, we confirmed that the organic solvent does not affect the antigen binding and the encapsulation process does not affect the binding activity of antibodies.



**Figure 3:** Antigen blot assay of free mAbs (a), mAb-loaded PEG-PLGA nanoparticles (b), BSA-loaded PEG-PLGA nanoparticles (c), and free Ab mixed with acetone (d).

#### 4. CONCLUSIONS

The anti-DENV E mAbs were successfully encapsulated in PEG-PLGA nanoparticles using the S/O/W method. The organic solvents (acetone, acetonitrile, and DMSO) did not affect the disulfide bond and binding activity of antibodies against DENV2 and DENV3. However, further steps must be investigated such as the internalization of mAb-loaded PEG-PLGA nanoparticles as well as the cytotoxic effect on the cell. This work provides an aspect for encapsulation of anti-DENV E mAbs which could be useful for the study of the effect of antibody-virus complex inside the cell.

#### 5. ACKNOWLEDGEMENT

This work was supported by the Alliance of International Science Organizations (ANSO),

Scholarship for young scientists, and TGIST scholarship (SCA-CO-2565-17169-TH). The researchers would like to thank Assoc. Prof. Dr. Nuttawee Niamsiri, MU-OU:CRC, and Faculty of Science, Mahidol University, and also BIOTEC, NSTDA for the facility and equipment.

## 6. REFERENCES

- [1]. Guzman MG, Gubler DJ, Izquierdo A, Martinez E, Halstead SB. Dengue infection. *Nature Reviews Disease Primers*. 2016;2(1):16055.
- [2]. Song Z, Liu L, Wang X, Deng Y, Nian Q, Wang G, et al. Intracellular delivery of biomaterialized monoclonal antibodies to combat viral infection. *Chem Commun (Camb)*. 2016;52(9):1879-82.
- [3]. Zhang K, Tang X, Zhang J, Lu W, Lin X, Zhang Y, et al. PEG-PLGA copolymers: Their structure and structure-influenced drug delivery applications. *Journal of Controlled Release*. 2014;183:77-86.
- [4]. Maeda T, Kitagawa M, Hotta A, Koizumi S. Thermo-Responsive Nanocomposite Hydrogels Based on PEG-b-PLGA Diblock Copolymer and Laponite. *Polymers*. 2019;11(2).
- [5]. Li Y-P, Pei Y-Y, Zhang X-Y, Gu Z-H, Zhou Z-H, Yuan W-F, et al. PEGylated PLGA nanoparticles as protein carriers: synthesis, preparation and biodistribution in rats. *Journal of Controlled Release*. 2001;71(2):203-11.
- [6]. Garinot M, Fiévez V, Pourcelle V, Stoffelbach F, des Rieux A, Plapied L, et al. PEGylated PLGA-based nanoparticles targeting M cells for oral vaccination. *Journal of Controlled Release*. 2007;120(3):195-204.
- [7]. Hu S, Zhang Y. Endostar-loaded PEG-PLGA nanoparticles: in vitro and in vivo evaluation. *Int J Nanomedicine*. 2010;5:1039-48.

# Combination of multiplex PCR and CRISPR detection enables simultaneous diagnosis of major pathogens in penaeid shrimp

Suthasinee Kanitchinda<sup>1</sup> and Thawatchai Chaijarasphong<sup>1,2\*</sup>

<sup>1</sup>Department of Biotechnology, Faculty of Science, Mahidol University, Bangkok, 10400, Thailand

<sup>2</sup>Center of Excellence for Shrimp Molecular Biology and Biotechnology, Faculty of Science, Mahidol University, Bangkok, 10400, Thailand

\*Correspondence to: Department of Biotechnology, Faculty of Science, Mahidol University, Bangkok, 10400, Thailand, E-mail: thawatchai.chi@mahidol.edu

**ABSTRACT:** Acute hepatopancreatic necrosis disease (AHPND), hepatopancreatic microsporidiosis (HPM), and white spot disease (WSD) represent the most devastating diseases in the cultivation of penaeid shrimp that have resulted in drastic economic losses around the world. While early detection is considered the best prevention, this suggestion is difficult to implement at farm levels due to low throughputs of conventional diagnostic methods. Here, we present a novel multiplex PCR-Cas12a method for simultaneous detection of three pathogens: *Vibrio parahaemolyticus* (AHPND strain, VP<sub>AHPND</sub>), *Enterocytozoon hepatopenaei* (EHP), and white spot syndrome virus (WSSV), which are the causative agents of AHPND, HPM, and WSD, respectively. The employment of multiplex PCR increased the detection throughput, while the use of highly specific CRISPR-Cas12a enabled naked eye visualization and prevented misinterpretation due to similar molecular weights of PCR products. Using *pirAB*, *ptp2*, and *vp28* as the targets, our multiplex PCR-Cas12a method yielded the detection limits of 100 DNA copies for VP<sub>AHPND</sub>, 1,000 DNA copies for EHP, and 1,000 DNA copies for WSSV, respectively. Moreover, the method displayed excellent specificity towards each intended target and did not generate false positive results towards non-target DNA. In lieu of agarose gel electrophoresis, the outcomes could be visualized by the naked eye simply by exposing the Cas12a reaction vials to blue light, providing results that are not obscured by the presence of non-specific PCR products or similar molecular weights of target PCR products. The whole procedure can be completed under 3 h, while demanding less amounts of reagents and labor compared to singleplex PCR protocols.

**Keywords:** Multiplex PCR, CRISPR-Cas12a, WSSV, EHP, AHPND

## 1. INTRODUCTION

Penaeid shrimp including Pacific whiteleg shrimp (*Penaeus vannamei*) and black tiger shrimp (*Penaeus monodon*) are among the most economically important animals of Thailand. It has been estimated that the total production of Pacific whiteleg shrimp can reach as high as 300,000 – 400,000 ton per year since 2014 [1]. However, one of the major bottlenecks in penaeid shrimp cultivation is the plethora of infectious diseases capable of rapidly killing shrimp or severely limiting their growth. For example, diseases such as acute hepatopancreatic necrosis diseases (AHPND) and white spot disease (WSD), caused by a specific strain of *Vibrio parahaemolyticus* and white spot syndrome virus (WSSV), respectively, have been reported to cause 100% shrimp mortality within a few weeks [2, 3]. While hepatopancreatic microsporidiosis (HPM), caused by infection with the parasite *Enterocytozoon hepatopenaei* (EHP), does not usually cause massive mortality, it is known to severely retard shrimp growth and increase variation in size [4], leading to an estimated economic loss of 232 million US dollars per year [5]

Routine disease surveillance is indispensable for ensuring that shrimp disease, if present, is detected and dealt with in a timely manner, preferably before the appearance of clinical symptoms.



Polymerase chain reaction (PCR) is often employed for this purpose due to its high sensitivity and specificity, but the majority of PCR assays for shrimp diseases are designed as “singleplex” protocols, and therefore can detect only one pathogen at a time [6-8]. To increase the throughput of PCR and decrease the cost per reaction, several primers targeting different pathogens can be simultaneously employed in the same PCR reaction. These “multiplex” protocols, however, face a number of constraints. For example, to interpret results using agarose gel electrophoresis (AGE), each pair of primers must be designed to generate a significantly different size of amplicon, or else their DNA bands may significantly overlap on agarose gel [9]. In addition, the use of multiple primer pairs increases the likelihood of primer dimerization, thereby lowering the sensitivity of multiplex PCR relative to its singleplex counterparts. Therefore, an alternative method that could distinguish different PCR products irrespective of their sizes and improve the sensitivity of multiplex PCR could potentially alleviate these pain points.

CRISPR detection has emerged as a novel strategy for rapid and isothermal disease detection [10, 11]. At the heart of this strategy is an enzyme called Cas12a, which is a programmable endonuclease that can be directed to cut any target DNA, provided that its sequence matches the “CRISPR-RNA” (crRNA) and is located next to a T-rich protospacer adjacent motif (PAM) [12]. The crRNA of Cas12a consists of two sections: a direct repeat (DR), which is constant in sequence and does not interact directly with the target DNA, and a spacer, which contains 20-28 nucleotides [12]. The sequence of the spacer must match the target DNA, as it must stably anneal with the latter to activate Cas12a for target DNA cleavage. Notably, Chen and colleagues (2018) discovered that, in addition to cutting the target DNA, Cas12a also proceeds to cleave ssDNA in a sequence-independent manner. This property, called “collateral cleavage,” is a pivotal factor that allows Cas12a to be employed for disease detection: by adding a reporter containing a fluorophore, a quencher, and an ssDNA linker (“FQ reporter”) to the reaction, Cas12a that has cut the target DNA will proceed to cleave the ssDNA linker in the FQ reporter, giving rise to strong fluorescence.

Here, we reported a novel combination of multiplex PCR and CRISPR detection for AHPND, HPM, and WSD that successfully improves upon the conventional multiplex PCR-AGE as in **Figure 1**. Our method not only increases the sensitivity of multiplex PCR, but also differentiates between three targets without ambiguity. The results can be visualized conveniently by placing vials on a transilluminator and observing the fluorescence by the naked eye.

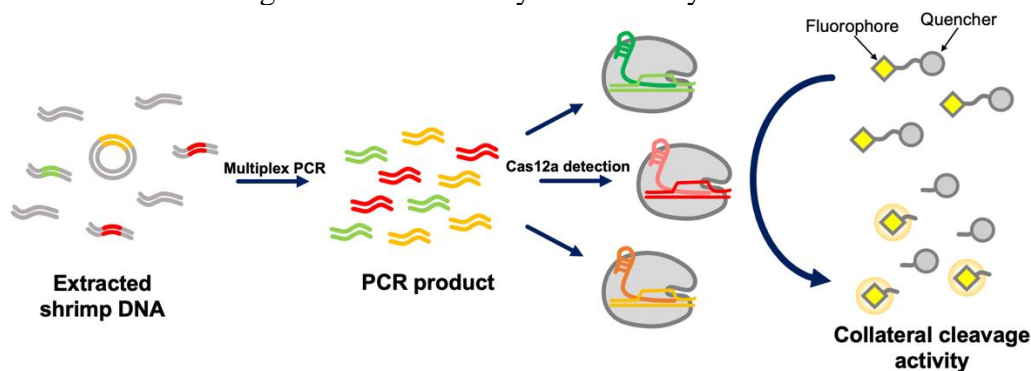


**Figure 1.** Workflow of multiplex PCR-Cas12a assay for AHPND, EHP, and WSSV detection

## 2. MATERIALS AND METHODS

### 2.1 Preparation of crRNA for LbCas12a

Each crRNA was designed based on previous studies as shown in **Table S1**. In this study, all crRNA was prepared using *in vitro* transcription (IVT). The DNA template for this purpose was prepared by overlap extension PCR using two overlapping DNA strands [14]. The unpurified PCR product was directly subjected to *in vitro* transcription using HiScribe® T7 Quick High Yield RNA Synthesis Kit (New England Biolabs, Ipswich, MA, USA), with incubation at 37°C for 16-18 h. To remove the DNA template, DNase I was added to the completed IVT reaction and incubated at 37°C for 1 hour. Then, the RNA product was purified using RNA clean & concentrator™-25 kit (Zymo-Research, Irvine, CA, USA). The concentration of each crRNA was measured using the Qubit™ RNA Broad Range (BR) assay kit (Invitrogen, Waltham, MA, USA).

### 2.2 Polymerase Chain Reaction (PCR)

The multiplex PCR reaction in this study used the following **Table S1**. Each reaction (25 µL) consisted of 1X PCR reaction buffer (without Mg), 0.4 mM dNTP, 200 nM of each pair of primers, 3 mM MgCl<sub>2</sub>, 1.5 U Taq DNA polymerase (Invitrogen, Waltham, MA, USA), and DNA template. The reaction was performed in Biometra Tprofessional Thermal Cycler (Analytik Jena Group, Jena, Germany), using the following temperature program: initial denaturation at 94°C for 3 minutes, followed by 35 cycles of 94°C for 30 s, 55°C for 1 minute, and 72°C for 1 minute, followed by final extension at 72°C for 10 minutes. The results were visualized via AGE or Cas12a assay. All of singleplex PCR reactions were performed using the same parameters as the multiplex PCR, except that only a single pair of primers was included in the reactions and change the annealing and extension times to 30 s and 20 s, respectively.

### 2.3 Cas12a fluorescence detection

A Cas12a reaction (20 µL) was established following the protocols with some modifications [14]. Each reaction consisted of 1x cleavage buffer (12.5 mM HEPES, 100 mM KCl, 10 mM MgCl<sub>2</sub>, 0.5 mM DTT, 1% glycerol, pH 7.5) and 50 nM MBP-LbCas12a, and 5 µL of multiplex PCR product. As each Cas12a reaction was capable of detecting one pathogen, three Cas12a reactions were required per one multiplex PCR product in order to detect all three pathogens. The fluorescence signal was quantified using SpectraMax iD3 (Molecular Devices, San Jose, CA, USA) with 526 nm excitation and 566 nm emission wavelengths, and calculated using an unpaired t-test with 95% confidence interval. Alternatively, the results were visualized with blue light using BluPad (Bio-Helix, Taiwan) and photographed with iPhone XR.

### 2.4 Determination of multiplex PCR-Cas12a specificity

The multiplex PCR-Cas12a assay was evaluated for specificity using DNA from non-target pathogens including infectious hypodermal and hematopoietic necrosis virus (IHHNV), and hepatopancreatic parvovirus (HPV). Archived DNA of shrimp infected with acute hepatopancreatic necrosis disease (AHPND), *Enterocytozoon hepatopenaei* (EHP), and white spot syndrome virus (WSSV) were also tested as positive controls.

### 2.5 Evaluation of field samples

Samples of archived DNA had previously been prepared from the hepatopancreatic or stomach tissues of disease-free *P. vannamei* or *P. monodon*, and those infected with either AHPND, EHP, or WSSV. Doubly- and triply-infected samples were artificially prepared by mixing two or three samples, each infected with a single pathogen. The field sample will be tested as a blind test to increase objectivity in disease diagnosis. All samples (n =15) were subjected to multiplex PCR,

followed by the Cas12a assay as described in Section 2.2 and 2.3. These samples were also analyzed using the gold standard method for each pathogen: AP4-AGE for AHPND [7], SWP-PCR for EHP [6], and VP28-PCR for WSSV detection [8].

## 2.6 Ethics statement

No shrimp was sacrificed in this study, as the DNA samples were either synthetic DNA or archived samples. The protocols involving archived DNA as well as the sources of these samples had been approved by the Faculty of Science, Mahidol University (Thailand) Animal Care and Use Committee (Protocol Number: MUSC64-040-589)

## 3. RESULTS AND DISCUSSION

### 3.1 Optimization of multiplex PCR-Cas12a assay

For PCR amplification of the target DNA in this study, we employed primers that were previously reported to be highly efficient for the amplification of their respective targets in either polymerase chain reaction (PCR) or recombinase polymerase amplification (RPA). Specifically, we employed PCR primers for WSSV [9], and RPA primers for AHPND [13] and EHP [14]. The PCR products generated using these primers were close in size (143, 157, and 221 bp for AHPND, WSSV, and EHP, respectively) and were accompanied by abundant amounts of non-specific products (**Figure S1** and **Figure 2**), making it challenging to determine whether the DNA bands corresponding to the targets were truly present. These ambiguous results highlight the difficulty of analyzing multiplex PCR products using AGE. However, these factors would be inconsequential in CRISPR detection due to the exemplary specificity of Cas12a.

To confirm whether an unpurified PCR product would inhibit the reaction of Cas12a, we assayed the PCR products with the Cas12a reactions, and found that all of the positive PCR products generated bright fluorescence in the Cas12a assay. Interestingly, the sensitivity obtained was 10 folds higher than the visualization using AGE, yielding detection limits of 10, 100, and 100 copies for AHPND, EHP, and WSSV, respectively (**Figure 2**). These results are consistent with the findings that AGE with ethidium bromide staining produces a visible DNA band only when the amount of DNA exceeds 5 ng (barely visible) [15], while the detection limit of Cas12a could be as low as 1 fmol or 3.3 ng [14].

Because the sensitivity of each pair of primers in singleplex PCR-Cas12a was satisfactory, we proceeded to test their performance in multiplex PCR-Cas12a, where all three DNA targets and the primers were simultaneously present in the PCR reaction. We also determined the effects of four different PCR annealing temperatures ( $T_a$ : 53, 55, 57 and 59°C) on the sensitivity of our method. The results show that all of the temperatures tested enabled multiplex PCR-Cas12a to detect 1,000 copies of each target DNA with comparable levels of fluorescence (**Figure S1**). To confirm the optimal  $T_a$ , the multiplex PCR-Cas12a assay was repeated in triplicate with the annealing temperatures of 53, 55, and 57°C. The  $T_a$  of 59 °C was excluded due to its subpar outcome. When the results were analyzed using AGE as in **Figure S2a**, smears and several DNA bands with low molecular weights were observed in all replicates. In comparison to 53 and 55°C conditions, using 57 °C as the annealing temperature failed to generate the band corresponding to EHP when 1,000 copies of target DNA was present. For conclusive interpretation of results, all of the PCR products were subjected to the Cas12a assay, in which the  $T_a$  of 55°C produced a higher sensitivity than 53°C at the detection limit of 1,000 copies per reaction for AHPND, EHP, and WSSV detection (**Figure S2b and S2c**). The fluorescence intensities between  $T_a$  were not significantly different in AHPND detection. However, at 1,000 copies, EHP and WSSV detection at 55°C  $T_a$  showed slight significance ( $p < 0.05$ ). Even though the positive result was easily distinguishable from the negative control, the fluorescence signal exhibited high fluctuations.

In order to increase the sensitivity of our method even further, we decided to optimize additional parameters of PCR, including the duration of annealing and extension, and the concentration of dNTPs, which had been reported to influence the efficiency of multiplex PCR [9]. The results show that increasing the duration of 30 s annealing and 20 s extension time to 1 min at both steps did not improve the detection limits that not significant between the conditions, but lowered the extent of signal fluctuations between replicates, as evidenced by the narrower standard deviations (**Figure S3b**). When the PCR step was performed with 0.2, 0.4, or 0.8 mM dNTPs (**Figure S4**), we found that 0.4 mM dNTPs reduced the detection limit for AHPND from 1,000 to 100 copies ( $p < 0.05$ ), while the sensitivity for WSSV and EHP remained unchanged. However, the 0.4 mM dNTP concentration at 100 copies of EHP detection exhibited significant differences ( $p < 0.05$ ) compared to the negative sample, although the fluorescence intensity remained indistinguishable from that of the negative sample. Therefore, we employed 1 min of annealing and extension, as well as 0.4 mM dNTPs, in all subsequent PCR experiments in this study.

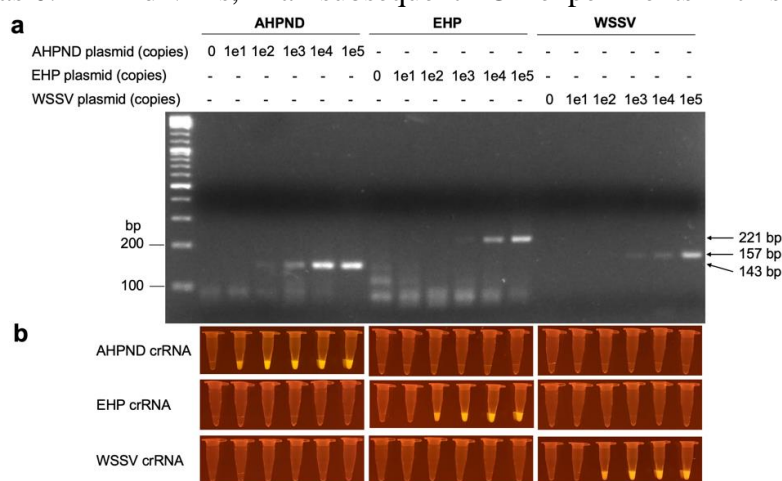


**Figure 2. Sensitivity test of the reference primers for AHPND, EHP, and WSSV detection using singleplex PCR method.** The template DNA was varied from 10 to  $10^5$  copies per reaction. The PCR product was analyzed both of a) agarose gel electrophoresis and b) Cas12a reaction visualized under blue light.

### 3.2 Multiplex PCR-Cas12a assay exhibited high sensitivity

To confirm the sensitivity of our multiplex PCR-Cas12a method, we performed the assay on samples containing  $1-10^6$  copies of AHPND-, EHP-, and WSSV- plasmids. The results revealed the detection limits for AHPND, EHP, and WSSV to be 100, 1,000, and 1,000 copies, respectively (**Figure 3a**). When the reaction vials were exposed to blue light, the fluorescence generated by the positive samples, including those at the detection limits, was easily distinguishable from the negative control and reactions containing fewer copies of target DNA than the detection limits.

As DNA extracts from shrimp will unavoidably contain background shrimp DNA, which may be able to interfere with the PCR or Cas12a steps, we sought to determine whether the presence of shrimp DNA would compromise the sensitivity of our assay. To this end, the sensitivity evaluation described above was repeated in the presence of 100 ng pathogen-free shrimp DNA in every reaction (**Figure 3b**). Interestingly, the introduction of background shrimp DNA decreased the detection limit for AHPND from 100 copies to 10 copies per reaction. It is possible that shrimp background DNA may contain a sequence that can effectively compete with non-specific targets of PCR, but is worse than the other non-specific targets at sequestering the DNA polymerase — i.e., the sequence in background shrimp DNA may be better at binding to the primers, but generate shorter amplicons compared to the original non-specific targets. Nonetheless, the real cause of this unexpected

observation remains to be investigated in the future. In contrast to AHPND, the detection limits for EHP and WSSV remained 1,000 copies per reaction, but the levels of fluorescence were largely attenuated, despite still being distinguishable from negative reactions.

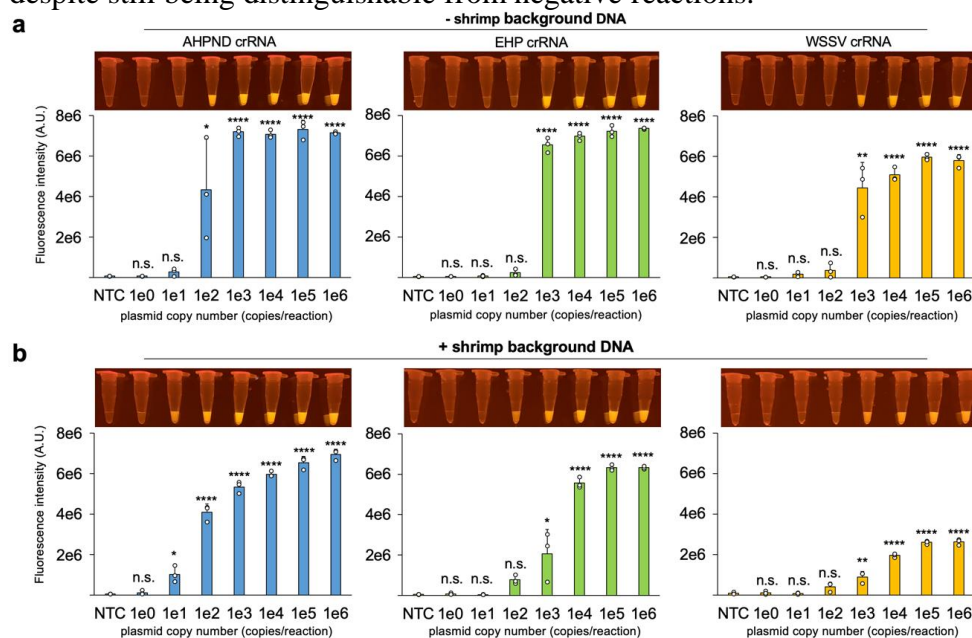


**Figure 3. Evaluation of sensitivity** between a) analytical sensitivity and b) sensitivity of presented 100 ng per reaction of shrimp background DNA visualized using BluPad and the fluorescence intensity as in each Cas12a with different crRNA. All error bar represents mean $\pm$ SD, (n = 3), unpaired student t-test; n.s., not significant; \*,  $p < 0.05$ ; \*\*,  $p < 0.01$ ; \*\*\*\*,  $p < 0.0001$ ).

### 3.3 Multiplex PCR-Cas12a with high specificity

In addition to confirmation of sensitivity, it is equally important to verify the specificity of an assay to ensure that it does not give rise to false positives due to non-target pathogens. To this end, a panel of archived DNA samples containing the genomic DNA of IHNV and *V. parahaemolyticus* (AHPND strain), and infected shrimp DNA of HPV, AHPND, EHP, and WSSV. A DNA extract from a disease-free shrimp was also tested as a negative control (**Figure 4**). The results show that our multiplex PCR-Cas12a assay exclusively detected AHPND, EHP, and WSSV, but not any of the non-target pathogens, thereby confirming the excellent specificity of this approach.

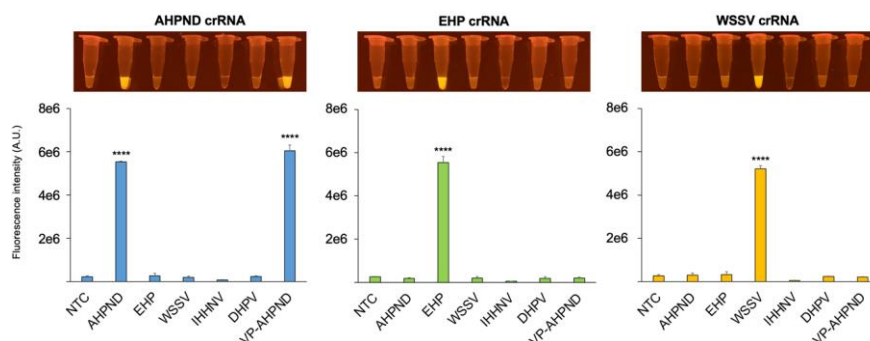


**Figure 4. Evaluation specificity of multiplex PCR-Cas12a method.** The Cas12a result was visualized under blue light and fluorescence signal of 566 nm emission was measured using microplate reader, error bars represent mean $\pm$ SD, (n = 3), unpaired student t-test; \*\*\*\*,  $p < 0.0001$ ).

### 3.4 Comparison efficiency between multiplex PCR-Cas12a and PCR-AGE method of field sample test

The three pathogens can be found using the multiplex PCR-Cas12a approach with great sensitivity and specificity. The results of the multiplex PCR-Cas12a could be compared to the gold standard PCR-AGE for each pathogen detection, as shown in **Table 1**. The outcome demonstrates the multiplex PCR-Cas12a's capability to identify three pathogens without producing false negative or positive results.

**Table 1. Comparison of detection method** between multiplex PCR-Cas12a method with gold standard PCR-AGE method

Sample number		1	2	3	4	5	6	7	8	9	10	11	12	13	14	15
PCR-AGE	AP4-AGE	+	+	+	+	-	-	-	-	-	+	+	-	-	-	+
	SWP-PCR	-	+	+	+	-	-	-	-	-	+	-	+	-	+	-
	VP28-PCR	+	+	+	+	-	-	-	-	-	-	+	+	+	-	-
Multiplex PCR-Cas12a	AHPND	+	+	+	+	-	-	-	-	-	+	+	-	-	-	+
	crRNA															
	EHP crRNA	-	+	+	+	-	-	-	-	-	+	-	+	-	+	-
	WSSV crRNA	+	+	+	+	-	-	-	-	-	-	+	+	+	-	-

## 4. CONCLUSIONS

Conventional multiplex PCR with AGE provides advantages in terms of high throughput and decreased cost per sample. However, the requirement that all PCR products be at significantly different sizes becomes an important challenge in the assay development, limiting the number of primer candidates that can be employed. In addition, as the sensitivity of PCR tends to decrease as amplicon length increases, this size requirement also impacts sensitivity, as it is difficult to resolve short PCR products on agarose gel. In this study, we demonstrated that the combination of multiplex PCR and Cas12a enabled highly sensitive and specific detection of three major shrimp pathogens within less than 3 h from sample to answer. Notably, the combination of primers chosen produced small amplicons that were close in size and exhibited moderate levels of non-specific amplification. This situation would have posed a significant challenge in interpreting results via AGE, but the integration of CRISPR detection increased the confidence of pathogen identification. Furthermore, it was observed that the incorporation of the Cas12a assay improved the detection limit of multiplex PCR, thereby enabling the detection of samples that did not produce DNA bands during AGE.

## 5. ACKNOWLEDGEMENTS

This research project is supported by Mahidol University (Fundamental Fund: fiscal year 2023 by National Science Research and Innovation Fund (NSRF)) (Grant no. FF-056/2566). We would like to thank Dr. Kallaya Sritunyaluksana Dr. Rungkarn Suebsing, and Miss Jiraporn Srisala for providing resources and valuable suggestions.

## 6. REFERENCES

- [1] Department of Fisheries (2019) Statistics of marine shrimp culture 2017. Fishery Information Technology Center, Department of Fisheries, Ministry of Agriculture and Cooperatives. No. 2/2020, 86 pp
- [2] Lightner, D.V. (1996). A Handbook of Pathology and Diagnostic Procedures for Diseases of Penaeid Shrimp. World Aquaculture Society, LA.
- [3] Thitamadee, S., Prachumwat, A., Srisala, J., Jaroenlak, P., Salachan, P.V., Sritunyalucksana, K., Flegel, T.W., and Itsathitphaisarn, O. (2016). Review of current disease threats for cultivated penaeid shrimp in Asia. *Aquaculture* 452, 69–87, DOI: 10.1016/j.aquaculture.2015.10.028.
- [4] Chaijarasphong, T., Munkongwongsiri, N., Stentiford, G. D., Aldama-Cano, D. J., Thansa, K., Flegel, T. W., Sritunyalucksana, K., and Itsathitphaisarn, O. (2021). The shrimp microsporidian enterocytozoon hepatopenaei (EHP): Biology, pathology, diagnostics and control. *Journal of Invertebrate Pathology*, 186, 107458, DOI: 10.1016/j.jip.2020.107458
- [5] Shinn, A. P., Pratoomyot, J., Griffiths, D., Trong, T. Q., Vu, N. T., Jiravanichpaisal, P., and Briggs, M. (2018). Asian shrimp production and the economic costs of disease. *Asian Fisheries Science*, 31, 29–58.
- [6] Jaroenlak, P., Sanguanrut, P., Williams, B.A.P., Stentiford, G.D., Flegel, T.W., Sritunyalucksana, K., and O. Itsathitphaisarn (2016). A nested PCR assay to avoid false positive detection of the microsporidian enterocytozoon hepatopenaei (EHP) in environmental samples in shrimp farms, *PLoS One* 11, DOI: 10.1371/journal.pone.0166320.
- [7] Dangtip, S., Sirikharin, R., Sanguanrut, P., Thitamadee, S., Sritunyalucksana, K., Taengchaiyaphum, S., Mavichak, R., Proespraiwong, P., and Flegel, T. W. (2015). AP4 method for two-tube nested PCR detection of AHPND isolates of *Vibrio parahaemolyticus*. *Aquaculture Reports*, 2, 158–162, DOI: 10.1016/j.aqrep.2015.10.002
- [8] Soowannayan, C., Phanthura, M., 2011. Horizontal transmission of white spot syndrome virus (WSSV) between red claw crayfish (*Cherax quadricarinatus*) and the giant tiger shrimp (*Penaeus monodon*). *Aquaculture* 319, 5–10, DOI: 10.1016/j.aquaculture.2011.06.012
- [9] Henegariu, O., Heerema, N. A., Dlouhy, S. R., Vance, G. H., and Vogt, P. H. (1997). Multiplex PCR: Critical parameters and step-by-step protocol. *BioTechniques*, 23(3), 504–511, DOI:10.2144/97233rr01
- [10] Chen, J. S., Ma, E., Harrington, L. B., Da Costa, M., Tian, X., Palefsky, J. M., & Doudna, J. A. (2018). CRISPR-Cas12a target binding unleashes indiscriminate single-stranded DNase activity. *Science*, 360, 436–439, DOI:10.1126/science.aar6245
- [11] Li, S.-Y., Cheng, Q.-X., Wang, J.-M., Li, X.-Y., Zhang, Z.-L., Gao, S., Cao, R.-B., Zhao, G.-P., and Wang, J. (2018). CRISPR-Cas12a-assisted nucleic acid detection. *Cell Discov.* 4 (1), DOI:10.1038/s41421-018-0028-z.
- [12] Zetsche, B., Gootenberg, J. S., Abudayyeh, O. O., Slaymaker, I. M., Makarova, K. S., Essletzbichler, P., Volz, S. E., Joung, J., van der Oost, J., Regev, A., Koonin, E. V., Zhang, F. (2015). Cpf1 is a single RNA-guided endonuclease of a class 2 CRISPR-Cas system. *Cell* 163, 759–771, DOI: 10.1016/j.cell.2015.09.038 Medline
- [13] Naranitus, P., Aiamsa-at, P., Sukonta, T., Hannanta-anan, P., and Chaijarasphong, T. (2022). Smartphone-compatible, CRISPR-based platforms for sensitive detection of acute hepatopancreatic necrosis disease in shrimp. *Journal of Fish Diseases*, 45(12), 1805–1816, DOI: 10.1111/jfd.13702
- [14] Kanitchinda, S., Srisala, J., Suebsing, R., Prachumwat, A., and Chaijarasphong, T. (2020). CRISPR-Cas fluorescent cleavage assay coupled with recombinase polymerase amplification for sensitive and specific detection of Enterocytozoon hepatopenaei. *Biotechnology Reports*, 27, e00485, DOI:10.1016/j.btre.2020.e00485
- [15] Tweedie, J. W., and Stowell, K. M. (2005). Quantification of DNA by agarose gel electrophoresis and analysis of the topoisomers of plasmid and M13 DNA following treatment with a restriction endonuclease or DNA topoisomerase I. *Biochemistry and Molecular Biology Education*, 33(1), 28–33, DOI:10.1002/bmb.2005.494033010410

## Supplementary Materials for

### Combination of multiplex PCR and CRISPR detection enables simultaneous diagnosis of major pathogens in penaeid shrimp

Suthasinee Kanitchinda<sup>1</sup> and Thawatchai Chaijarasphong<sup>1,2\*</sup>

\*Correspondence to: Thawatchai Chaijarasphong (thawatchai.chi@mahidol.edu)

#### This PDF file includes:

Materials and Methods

Figs. S1 to S4

Tables S1

#### Materials and Methods

##### 1. Preparation of MBP-LbCas12a protein

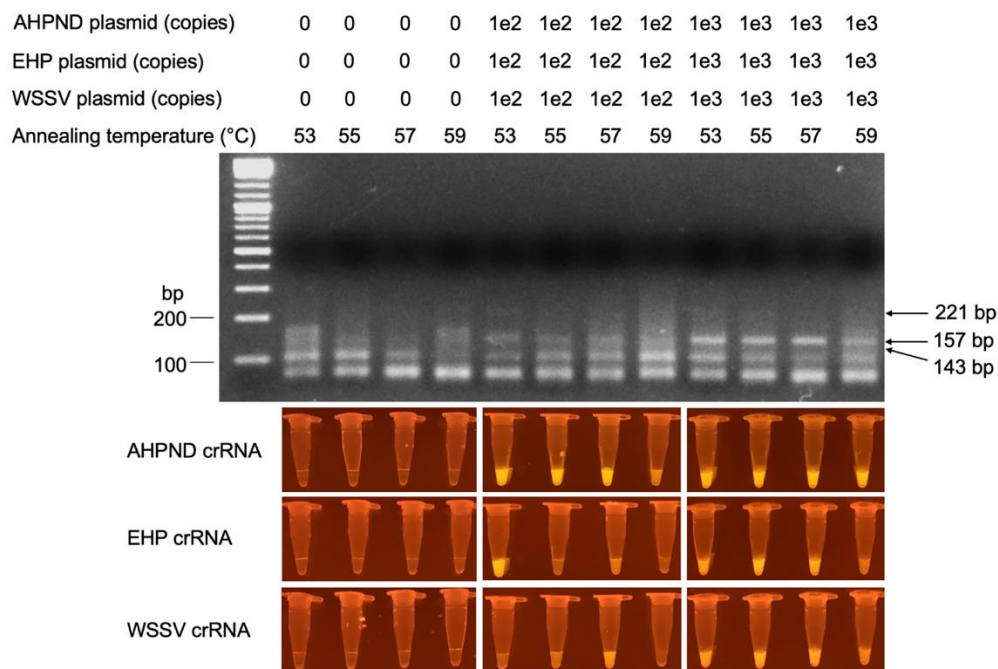
MBP-LbCas12a is a fusion protein consisting of Cas12a from *Lachnospiraceae bacterium* ND2006 (LbCas12a) fused with maltose binding protein (MBP), expressed and purified following Chen et al. (2018) with some modifications. The expression plasmid (pMBP-LbCas12a) was a gift from Jennifer Doudna (Addgene plasmid #113431). The plasmid was introduced to *E. coli* Rosetta 2 (DE3) competent cells through chemical transformation. The transformants were spread on LB agar with 50 µg/ml ampicillin and 12.5 µg/ml chloramphenicol for selection. A single colony was picked and grown in 7 mL of LB broth supplemented with the same concentrations of antibiotics at 37°C overnight in an incubator shaker with (250 RPM) and subsequently diluted in a larger volume of LB broth (500 mL) to the OD<sub>600</sub> of 0.05. This culture was grown at 37°C with a shaking speed of 250 rpm until the OD<sub>600</sub> reached 0.5-0.7, at which point IPTG was added to the culture at a final concentration of 0.2 mM to induce protein expression. After 16 h of induction at 16 °C and a shaking speed of 250 RPM, the cells were harvested by centrifugation at 7,000xg for 10 min, and stored at -80°C until purification.

To initiate the purification, the frozen cell pellet was resuspended in lysis buffer (20 mM Tris, 500 mM NaCl, 10 mM Imidazole, pH 8) and sonicated using the following parameter: 40% amplitude, on/off: 9s, total on time 2 min. The crude lysate was centrifuged at 12,000xg for 30 min, before the supernatant was isolated and incubated with Ni-NTA agarose resin (Qiagen, Hilden, Germany) for 1 h. The resin was then transferred to a gravity-flow chromatography column (Bio-Rad) and washed with wash buffer (20 mM Tris, 500 mM NaCl, 50 mM imidazole, pH 8) for 10 column volumes (CV), eluted with elution buffer (20 mM Tris, 250 mM NaCl, 250 mM imidazole, pH 8) in fractions, each containing 1 CV of the eluent (except for the first fraction, which contained 0.5 CV of eluent.) The eluted fractions were analyzed using SDS-polyacrylamide gel electrophoresis (SDS-PAGE), and those with high abundance of MBP-LbCas12a and high purity was dialyzed against dialysis buffer (25 mM Tris, 250 mM NaCl, pH 7.5), and concentrated using Amicon Ultra centrifugal filter unit with 3 kDa cutoff (MERCK, Millipore, Burlington, MA, USA). Prior to storage, the following additives were introduced to the dialyzed protein to the final concentrations specified: 10% glycerol, 10 mM DTT, and 1 mM PMSF. Therefore, the final composition of the storage buffer consisted of the following: 20 mM Tris, 200 mM NaCl, 10% glycerol, 10 mM DTT, and 1 mM PMSF, pH 7.5. The protein was stored at -80°C for further experiments.



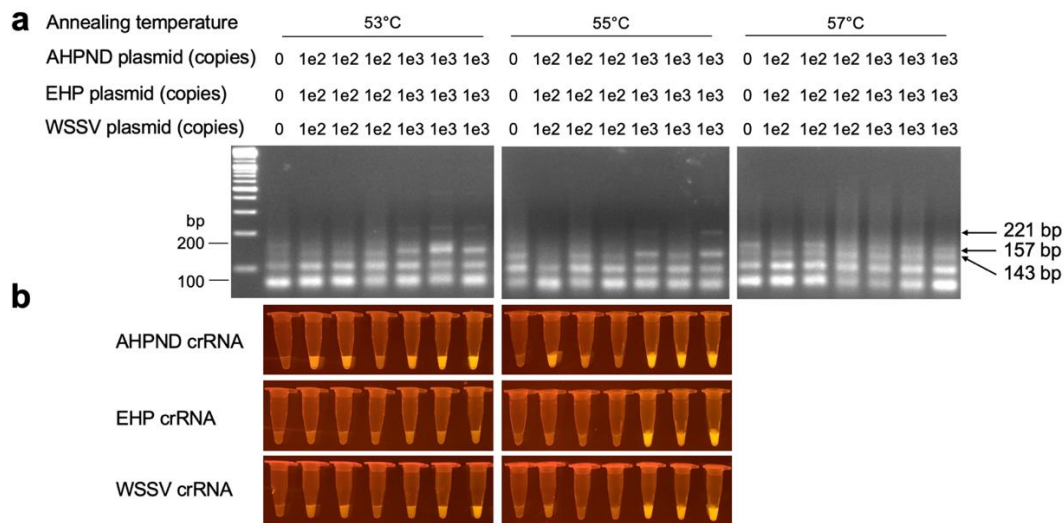
Supplementary Figures

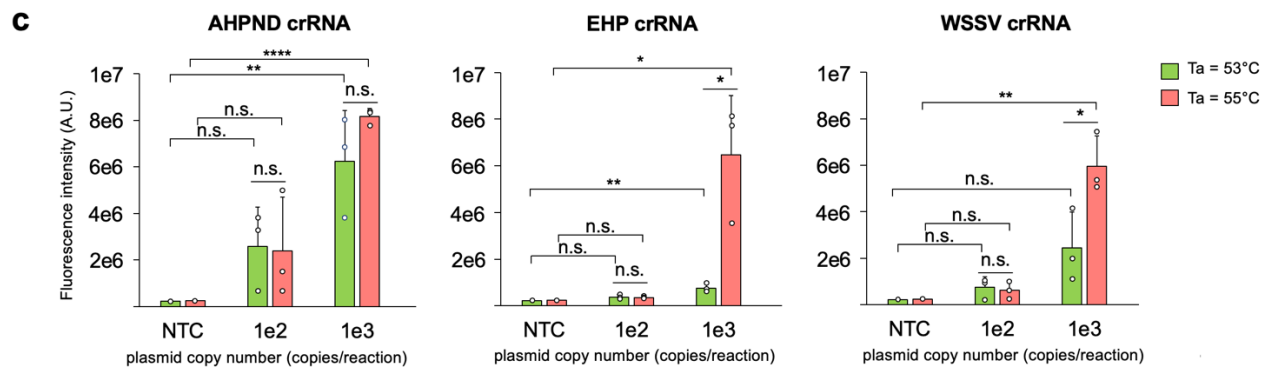
Figure S1



**Fig. S1**  
**Optimization of the annealing temperature of multiplex PCR-Cas12a assay** The annealing temperature was performed at 53, 55, 57, and 59°C using 3 concentrations of target DNA: 0, 100, and 1,000 copies/target DNA/reaction (n=1). All multiplex PCR samples were visualized on agarose gel electrophoresis and BLU-Pad for the PCR product and Cas12a reaction, respectively.

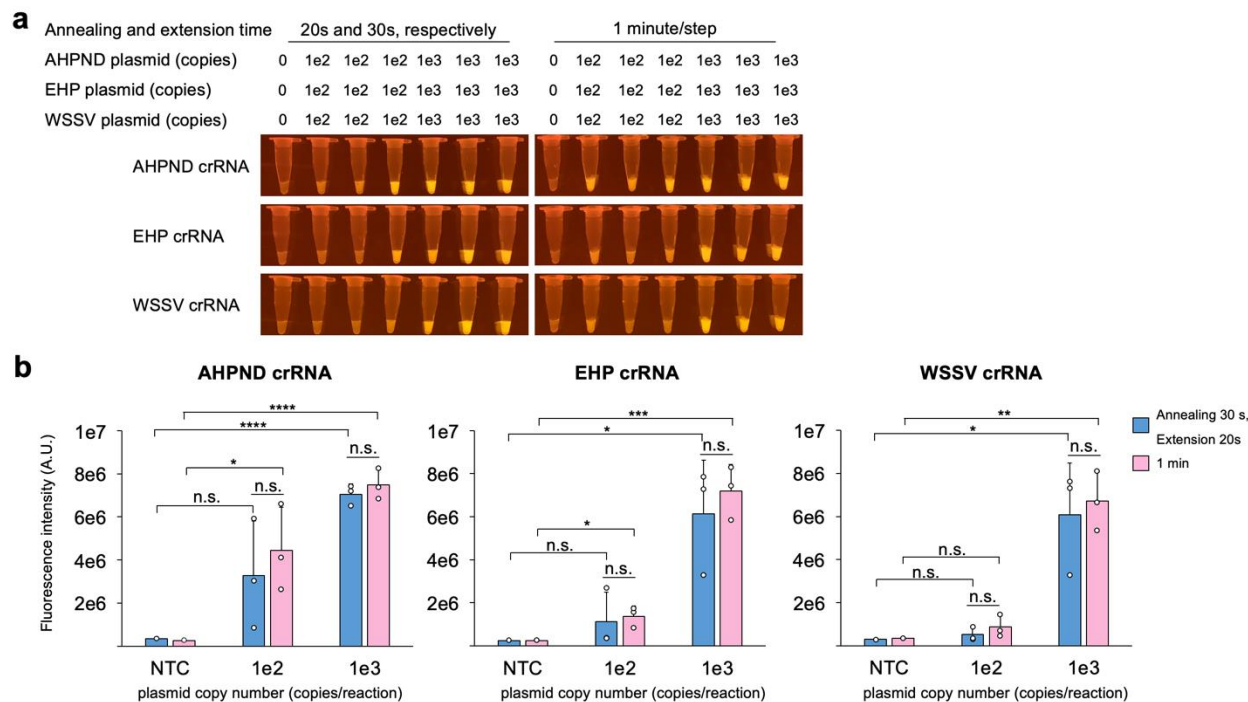
Figure S2





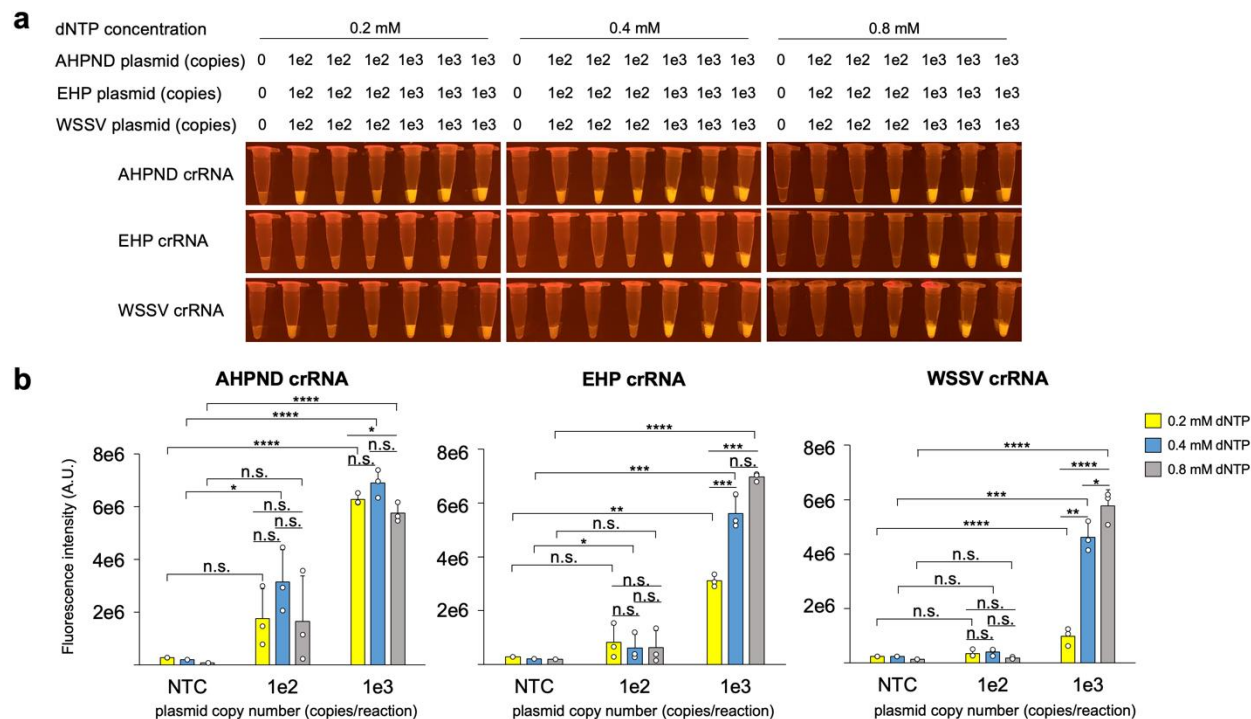
**Figure S2.**  
**Evaluation of promising annealing temperatures for multiplex PCR-Cas12a assay at 53, 55, and 57°C**  
 The results were pre-screened for efficiency on a) agarose gel electrophoresis. b) The Cas12a reaction of specific crRNA visualized under blue light and measured c) the fluorescence intensity at 566 nm of emission using a microplate reader; Error bars represent mean±SD (n=3; technical replicate, except NTC; n=1, unpaired student t-test; n.s., not significant; \*,  $p < 0.05$ ; \*\*,  $p < 0.01$ ; \*\*\*\*,  $p < 0.0001$ ). There was a noticeable distinction between the EHP and WSSV detections at 1,000 copies per reaction, with a slightly greater difference in fluorescence intensity between them. The overall limit of detection and fluorescence intensity for positive samples of the three pathogens detected at an annealing temperature of 55°C were superior to those at 53°C

**Figure S3**



**Figure S3.**

**Evaluation of increasing the annealing and extension time of multiplex PCR-Cas12a method.** The annealing and extension steps were increased from 20 s and 30 s, respectively, to 1 minute per step. a) The Cas12a reaction was visualized under blue light; b) fluorescence signal of 566 nm emission was measured using microplate reader. Error bars represent mean $\pm$ SD (n=3; technical replicate, except NTC; n=1, unpaired student t-test; n.s., not significant; \*,  $p<0.05$ ; \*\*,  $p<0.01$ ; \*\*\*,  $p<0.001$ ; \*\*\*\*,  $p<0.0001$ ). The difference in improvement between the conditions was not significant. However, the fluorescence intensity was more consistent under the 1-minute condition.

**Figure S4****Figure S4.**

**Optimization of dNTP concentration of multiplex PCR-Cas12a method.** The dNTP concentrations at 0.2, 0.4, and 0.8 mM were determined using the specific gene containing plasmid at 0, 100, and 1,000 copies/target DNA/reaction. a) The Cas12a reaction was visualized under blue light, and b) fluorescence signal of 566 nm emission was measured using microplate reader. Error bars represent mean $\pm$ SD (n=3; technical replicate, except NTC; n=1, unpaired student t-test; n.s., not significant; \*,  $p<0.05$ ; \*\*,  $p<0.01$ ; \*\*\*,  $p<0.001$ ; \*\*\*\*,  $p<0.0001$ ).

## Supplementary Table

Table S1. Lists of oligonucleotides used in this study

Name	Sequence (5'→3')	Description	References
227F	TGATGAAACTTACCATTTACAACGCCCTG ATA	Primers for multiplex PCR targeting AHPND, EHP, and WSSV in this study.	Naranitus et al. (2022)
339R	GTTACAACGTATTCGTTAGTCATGTGAGC ACC		Kanitchinda et al. (2020)
F1	CACTCAAGGAATGGCTCAAGGGTTCAAA AT		
R1	ACCTGTGAATTGATCATATCTCCTGCC T		Soowannayan and Phanthura, (2011)
VP28-HF	TGTGACCAAGACCATCGAAA		
VP28-HR	ATTGCGGATCTTGATTTTGC		
T7-DR	CACCAAAGCTAATACGACTCACTATAGG GTAATTTCTACTAAGTGTAGAT	Sequences of oligos used to prepare the DNA templates for in vitro transcription of crRNA.	Naranitus et al. (2022)
Spacer-crRNA AHPND 01	TAGTGGTAATAGATTGTACAATCTACACT TAGTAGAAATTACCCTATAGTGAG		Kanitchinda et al. (2020)
Spacer-crRNA EHP 02	ACTACGTTCTTAAACACATCATCTACACT TAGTAGAAATTACCCTATAGTGAG		
Spacer-crRNA WSSV 02	TTTGACAGCGACACCTTGGGATCTACACT TAGTAGAAATTACCCTATAGTGAG		Chaijarasphong et al. (2019)
crRNA AHPND	<u>GUAAUUUCUACUAAGUGUAGA<u>UUGUAC</u></u> <u>AAUCUAUUACCACUA</u>	The expected sequences of crRNA from in vitro transcription	Naranitus et al. (2022), Kanitchinda et al. (2020), Chaijarasphong et al. (2019)
crRNA EHP	<u>GUAAUUUCUACUAAGUGUAGA<u>UGAUGU</u></u> <u>GUUUAAAGAACGUAGU</u>		
crRNA WSSV	<u>GUAAUUUCUACUAAGUGUAGA<u>UCCCAA</u></u> <u>GGUGUCGCUGUCAAA</u>		
FQ	/5HEX/TTATT/3IABkFQ/	Fluorophore- quencher connected by ssDNA linker, serving as the reporter for Cas12a reactions	Chen et al. (2018)

## Preliminary study on free radical scavenging activity in the different fractions of lactic acid bacteria-derived postbiotics

**Sareeya Reungpatthanaphong**\*, Monchanok Bumrungrchai,  
Tanaphol Thanagornyothin, and Neungnut Chaiyawan

\*Correspondence to: Biodiversity Research Centre, Thailand Institute of Scientific and Technological Research, Pathum Thani 12120

E-mail address: sareeya@tistr.or.th

**ABSTRACT:** Probiotics, live microorganisms, have been known to provide health benefits to the host when consumed in sufficient quantities. Postbiotics or inactive probiotics and their metabolic by-products also help to promote host's health. They have been reported to exhibit several biological effect which generally characterized by the probiotics used as starting point of bioprocessing and inactivation procedures used for their production. In this study, the free radical scavenging activity in three difference fractions of Lactic Acid Bacteria-derived postbiotics including *Lactobacillus acidophilus*, *Lactobacillus paracasei* and *Lactobacillus zae* were determined. Due to the byproduct utilization, postbiotics are interested and can be applied to the various products. Furthermore, the application of postbiotics is widely used in many industries worldwide such as food, beverage, personal care products, cosmetics, and nutraceuticals.

**Keyword:** Probiotics; Postbiotics; Free Radical Scavenging; Byproduct Utilization; Lactic Acid Bacteria

### 1. INTRODUCTION

Postbiotics are soluble factors secreted by living bacteria or released by bacterial lysis which have been generally known as metabolites or bacterial components of the live probiotics and can promote health benefits to the host.<sup>[1]</sup> They have several biological activities such as antimicrobial, antioxidant, anti-inflammatory and immunomodulatory effects.<sup>[2],[3]</sup> Recently, clinical study suggested that postbiotics are safe to improve diarrhea, immune function, allergic reactions and neurodegenerative diseases. Moreover, postbiotics play an important role in the GI tract, oral cavity, skin, nasopharynx and other parts of human body. Over the past decade, the number of global research about postbiotics has been increasing and their commercialization process will be accelerated. The global market of postbiotics is mainly in the United State, Japan and Europe. Therefore, the application use of postbiotics is widespread in various industries.<sup>[4],[5]</sup>

The objective of this study was to determine free radical scavenging activity in three difference fractions of Lactic Acid Bacteria-derived postbiotics including *Lactobacillus acidophilus*, *Lactobacillus paracasei* and *Lactobacillus zae* which were processed by Innovative Center for Production of Industrially used microorganisms (ICPIM), Thailand Institute of Scientific and Technological Research (TISTR).

### 2. MATERIALS AND METHODS

1) *Materials:* All Chemicals were analytical-grade reagens. Ethanol, methanol and potassium persulfate were purchased form RCI Labscan, Thailand. DPPH, ABTS and trolox were obtained from Sigma-Aldrich.

2) *Preparation of postbiotics:* Three different fractions of each LAB including *Lactobacillus acidophilus*, *Lactobacillus paracasei* and *Lactobacillus zae* were used. Ferment solution of each postbiotics was collected after processing and then centrifuged at 6,000 rpm for 10 minutes. Supernatant was separated from pellet. The pellet was heated by boiling at 80° C for 30 minutes and

then kept at  $-20\text{ }^{\circ}\text{C}$ .

3) *DPPH radical scavenging activity assay*<sup>[6]</sup>: The free radical scavenging activity of postbiotic was assessed by measuring their scavenging abilities to 2, 2-diphenyl 1-picrylhydrazyl stable radical. A solution of the radical is prepared by dissolving 3.944 mg DPPH in 50 mL methanol. A test solution was added to methanolic DPPH. The mixture was vortexed thoroughly for 1 minute. Finally, the absorbance of the mixture was measured at 517 nm after standing at ambient temperature for 20 minutes. The assay was carried out in triplicate.

4) *ABTS radical cation-scavenging assay*: For the ABTS assay, the procedure followed a modified version of Giao *et al.*'s method.<sup>[7]</sup> the stock solutions included 7 mM ABTS<sup>++</sup> solution and 2.45 mM potassium persulfate solution. Then, the working solution was prepared by mixing the two stock solutions in a ratio of 1:0.5, and they were permitted to react for 12-16 h in the dark at room temperature. The solution was then diluted by mixing with diluted water (1:25) to acquire an absorbance of 0.7-0.9 units at 734 nm using the microplate reader. Fresh ABTS<sup>++</sup> solution was prepared for each assay. The postbiotics reacted with the ABTS<sup>++</sup> solution for 2 h in a dark condition. The absorbance was measured at 734 nm using the microplate reader.

### 3. RESULTS AND DISCUSSION

In this study, DPPH and ABTS radical scavenging activity were analysed to estimate antioxidant activity of three fractions of postbiotics derived from LAB, and the results are shown in Table 1. Among these postbiotics, *L. paracasei* showed the highest antioxidant activity in DPPH radical scavenging assay compared to *L. acidophilus* and *L. zeae*. The value of %DPPH scavenging activity of all fractions; ferment, heat-killed and supernatant, were  $73.2 \pm 0.2\%$ ,  $87.0 \pm 1.3\%$  and  $82.1 \pm .15\%$ , respectively.

ABTS scavenging ability was also evaluated. The results showed that *L. paracasei* exhibited a high scavenging activity. %ABTS scavenging activity of all fractions; ferment, heat-killed and supernatant, were  $92.9 \pm 0.2\%$ ,  $93.9 \pm 0.1$  and  $93.9 \pm 0.1\%$ , respectively.

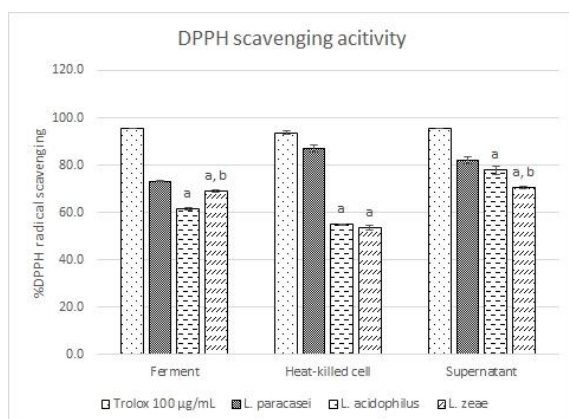


Figure 1 DPPH scavenging activity

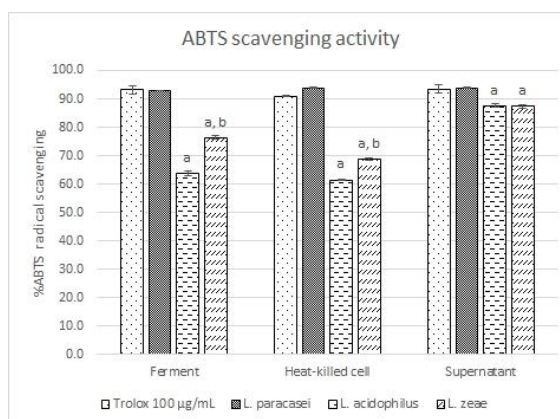


Figure 2 ABTS scavenging activity

Table 1 Free radical scavenging activity of postbiotics determined by DPPH and ABTS assay.

Assay	Species	Radical scavenging activity (%)		
		Ferment	Heat-killed cell	Supernatant
DPPH assay	Trolox 100 $\mu\text{g/mL}$	95.5 $\pm$ 0.1	93.7 $\pm$ 0.9	95.7 $\pm$ 0.1
	<i>L. paracasei</i>	73.2 $\pm$ 0.2	87.0 $\pm$ 1.3	82.1 $\pm$ 1.5
	<i>L. acidophilus</i>	61.6 $\pm$ 0.5 <sup>a</sup>	54.9 $\pm$ 0.4 <sup>a</sup>	77.8 $\pm$ 1.7 <sup>a</sup>
	<i>L. zeae</i>	68.9 $\pm$ 0.6 <sup>a, b</sup>	53.7 $\pm$ 1.1 <sup>a</sup>	70.6 $\pm$ 0.4 <sup>a, b</sup>
ABTS assay	Trolox 100 $\mu\text{g/mL}$	93.3 $\pm$ 1.4	91.1 $\pm$ 0.1	93.4 $\pm$ 1.4
	<i>L. paracasei</i>	92.2 $\pm$ 0.2	93.9 $\pm$ 0.1	93.9 $\pm$ 0.1
	<i>L. acidophilus</i>	63.8 $\pm$ 0.8 <sup>a</sup>	61.5 $\pm$ 0.3 <sup>a</sup>	87.6 $\pm$ 0.7 <sup>a</sup>
	<i>L. zeae</i>	76.4 $\pm$ 0.6 <sup>a, b</sup>	68.8 $\pm$ 0.4 <sup>a, b</sup>	87.4 $\pm$ 0.6 <sup>a</sup>

Notes: Mean of three replications  $\pm$  standard deviation (SD).

"a" means significantly different ( $P \leq 0.05$ ) when compared with *L. paracasei*.

"b" means significantly different ( $P \leq 0.05$ ) when compared with *L. acidophilus*.

#### 4. CONCLUSIONS

Postbiotics are bioactive substances that are secreted by probiotics. In this study, *L. paracasei* derived postbiotic exhibited the strongest radical scavenging activity. In addition, the supernatant of all postbiotics was a fraction that showed higher activity than the other fractions. The usage of postbiotics, a novel class of substances derived from probiotics confer a health benefit on the host. The use of postbiotics as cosmetic ingredient is more increasingly due to their significant biological effects such as antioxidant, anti-inflammatory and antimicrobial activities. In addition, postbiotics possess the potential for skin care applications and they have the ability to up- or down-regulate specific genes, potentially reducing inflammatory response.<sup>[8]</sup> The results of this study indicated that *Lactobacillus sp.* exhibited their free radical scavenging activity which may provide an information of byproduct utilization from probiotics as benefit ingredients in the health care products.

#### 5. ACKNOWLEDGEMENT

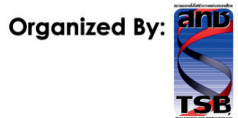
The authors would like to gratefully thank the National Research Council of Thailand for financial support. We would like to extend our thanks to the Biodiversity Research Centre, Thailand Institute of Scientific and Technological Research for the provision of equipment and facilities.

#### 6. REFERENCES

- [1] Aggarwal, S., Sabharwal, V., Kaushik, P., Joshi, A., Aayushi, A., & Suri, M. (2022). Postbiotics: From emerging concept to application. *Frontiers in Sustainable Food Systems*, 6, 887642. <https://doi.org/https://doi.org/10.3389/fsufs.2022.887642>
- [2] Aguilar-Toalá, J., Garcia-Varela, R., Garcia, H., Mata-Haro, V., González-Córdova, A., Vallejo-Cordoba, B., & Hernández-Mendoza, A. (2018). Postbiotics: An evolving term within the functional foods field. *Trends in food science & technology*, 75, 105-114. <https://doi.org/https://doi.org/10.1016/j.tifs.2018.03.009>
- [3] Salminen, S., Collado, M. C., Endo, A., Hill, C., Lebeer, S., Quigley, E. M., Sanders, M. E., Shamir, R., Swann, J. R., & Szajewska, H. (2021). The International Scientific Association of Probiotics and Prebiotics (ISAPP) consensus statement on the definition and scope of postbiotics. *Nature Reviews Gastroenterology & Hepatology*, 18(9), 649-667.
- [4] Mosca, A., Abreu Y Abreu, A. T., Gwee, K. A., Ianiro, G., Tack, J., Nguyen, T. V. H., & Hill, C. (2022). The clinical evidence for postbiotics as microbial therapeutics. *Gut Microbes*, 14(1), 2117508. <https://doi.org/https://doi.org/10.1080/19490976.2022.2117508>

- [5] Liang, B., & Xing, D. (2023). The Current and Future Perspectives of Postbiotics. *Probiotics and Antimicrobial Proteins*, 1-18.
- [6] Thaipong, K., Boonprakob, U., Crosby, K., Cisneros-Zevallos, L., & Byrne, D. H. (2006). Comparison of ABTS, DPPH, FRAP, and ORAC assays for estimating antioxidant activity from guava fruit extracts. *Journal of food composition and analysis*, 19(6-7), 669-675. <https://doi.org/https://doi.org/10.1016/j.jfca.2006.01.003>
- [7] Gião, M. S., González-Sanjósé, M. L., Rivero-Pérez, M. D., Pereira, C. I., Pintado, M. E., & Malcata, F. X. (2007). Infusions of Portuguese medicinal plants: Dependence of final antioxidant capacity and phenol content on extraction features. *Journal of the Science of Food and Agriculture*, 87(14), 2638-2647. <https://doi.org/https://doi.org/10.1002/jsfa.3023>
- [8] Duarte, M. F. P. (2022). *Sustainable postbiotics for cosmetic and skincare applications*





In collaboration with:

Thai Probiotics and Lactic Acid Bacteria



Supported By:

